Fall 12-18-2014

The Garnet Line in Oxford County, Maine Pegmatites.

Myles Mathew Felch
The University of New Orleans, mmfelch@uno.edu

Myles M. Felch
myles.felch@maine.edu

The Garnet Line in Oxford County, Maine Pegmatites.

A Thesis

Submitted to the Graduate Faculty of the
University of New Orleans
in partial fulfillment of the
requirements for the degree of

Master of Science
in
Earth and Environmental Sciences

By

Myles Felch

B.A., University of Maine at Farmington, 2012

December 2014

Acknowledgments

I would first like to thank Jim Nizamoff, whom I contacted a few years ago and eventually introduced me to the MP^2 group. With that said, I would like to thank Al, Skip and Karen for allowing me to further my education here at the University of New Orleans. Of course this would also not be possible without the help of my officemates Drew, John, Karen, Kim, Leah, Mark and Sasha. I also need to thank all the Maine pegmatite miners who have given me access to their property over the past few summers and all other involved in their projects: Jeff Morrison, Gary Freeman, Ray Sprague, Frank Perham and company and Mary Groves and her crew at the Poland Mining Camp.

I want to thank my professors at the University of Maine at Farmington, Dr. Eastler, Dr. Gibson and Dr. Reusch. You were the first people to show me the beauty that lies beneath my feet. Thank you for inspiring me.

For all involved at the Maine and Mineral and Gem Museum, past and present. Thank you for everything you have given me. What I admire most about you all is the sense of family you all bring to this amazing project. Thank you for making me feel at home, you guys and gals are the best.

Lauren El-Hajj, thank you for everything… and I mean everything. Seriously though, I would have never made it through this without you. I wish you the best, with love always.

Sam and Gavin, you are the best brothers and friends anyone could ask for. You both mean the world to me, thank you for all your support.

Ultimately this one goes out to my parents, without them this would not be possible. You both have given me everything; I am so lucky to have parents like you. Words cannot describe my love for you both. Hats off to you.

Table of Contents

List of Figures

List of Tables

Abstract:

The garnet line is a planar fabric occurring within the either the intermediate or core zone in many of the Oxford County, Maine pegmatites. This study focuses primarily on the textural and chemical characteristics of the garnet line within the Mt. Mica and western Mt. Apatite quarries. Smaller, but similarly textured garnet line analogs from the Bennett, Emmons, Havey and Tamminen quarries are also investigated. All of these textures represent specific fractionation events within their respective dikes. In some of these locations, multiple stages of crystallization occur and appear to be post-magmatic, related to late stage metasomatism. These late stage fluids are believed to have migrated from localized and highly evolved regions within these pegmatites. The garnet line at Mt. Mica has the greatest diversity of secondary mineral assemblages, e.g. tourmaline and/or muscovite rims around garnets and ferric pollucite. None of these late stage textures have ever been described before.

Keywords: Pegmatite, Maine, “Garnet Line”, Tourmaline rim, Metasomatism.

Introduction:

Pegmatite Petrogenesis:

Pegmatites are coarse-grained igneous rocks (>2 cm), typically granitic, which may at times contain high concentrations of minor and trace elements capable of producing an array of unique mineral assemblages. These rocks are found in many locations around the world, where they often serve an economic purpose. A small portion of these intrusions contain an abundance of Li, Cs, U, Sn and Be ores, whereas others have been mined exclusively for their exotic minerals and world class gem rough. In the beginning, many of these intrusions were primarily mined for their industrial minerals (feldspar and mica) and only later were they exploited for their gemstones, whereas some locations were mined only for gem production.

Pegmatite genesis is not yet fully understood. There are three basic models of formation, including fractional crystallization from a parent melt, anatectic partial melting of country rock and hydrothermal processes. There is no certainty that there is ever only one mechanism producing the pegmatitic melt.

Fractionation from parent magma has been the most widely used explanation for pegmatite genesis (Černý 2005). However, there is a large body of evidence surrounding anatexis as a mechanism capable of producing highly evolved melts through partial melting (Swanson 2012, Simmons 2007, Grew *et al.* 2004). Though fractionation of a partial melt is likely to occur, the extent depends on the volume and composition of melt that is initially produced and its distance travelled from the source.

Many classification schemes have developed to attempt to divide these intrusions into a series of differ rent types. Depth of emplacement: abyssal (deep crustal levels), muscovite, rare-earth element, miarolitic (shallow crustal levels) is based largely on country rock-pegmatite relations as well as mineral content. The existing mineralogy in each of these different pegmatite types is a reflection of the starting melt composition. Distinctions between these types, which lead to the development of many different classes and subclasses is based on the specific mineral assemblages found in these intrusions. Pegmatites that crystallized in high pressure regimes are generally barren (containing only feldspar, quartz and some mica), representing the early stages of fractionation. Pegmatites that are emplaced at shallow depths may contain miarolitic cavities and high concentrations of rare-earth element bearing minerals. These pegmatite are an example of a higher degree of fractionation crystallization (Simmons *et al.* 2012) compared to the more barren types.

LCT (Li-Cs-Ta) and NYF (Nb-Y-F) type pegmatites are two broad families in a classification scheme that is widely accepted in modern research (Černý *et al.* 2012).The acronyms signify an abundance of select elements (listed above), which translate to the mineral assemblages exhibited by a pegmatite. These two families are each generated by different starting melt compositions, which are produced from different source materials. LCT pegmatites are derived from S-type granites through partial melting of metasedimentary rock and result in a peraluminous melt composition (Al_2O_3> ($CaO+Na_2O+K_2O$)). NYF pegmatites are derived from I and A-type granites, produced by melting pre-existing igneous material. Metaluminous (Al_2O_3< ($CaO+Na_2O+K_2O$)) to subaluminous (Al_2O_3≈ ($CaO+Na_2O+K_2O$)) compositions are characteristic of these melt types.

The two families have been used to some extent in relation to tectonic setting, as they tend to show an affinity for certain regimes. NYF suites are generally associated with anorogenic extensional settings and LCT suites with orogenic collisional regimes. However, there are many variables associated with melt generation. Orogenic, anorogenic and the transitional tectonic events all occur at different rates and involve the contribution of differing crustal materials and mantle components. Localized contamination from assimilated country rock or metasomatized crustal blocks may influence a melt resulting in overprinting NYF and LCT signatures (Martin and De Vito 2005). An attempt to categorize pegmatites in this fashion is difficult because the duration of the phases involved with relaxation and mountain building events and the degrees of metamorphism and magmatization all occur at different stages and rates. Future classification schemes will likely involve tectonic indicators as well as the now popular rare element categories (see Černý *et al.* 2012).

The "garnet line":

The "garnet line" is a distinctive layer of reddish-brown euhedral to anhedral garnet crystals ranging in size from a few mm to some as large as a cm. In some places the garnets are rimmed by fine-grained blue tourmaline. Prismatic schorl crystals occur above and below the garnet line. The "garnet line" has a particularly interesting historical background. It has been used as an indicator for the pegmatite miners at the Mt. Mica and Mt. Apatite Quarries, since their early beginnings over a century ago (Bastin 1911). Mining above the garnet line has proven to be an invaluable strategy for extracting gemstones; "to explore beneath has been thus far a waste of time and labor" (Hamlin 1895). The texture is still used to this day as an aid

for mining gemstones and mineral specimens at these two locations. Similar odd textures have been used as exploration guides by other Maine pegmatite mines, e.g. discontinuous schorl lines have been used as pocket zone indicators at the Havey (see Fig. 10) in Havey chapter, and Emmons quarries, (*Person. comm.* Ray Sprague 2013). However, no other feature is more prominent and well known by Maine pegmatite miners than the garnet line at the Mt. Mica and Mt. Apatite Quarries.

Mineralogical descriptions for many of the western Maine's highly evolved pegmatites are available in the literature, to include Mt. Mica (Hamlin 1895, Cameron *et al.* 1954, Simmons 2006, Marchal 2014), Mt. Apatite (Rose *et al.* 1997, Francis *et al.* 1993) and the Bennett (Wise *et al.* 2000). Many are reviews on the mineral occurrences in single pegmatites with minimal chemical studies, whereas others focus on comparing select mineral species from different locations (Wise and Brown 2010). None of these sources have yet focused on the development of the garnet line. Fortunately, these pegmatites have been extensively mined for their mineral resources and exposures are plentiful. The garnet line texture has prompted the author to question its significance with respect to pegmatite melt evolution. The Mt. Mica and Mt. Apatite quarries have produced a range of valuable minerals and the pegmatites themselves show differences in trace element enrichment, owing to their degree of melt evolution.

This thesis looks at the continuous garnet line of Mt. Mica and Mt. Apatite as well as the discontinuous "stringers" of garnets that occur in other Oxford County pegmatites: the Emmons, Havey and Tamminen, in addition, garnets from an aplite at the Bennett quarry are also investigated. These features are like the more pronounced garnet line of Mt. Mica and Mt. Apatite in that they represent a specific moment in the pegmatites crystallization history as

they generally occur in one particular zone. Less well known garnet “train textures” have been reported from pegmatites and plutons in other parts of the world (Hönig *et al.* 2011, Macleod 1992), but neither case are as texturally pronounced as these occurrences in Maine.

Garnets in pegmatites:

Garnets are a common accessory phase found in a range of different rock types (Jaffe 1951) to include granitic pegmatites where their chemistry is found to range greatly depending on the parental melt. Granitic pegmatites generally host almanditic to spessartitic varieties. The most highly evolved pegmatites tend to have garnets with a considerable spessartine component (Baldwin 1983, Sokolov and Khlestov 1990) and at times end member compositions (Laurs 2001, Foord 1976). For this reason garnets serve as good indicators of melt evolution when comparing granitic pegmatites.

Evolved pegmatites often develop a series of zones, each signifying distinct chemical and thermal transitions that the melt experienced during its crystallization history. The Mn/Fe in granitic pegmatites has been shown to increase as the melt fractionates. Garnets are a good indicator of the Mn enrichment because Fe and Mn are both compatible in the crystal structure and garnets often grow in multiple zones of a pegmatite and can potentially show a progression; wall, intermediate and core zones. Though Mn is compatible with other accessory minerals that may crystallize simultaneously with garnet e.g. schorl and biotite, which have a stronger affinity for Fe and are more likely to preferentially incorporate this divalent ion into

their structure (London 2001), the Mn/Fe ratio of the later melts increases and is reflected in the later garnets.

Baldwin *et al.* 1983, were able to show a relationship between the Mn/Fe ratio in garnet chemistry and pegmatite zones. Furthermore, they illustrated that garnets with the highest spessartine component are found in core/replacement zones of lithium-rich pegmatites verse those found in the cores of lithium deficient systems. Though a trend is identified the resulting garnet compositions are ultimately determined by the starting melt composition. A melt may already be highly enriched in Mn long before it is emplaced and begins to crystallize. Such a composition will reflect overall higher Mn/Fe ratios in garnets from all zones than a melt that is Mn-depleted prior to fractionation.

Within individual crystals, the amount of Mn and Fe may change systematically from core to rim, which is dependent on the composition of the melt along the crystallization front. There are many reports of Mn/Fe enrichment from rim to core (Manning 1983, Whitworth 1992, Nakajima 2006, Müller 2012), however, the opposite has been seen to occur (Foord 1976). In some cases, major cation zoning is nonexistent (Müller 2012). In all instances the Mn/Fe ratio increases from wall-zone to core of the pegmatite. Single garnet crystals from separate zones show the melt characteristics of a brief moment during the crystallization history

Geologic Background:

The Mt. Mica, Tamminen, Havey, Emmons, Bennett and Western Mt. Apatite quarries are all separate, cavity and RE-bearing pegmatites within the Oxford County, ME pegmatite field (Wise and Francis 1992). The pegmatites are concentrated in a portion of the Central Maine Belt (CMB), a NE-SW trending synclinorium (Fig. 1),

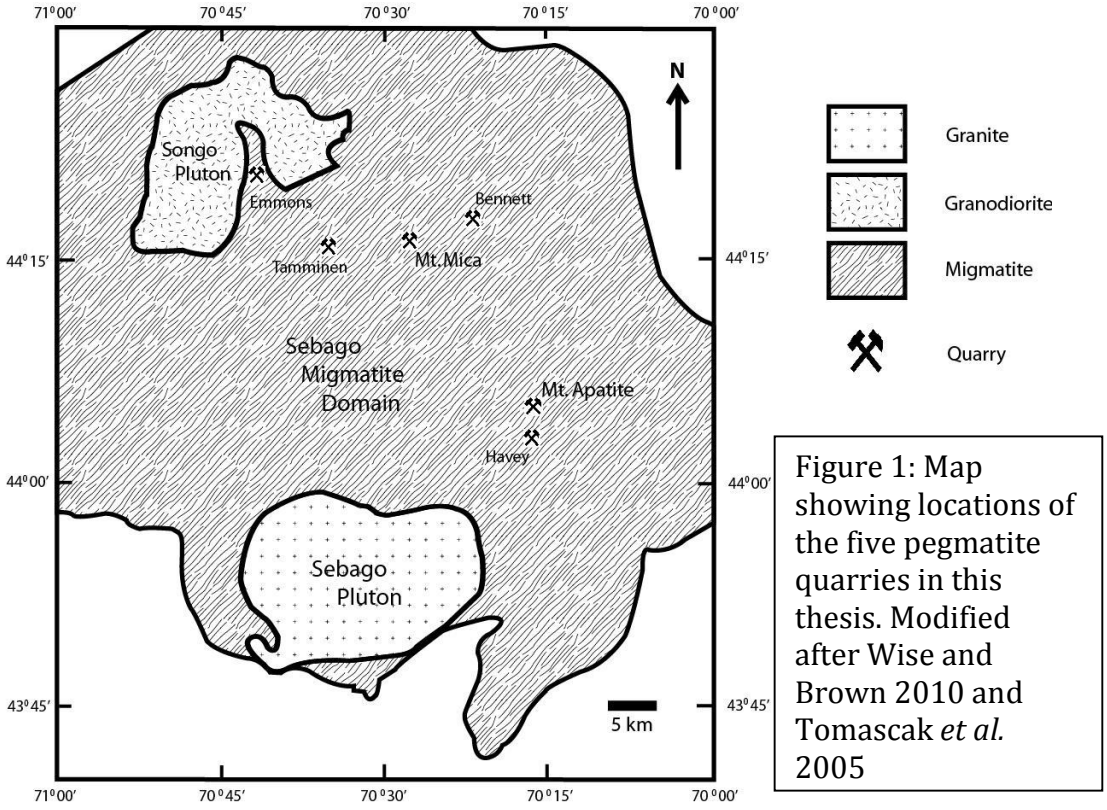

Figure 1: Map showing locations of the five pegmatite quarries in this thesis. Modified after Wise and Brown 2010 and Tomascak *et al.* 2005

which is the result of a very complex tectonic history that was active through much of the Proterozoic (Cambrian - Devonian) (Moench 2003) involving multiple orogenies (Penobscottian, Taconic and Acadian). The unit extends from New Brunswick, Canada into Connecticut and is primarily composed of Silurian-Devonian metasediments (Reusch and van Staal 2012) with

individual igneous plutons of Mesozoic-Ordovician ages sporadically emplaced and ranging in size from 10-25 km in diameter (Tomascak *et al.* 2005).

The portion of the CMB surrounding the Oxford county pegmatites in western Maine has endured extensive deformation. The sillimanite grade metamorphism and migmatite textures are believed to be the result of a regional metamorphic event caused by the Acadian orogeny and coupled with localized plutonism (Solar and Brown 2001, Guidotti and Johnson 2002, Holdaway *et al.* 1988.). Furthermore, the area where much of western Maine's pegmatites have intruded has such an abundance of migmatitic textures the geograds for the region have been remapped. The area has been named the Sebago Migmatite Domain, SMD (Tomascak *et al.* 2005). Regionally, outcrops in this area consist of metapelites, metasandstones and calc-silicate granofels, whereas numerous other areas show a high degree of partial melting with dominant igneous fabrics. Pegmatites throughout the Oxford County pegmatite field intrude into all rock types associated with the SMD, showing no intrusive preference with respect to metasediments or partially melted material, but generally are emplaced concordantly with country rock fabric.

Genetic correlation between temporally and spatially related plutons and the Oxford county pegmatites have been hypothesized in the past. Preference was first given to the Sebago Pluton as it shares similar age (293 ± 2 Ma, Tomascak *et al.* 1996) with the few Oxford County pegmatites that have been dated; U-Pb zircon ages 274 and 264 Ma Bradley *et al.* 2013, McCauley and Bradley 2013 and 2014 and in this study U-Pb monazite ages dates for Mt. Mica are 255.4 Ma and Mt. Apatite are 258.7 Ma. However, recent reconnaissance mapping in western Maine has forced a paradigm shift on previous assessments of pluton-pegmatite

relations. The dimensions of the Sebago pluton have decreased considerably and subsequently make genetic relations based on spatial proximity highly unlikely; pegmatite distances from the Sebago pluton range from 10-30 km. Further investigation should be done with other smaller, localized leucogranite bodies in the SMD to answer potential genetic parental melt relations with the Oxford county pegmatites.

Direct anatexis of the host country rock has also been considered as a potential genesis for these pegmatites as well, but metamorphic rocks of the Perry Mountain Formation in the Rumford quadrangle, just north of the Lewiston quadrangle (area of this study) record a much older deformation age (U-Pb monazite date; 405 to 399 ± 2 Ma, Smith and Barreiro 1990) than the emplacement of the pegmatites and Sebago pluton, but the granites in the migmatites have U-Pb zircon and monazite ages that range from 408-404 Ma, Solar *et al.* 1998. Furthermore, in greater proximity to the pegmatites in this study, zircon grains from migmatites have a date of 376 ± 15 Ma (Tomascak and Solar 2013). By the time the pegmatites were emplaced, given the reported age dates, the SMD had already partially melted and cooled Tomascak and Solar 2013. Therefore, partial melting of the country rock hosts are not likely cogenetic with pegmatite generation and emplacement. However, precaution is needed for interpreting age dates from zircons as these crystals are often highly metamict and may be xenocrystic McCauley and Bradley 2014.

Given the problems with obtaining age dates, their validity becomes questionable leaving further interpretations based on geochemistry to ascertain the genetic link between pegmatites and source materials. Textural and geochemical evidence at the Mt. Mica pegmatite support the anatexis hypothesis. Rare-earth element content from the pegmatite closely

resembles that of leucosomes from numerous areas within the SMD (Simmons *et al.* 2013). Therefore, this presents a very strong argument for the capability of direct anatexis of the SMD metapelites to produce the pegmatites seen in western Maine.

Quarry Descriptions

Mount Mica:

The Mt. Mica pegmatite is located in Paris, Maine, about 4 miles east of route 26. The mine is known for being the first producer of gem tourmaline in North America, beginning in 1820. Mining has been sporadic at this location through the years; however, beginning in 2003 till the present, the mine is still operational and continues to produce a variety of gemstones and mineral specimens.

The Mt. Mica pegmatite is a single lens shaped dike intruding concordantly into migmatite of the SMD (Solar & Tomascak 2009, Marchal et al. 2014) composed of a Silurian to Devonian aged sequence. The dike ranges in thickness 1.5-8m, strikes northeast-southwest and dips ~ 25° SE on average. The pegmatite has an abundance of cavities that range in size (20 cm to 6m in diameter) and host different mineral assemblages. The abundant lithian (lepidolite), cesian (pollucite) and boron (tourmaline) mineralization are indicative signatures of highly evolved.

The zones of the pegmatite are not well defined; however, mineralogical and grain size differences divide the dike into three distinguishable sections. The contact is well exposed

along the hanging wall, country rock leucosome appear to grade into the dike whereas melanosome contacts have sharper contrast but corroded margins. The footwall contact is rarely exposed, but has a similar contact as the hanging wall. The core is composed primarily of quartz, muscovite and to a lesser extent, K-feldspar and tourmaline. The wall zone is coarse to very coarse-grained quartz, plagioclase and muscovite with accessory schorl. It is within the wall zone on the footwall-side where the garnet line is found. Light gray cleavelandite is somewhat localized and restricted to the inner portions of the dike adjacent to the garnet line. Lepidolite pods are locally developed throughout the core of the pegmatite and host other rare mineral species e.g. altered spodumene and pollucite.

The garnet line is generally 2-6 cm thick and hosts garnet, muscovite, schorl and feldspar. It is often a boundary between blocky plagioclase feldspar and cleavelandite (Figs. 2 and 3)**.** Garnets are deep red in color, are 0.5-3.5cm in diameter and generally euhedral. Tourmaline overgrowths (0.5-2mm) on garnet crystals are commonly encountered. This is a trademark texture for the Mt. Mica pegmatite, but Buřival and Novák 2014, have recently reported a similar occurrence from the Sahatany Valley, Madagascar. The tourmaline coronas are blue to black in color and zoning from black to blue occurs with distance from the garnet crystal margin. There are areas within the garnet line along strike of the pegmatite where the tourmaline rims are absent. The tourmaline rimming appears to be most abundant in areas where highly evolved mineral species and pockets occur.

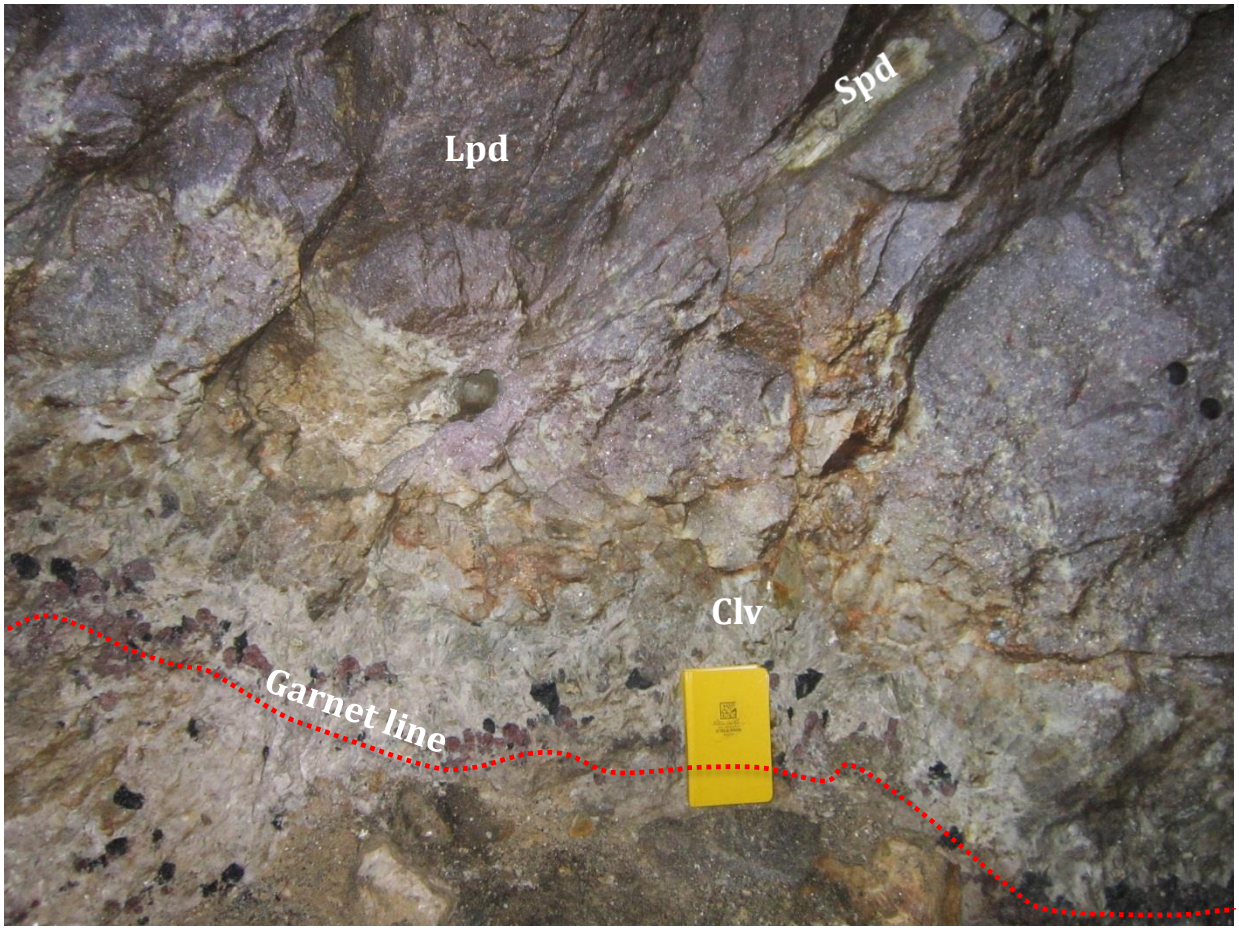

Figure 2: Partial pegmatite cross section highlighting the area beneath garnet line (footwall side) and core portion. Lepidolite (Lpd), cleavelandite (Clv), spodumene (Spd). Red dotted line marks garnet line.

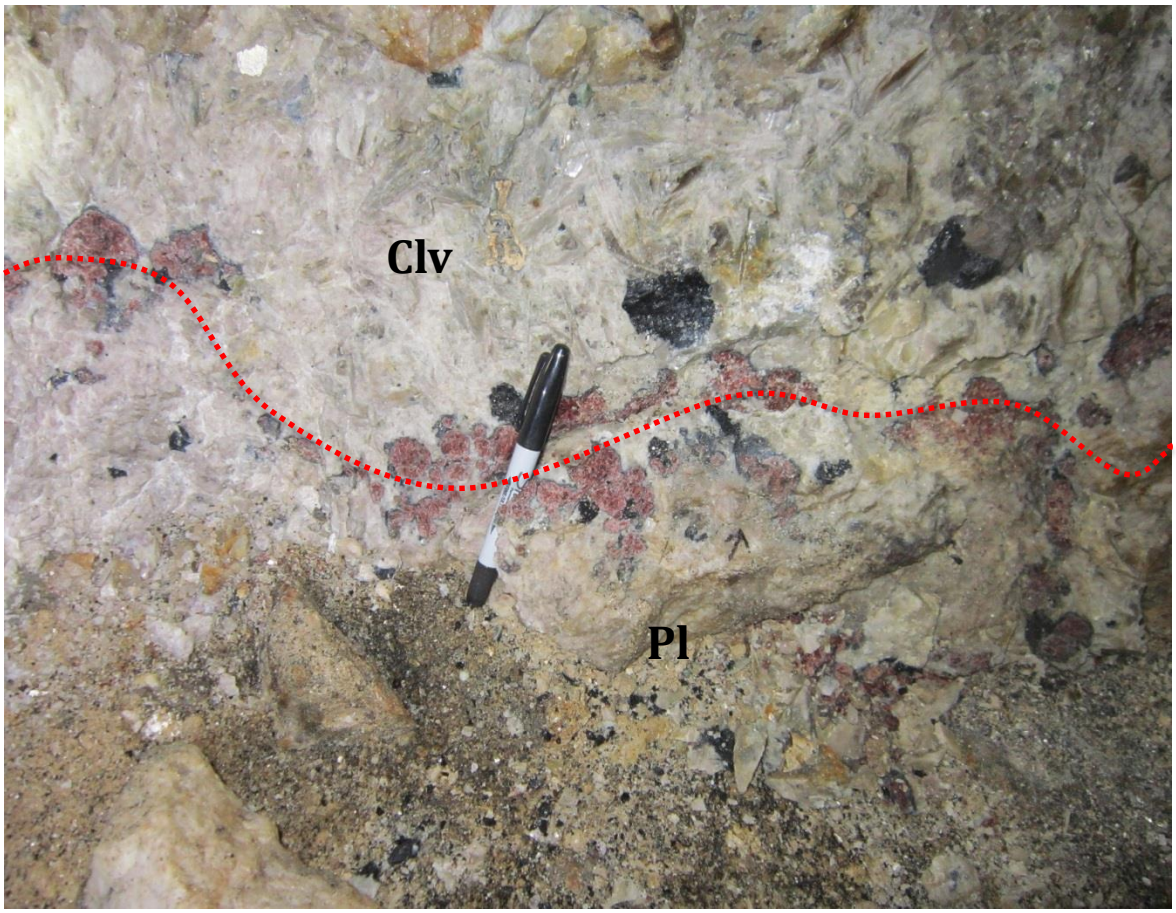

Figure 3: Closer image of the garnet line from previous image illustrating its significance as a common boundary layer transition of cleavelandite and pegmatitic plagioclase (Pl) and quartz. The garnet line is highlighted with red marks and arrow points toward the core.

Schorl is a common accessory mineral phase throughout the Mt. Mica pegmatite. Schorl occurs in portions of the wall zones and core zone. Large subhedral masses (≤40cm) schorl are sometimes present growing from above and into pockets below, where they grade into elbaitic compositions. Gem green and pink tourmalines have been recovered from many of the pockets in the core zone. Also, roughly parallel lines of schorl occur both above and below the garnet line in some pegmatites. However, schorl also occurs within the garnet line itself. The crystals range from 1 to 4cm, show no preferred orientation, are usually highly fractured and may host inclusions of garnet, quartz and very small siderite/rhodochrosite masses.

Fe/Mn carbonate pods, primarily siderite-rhodochrosite, exist in the central core portion of the Mt. Mica pegmatite, where they host a range of exotic and rare phosphates (eosphorite – childrenite, mccrillisite, kosnarite) and heavy mineral phases (Johnson 2013). The pods are pale yellow to white in color and are commonly rimmed with blue/black tourmaline. The carbonate pod associated with the garnet line perhaps marks the onset of this occurrence, as their size and abundance seems to increase within the core portions near pollucite and lepidolite pods. The phosphate assemblages in the core suggest they are late stage and crystallized at low temperatures (Johnson 2013).

Within the garnet line, these carbonate pods are commonly rimmed with tourmaline in a similar fashion to the garnets (Fig. 4), but muscovite is also seen rimming the pods. They also occur within tourmaline crystals and between blades of cleavelandite.

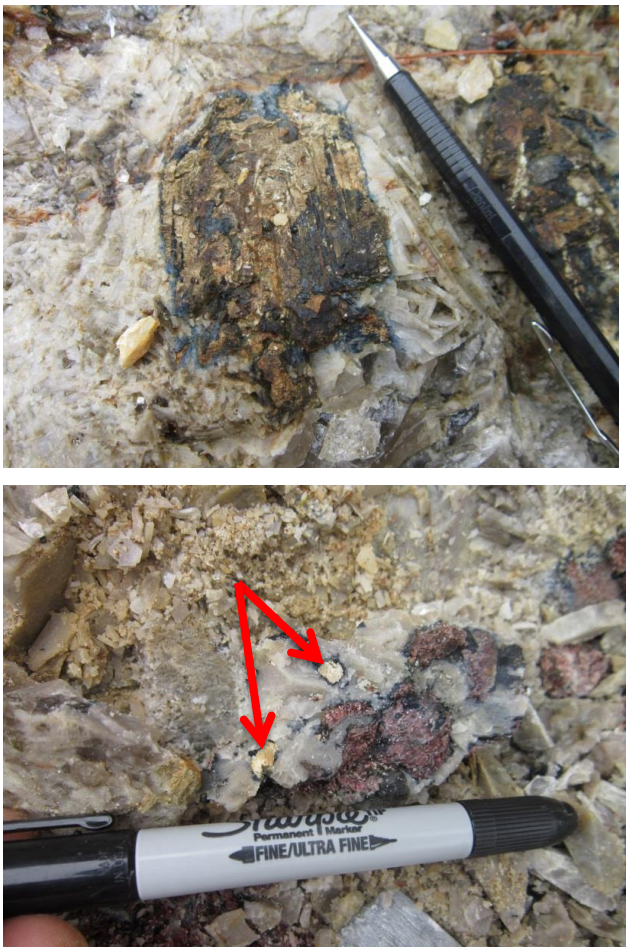

Figure 4: Two examples of carbonate pods with blue tourmaline rims, found among cleavelandite within the garnet line.

A localized area of extensive hydrothermal alteration occurred in the garnet line in the proximity of a large cavity (~6 m diameter). This pocket was not tourmaline bearing, but contained abundant apatite, pyrite, rhodochrosite and bertrandite. The garnets in the garnet line, beneath this pocket are partial or fully replaced by green to pale yellow muscovite. Along garnet crystal margins tourmaline is absent, instead anhedral to cubic pyrite crystals, löllingite are found.

Mount Apatite:

The Western Mt. Apatite quarries have been prolific producers of royal purple apatite as well as gem tourmaline (Rochester 1997, Francis 1985). A sequence of five different quarries and some minor prospects stretch ~400 m along the western side of Hatch Mountain road (Fig. 5). These quarries were each opened at different times in the early 1900's, but select pits have been mined periodically for the past century. Only one quarry is still actively mined to this day.

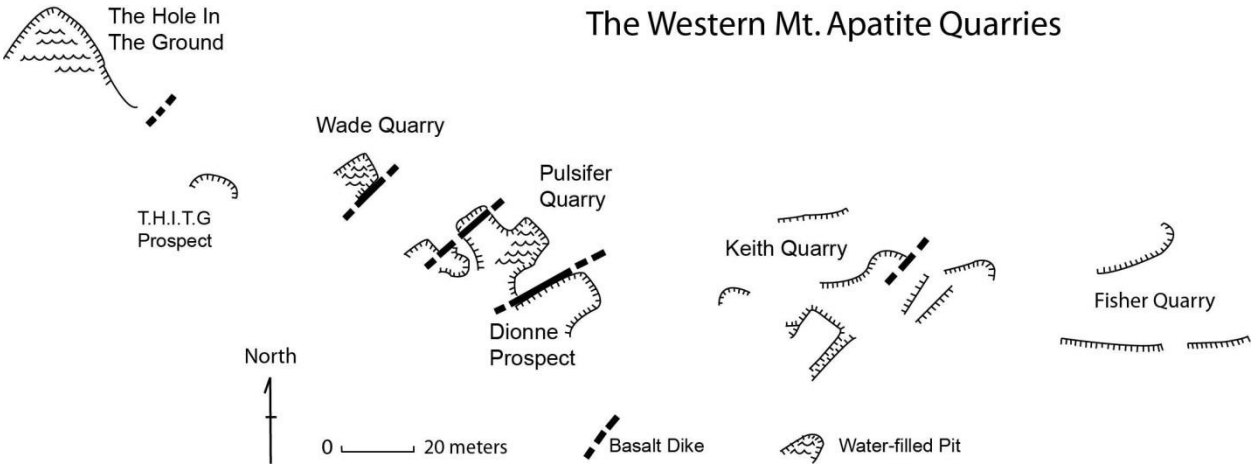

Figure 5: The Western Mt. Apatite quarries, modified from Rose and Wise 1997

The set of quarries on the western side of Mount Apatite are located about 5.5 km southwest of the city of Auburn in Androscoggin County, Maine. They are believed to be all part of the same pegmatite. The assumption is based on the occurrence of similarly textured units that can be seen in each quarry; like the garnet line and hanging and footwall zones comprised of graphic granite. The quarries also all fall along strike with one another and their hanging wall contacts are exposed revealing the similar concordant emplacement style, and gentle westerly dip. The pegmatite intrudes a metasedimentary package

consisting of fine-grained calc-silicate granofels and metapelites of the Sangerville formation, likely the Patch mountain member (Creasy 1979).

Outcrops at the Pulsifer, The-Hole-In-The-Ground (T.H.I.T.G) and The-Hole-In-The-Ground prospect were the only sampled locations. The Wade quarry was submerged during the field work season; however, the occurrence of the garnet line has been reported in this quarry (Rose *et al.* 1997, Huberty and Brown 2007). The line was not seen by the author in the Keith or Fischer quarries and is not mentioned in earlier reports by Bastin, 1911.

Pulsifer:

The Pulsifer Quarry had minimal exposure of the garnet line, however, what was uncovered was seen to mimic the descriptions of Bastin 1911 (Figs. 6 a & b). Mine tailings also support the description. Two garnet layers, parallel to one another, are separated by a fine grained graphic granite intergrowth of white plagioclase and light gray quartz. Beneath the lower garnet layer is coarser grained graphic granite, which may very well continue to the footwall. However, no exposure is available to support this claim. Above the upper garnet layer are primarily coarse-grained blocky white plagioclase, smoky gray quartz and accessory muscovite and garnet. Plumose muscovite pods are abundant within the unit and range in size from 10-40 cm in width. The garnet line closest to the core tends to have a higher abundance of garnets, single crystals ≤0.75 cm in diameter. These garnets in the lower line are generally less than 2 mm in diameter. The hanging wall is a graphic granite unit similar to the zone beneath the garnet seam.

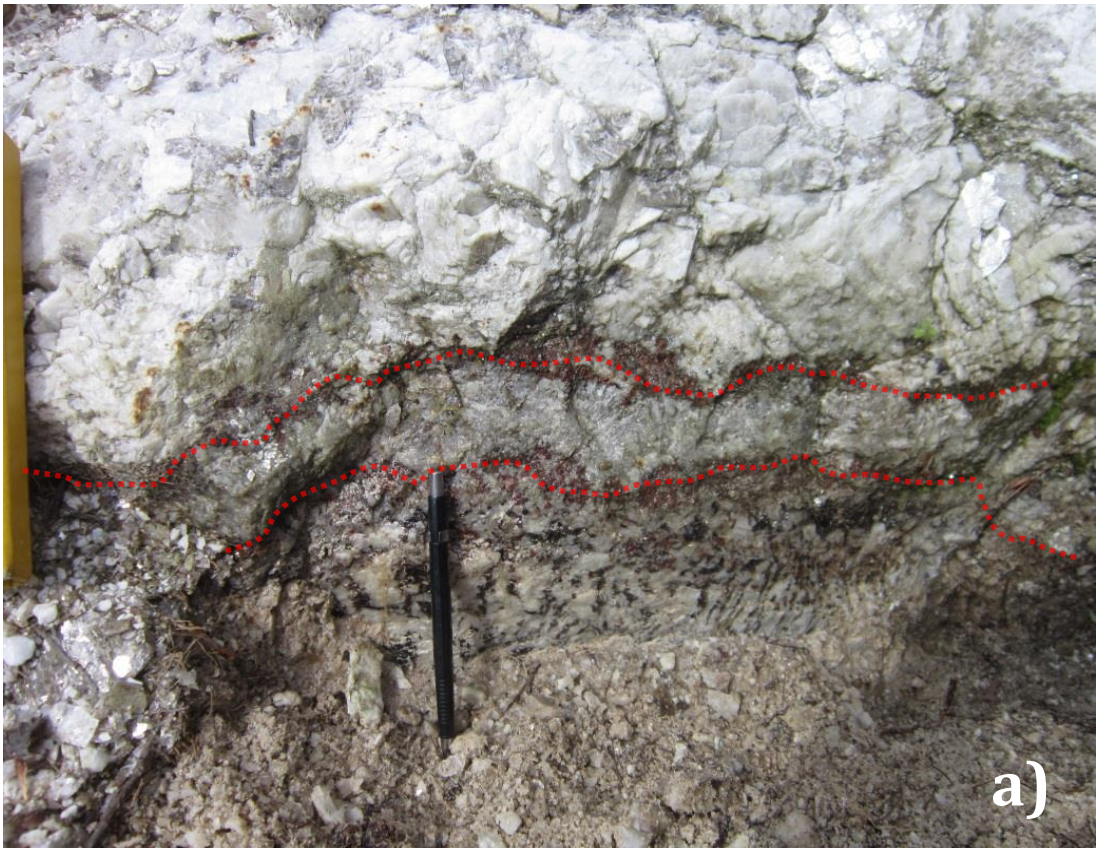
a)

Figure 6: (a) Both garnet lines at the Pulsifer quarry, pen is pointing down toward footwall. Note grain size differences core-ward; coarse grained graphic granite>garnet line> med-fine grained graphic granite>garnet line>blocky plagioclase. (b) Boulder from the Pulsifer Quarry. Note three texturally distinct zones, each separated by a layer of garnet. Hammer handle points toward the pegmatite core.

The-Hole-In-The-Ground:

The-Hole-In-The-Ground quarry is the most recently worked mine of the five quarries and provided an ideal cross section of the pegmatite apart from the footwall contact, beginning at the garnet line and ending at the hanging wall contact, with minimal exposure of the graphic granite zone beneath the line (~30 cm). The graphic zone adjacent to the hanging wall contains biotite laths (1-6 cm) grown perpendicular to the wall zone that mimic comb textures of tourmalinization. Plumose muscovite pods also occur in this portion of the dike as well as euhedral garnet (≤1.5 cm), plagioclase and quartz. The graphic zone beneath the garnet seam is composed of white plagioclase and smoky quartz with minor, small plumose muscovite pods (1-2 cm), which fan out in the direction of the core of the dike.

The garnet line is well exposed (Figs. 7 and 8) and ranges in size, but can be up to 25 cm thick. A second more discontinuous line (2-5 cm thickness) runs roughly parallel, 6-12 cm, above the thicker lower line. It is similar to the findings in the Pulsifer pit, but differs with respect to thickness and grain size.

Figure 7: At The-Hole-In-The-Ground quarry, only the portions above the garnet line have been excavated. The line has been enhanced (red), but shows the extent of the features planar fabric. The active portion of the quarry is submerged at right of the photograph. Intermediate and hanging wall portions are protruding from the water at top right of photograph.

Figure 8: Pointing to the garnet line in The-Hole-In-The-Ground quarry, note the rusted weathering. This is the portion of the dike that is protruding from the water in the top right of the previous figure.

The line is composed of euhedral (≤1.5 cm) garnets that are deep red in color and have a vitreous luster, but are often highly fractured. Subhedral smoky quartz is the predominant interstitial phase; accessory muscovite books (≤1 cm) are not uncommon.

The blocky plagioclase feldspar zone is the pocket bearing portion of the pegmatite. It ranges from a 0.5-2m thickness. Large 15cm K-feldspar crystals and cleavelandite pods are localized, with pocket development occurring near cleavelandite. Massive green apatite is also localized in this zone (Fig. 9). The apatite displays a pattern similar to exsolution lamellae in feldspar, with alternating bands of white, porous material and more green vitreous sections. Dark green/black euhedral gahnite is found in this zone and displays

some interesting morphological differences. Crystals are homogenous and typically covered with an overgrowth of muscovite.

Garnets in the blocky feldspar zone are euhedral, 2-4 cm in diameter, homogenous and generally free of inclusions. Tourmaline is uncommon and seen partially replaced by muscovite. Columbite is rare and typically found in association with cleavlandite.

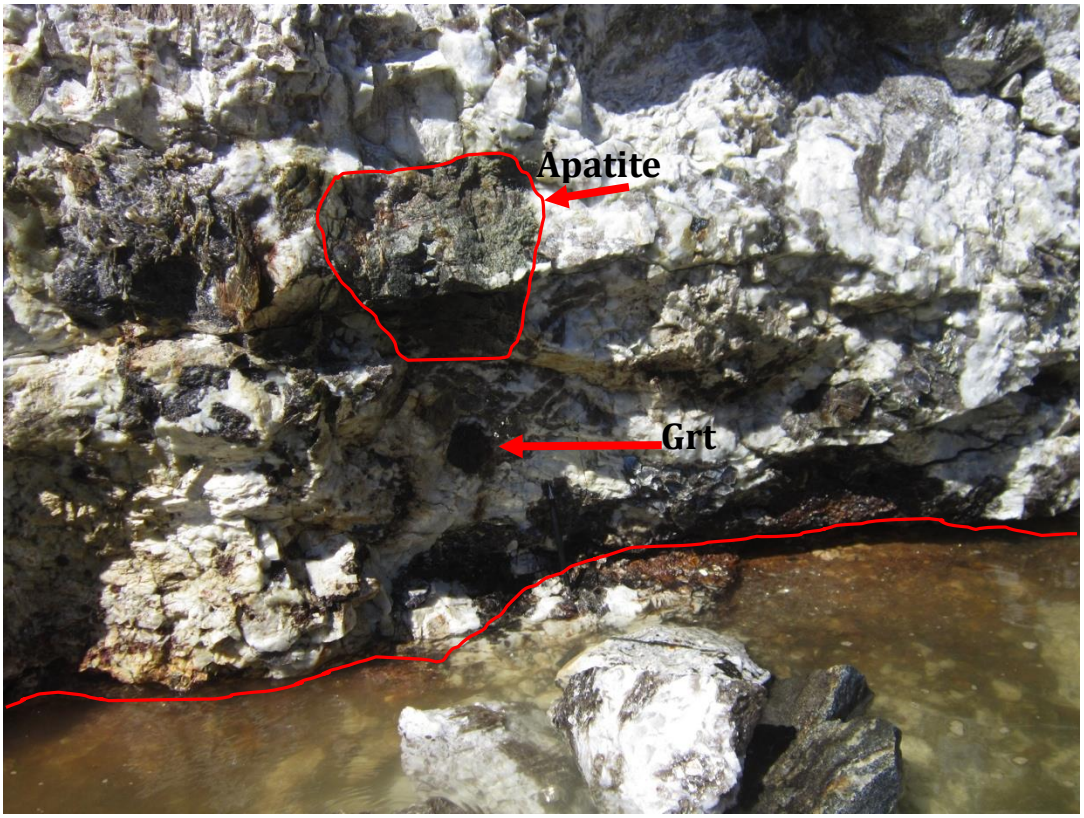

Figure 9: Apatite in massive form in the blocky feldspar zone of The-Hole-In-The-Ground (outlined in red). Also note 3cm garnet crystal beneath and red line marking boundary of the garnet line. Pencil is beneath the garnet for scale.

T.H.I.T.G. prospect:

A small (3x1.5x2m) prospect is located between the Wade and T.H.I.T.G. quarries. The bench of the pit is entirely garnet line. Miners had practiced what they had learned from their past experiences and opted not to mine below it. The line is thicker than reported in the Pulsifer, but thinner than in T.H.I.T.G. The mineralogy is similar to that found in T.H.I.T.G. However, the hanging wall portion containing biotite is absent, likely due to erosion.

The Bennett Pegmatite:

The Bennett quarry is a well-documented, highly evolved, miarolitic pegmatite. The dike intrudes amphibolite grade metapelites of the CMB, striking E-W and dipping ~70° on average (Wise and Rose, 2000). It is unique in comparison to many of the other Oxford County pegmatites in that there is an aplitic unit associated with the intrusion, texturally like what is described at the Himalaya pegmatite in San Diego, CA (Webber et. *al* 1997, Foord, 1997). There is some controversy over the origin of the aplitic portion; however, there has not yet been a study dedicated to understanding its genetic relationship with the pegmatitic portion of the dike. The aplite is assumed to represent an early stage in the crystallization history.

The size of the aplite is interesting as it is exceedingly large compared to other similarly described pegmatite-aplite systems found worldwide, but it's textural and mineralogical features also set it apart from any other pegmatite in the area. It is equigranular, predominantly consisting of quartz and plagioclase with accessory biotite and subhedral garnet grains. Large ≤3cm black tourmaline phenocrysts, with poikilitic

quartz grains (≤1mm) occur in the aplite. Similar poikolitic tourmaline and aplitic textures have been reported from other nearby quarries/exposures; Westinghouse quarry (Wise and Brown) and Streaked Mountain (Wise and Rose) respectively.

The Havey:

The Havey quarry is located in Minot, Maine about 2km due south of the Western Mt. Apatite quarries. The pegmatite is a highly evolved, rare-element, cavity bearing pegmatite with a complex-multi-zoned internal structure (Roda-Robles *et al.* 2011). It is currently mined for gemstones and mineral specimens. The dike intrudes amphibolite grade schist and is cross-cut by multiple mafic dikes. The attitude of the dike is difficult to constrain with its current exposure.

The pegmatite contains four texturally distinct outer zones, to include quartz, plagioclase, K-feldspar, plagioclase, mica (biotite and muscovite), tourmaline (schorl dominant) and garnet. The core is the most mineralogically complex portion of the dike. It includes all mineral species found in the outer zones, but shows a striking enrichment in Li (lepidolite and montebrasite), P (Fe-Mn phosphates including apatite, hydroxyl-herderite), Be (beryl) and rare pollucite. Columbite, cassiterite and pink/green tourmaline (gem quality) are also found in the core.

Schorl pods are localized, aligning in the intermediate zone of the dike (Fig. 10) and contain tourmaline crystals ≤15 cm in diameter intergrown with very coarse grained graphic feldspar and quartz. Euhedral garnet crystals ≤3 cm are found amongst these boron rich regions, but do not constitute and distinct garnet line. However, garnet samples were

analyzed from this 'schorl line' to compare to the other garnet line fabrics in this study. Muscovite is a common accessory mineral in this portion of the dike as well.

Figure 10: Aligned clusters of schorl in the intermediate zone of the Havey. A mafic dike is seen cross-cutting the pegmatite at the right of the photograph.

The Tamminen Quarry:

The Tamminen quarry is located in Greenwood, Maine, is a single pegmatite with a near vertical dip, striking E-W. It intrudes a Silurian aged medium grained pelitic schist and calc-silicate rock sequence. Country rock has a near vertical dip and the pegmatite is oriented concordantly. The pegmatite is pocket bearing and Li-rich containing petalite, lithian micas, spodumene, montebraisite and elbaite. Pollucite and lithiophilite also occur at this location. Some country rock xenoliths occur in the pegmatite wall zones. The slabs are rounded and commonly surrounded with rings of garnet and likely represent partial digestion of the xenolith (Fig. 11)

Figure 11: Country rock – pegmatite contact, note rounding of country rock and abundant garnet surrounding it in the pegmatitic portion.

The garnets stringers are more or less discontinuous and occur near the wall zones of the pegmatite in blocky perthite (Fig. 12). Garnets are (≤0.75cm) and commonly associated with muscovite and schorl.

Figure 12: Two separate discontinuous garnet and tourmaline stringers at the Tamminen quarry marked with red arrows.

The Emmons:

The Emmons pegmatite is located in Greenwood, ME along the south-eastern slope of Uncle Tom Mountain. The pegmatite is gently dipping to the east 40°, striking N-S and intrudes a **%$%$#**The pegmatite is highly evolved with abundant Ta-species, pollucite and Li- phosphates.

A localized garnet line is exposed along the footwall side of the dike in the intermediate zone (Fig. 13). The garnets are 1cm or less in diameter, euhedral to subhedral and are deep red colored. The garnets are accompanied by ≤4cm (c-axis) schorl crystals that are predominantly euhedral, black in color and at times poikioltically include anhedral quartz grains. The matrix is blocky plagioclase feldspar and anhedral gray quartz.

Figure 13: Section of the garnet line at the Emmons Quarry. Yellow arrow and chisel point to the feature.

Methods:

Multiple garnet line samples, complete with matrix, were collected along strike from the Mt. Mica and Western Mt. Apatite (T.H.I.T.G, T.H.I.T.G prospect and Pulsifer) quarries. Garnets from similar line textures were collected from the Tamminen, Havey, Emmons and Bennett quarries. T.H.I.T.G and Pulsifer quarries provided the necessary exposures allowing for garnet sampling from the hanging wall and inner blocky feldspar zones apart from the defined garnet line, which is an outer intermediate and lower portion of the dike. The line at Mt. Mica and garnets from the Emmons and Havey quarries are located in the outer intermediate, foot-wall portions of their respective pegmatites. The Tamminen is the only location where the garnets appear to be close to the wall zone, near margins of the schistose country rock.

Pieces of the samples from all locations were cut and generally encased in epoxy, ground and polished to 0.3 microns for analysis at the University of New Orleans by scanning electron microscopy (SEM) and electron microprobe (EMPA). These sections were chosen for analysis based on their apparent mineralogical content (garnet, feldspar, black tourmaline, muscovite, biotite, columbite, zircon and gahnite).

Dark fracture-filling micas from garnets at Mt. Mica were carefully handpicked, pulverized and digested in a HF solution for Directly Coupled Plasma Mass Spectrometry (DCP) analysis to estimate Li_2O content.

Several rock sections were sent to Applied Petrographic Services, Inc. where they were made into thin sections. These were used to correlate petrographic textures with microprobe analysis.

SEM:

Scanning electron microscope analyses used an AMRAY 1820 digital SEM (Fig. 14). Operating conditions included an accelerating voltage of 20kV, 18 mm working distance, ~15 degrees. Samples ranged from single garnet crystals to complete matrix sections (2.5 x 4.5cm) and were ground, polished and coated with 250 Å of carbon prior to analysis. Qualitative spot analysis, line scans, back-scattered electron images collected at 2048x2048 pixels, and X-ray maps collected at 1048x1048 pixels were obtained with the SEM. An Iridium integrated software package by IXRF systems was used for the acquisition of all data and images.

Figure 14: AMRAY 1820 digital SEM at the University of New Orleans.

EMPA:

Electron microprobe analyses were carried out with an ARL-SEMQ instrument (Fig. 15). Acceleration voltage of 15kV and a beam current of 15nA with 30 second count rates and a beam size of 2μ was used for garnet, feldspar, micas, tourmaline, pollucite and phosphates. Background was determined by MAN (mean atomic number). The peak standards for these species included: Albite (Si K_α, Al K_α, Na K_α), Andalusite (Si K_α, Al K_α), Barium sulfate (Ba L_α), Cerro de Mercado apatite (Ca K_α, F K_α, P K_α), Clinopyroxene (Si K_α, Ca K_α, Fe K_α, Mg K_α, Ti K_α), Fayalite (Si K_α, Fe K_α), Fibbia adularia (Si K_α, Al K_α, K K_α), Fluortopaz (Al K_α, F K_α, Si K_α), Plagioclase An_{50} (Al K_α, Ca K_α, Si K_α), Pollucite (Cs L_α), Rhodonite (Mn K_α, Si K_α), Rubidium Leucite (Rb L_α), Strontium sulfate (Sr L_α).

Zircon, Nb/Ta oxides, cassiterite, tungstates, xenotime and monazite required operating conditions; 20kV accelerating potential, a beam current of 20nA and 30 second count times with a beam diameter of 2μ. Background was determined by MAN. Peak standards for these minerals included: Bismuth germanate (Bi M_α), synthetic HfO_2 (Hf K_α), Hematite (Fe K_α), Manganotantalite (Mn K_α, Ta M_α), Rutile (Ti K_α), Stibiotantalite (Sb L_α), synthetic ThO_2 (Th L_α), Tin (IV) oxide (Sn L_α), synthetic UO_2 (U L_α), yttrium niobate (Nb L_α), Zirconium (IV) oxide (Zr L_α). Additional standards for xenotime and monazite include: synthetic $REEPO_4$ (La, Ce, Pr, Nd, Sm, Eu, Gd, Dy, and Yb L_α) and Y PO_4 (Y L_α).

Figure 15: ARL-SEMQ electron microprobe at the University of New Orleans.

DCP:

Select dark mica grains were extracted from single garnet crystals from Mt. Mica. Samples were crushed, sieved and handpicked and analyzed for a bulk Li_2O with the Directly Coupled Plasma Mass Spectrometry unit (Fig. 16)

Figure 16: Beckman Directly Coupled Plasma Mass Spectrometry unit.

***Textural Descriptions*:**

Garnet line petrography; megascopic images of the garnet line from each quarry has been shown in the previous sections. The next segment describes the many micro-inclusions found in the garnet line, reveals the chemical heterogeneity with BSE imaging and X-ray maps and exposes the unexplored and complex textures encountered in the garnet line from each quarry.

Mt. Mica:

Photomicrographs of the tourmaline rims around garnet crystals display a distinct color transition (Fig. 17a). BSE (Fig. 17b) and false colored X-ray maps (Fig. 17c, d) highlight the compositional differences. The darker, proximal portions show relatively higher concentration of Fe compared to the distal portions, whereas Mn shows an opposite effect. The garnet crystal margin is often corroded what the tourmaline rim is present and the tourmaline rim often encapsulates sub-rounded fragments of garnet (Figs. 18a and b)

The garnets beneath a large altered pocket also have rimmed textures. However, there is a marked absence of tourmaline. Instead yellow-green micas and pyrite, arsenopyrite, and löllingite are found along the rims (Fig. 19a). Gypsum is also found within the micaceous overgrowths. The garnets show no change in composition, compared to garnets from elsewhere in the garnet line, despite having experienced extensive decomposition, which is apparent given their corroded and porous crystal margins and as well as areas along fractures (Fig. 19b). Blocky plagioclase in this area also has veins of sulfides filling in fractures.

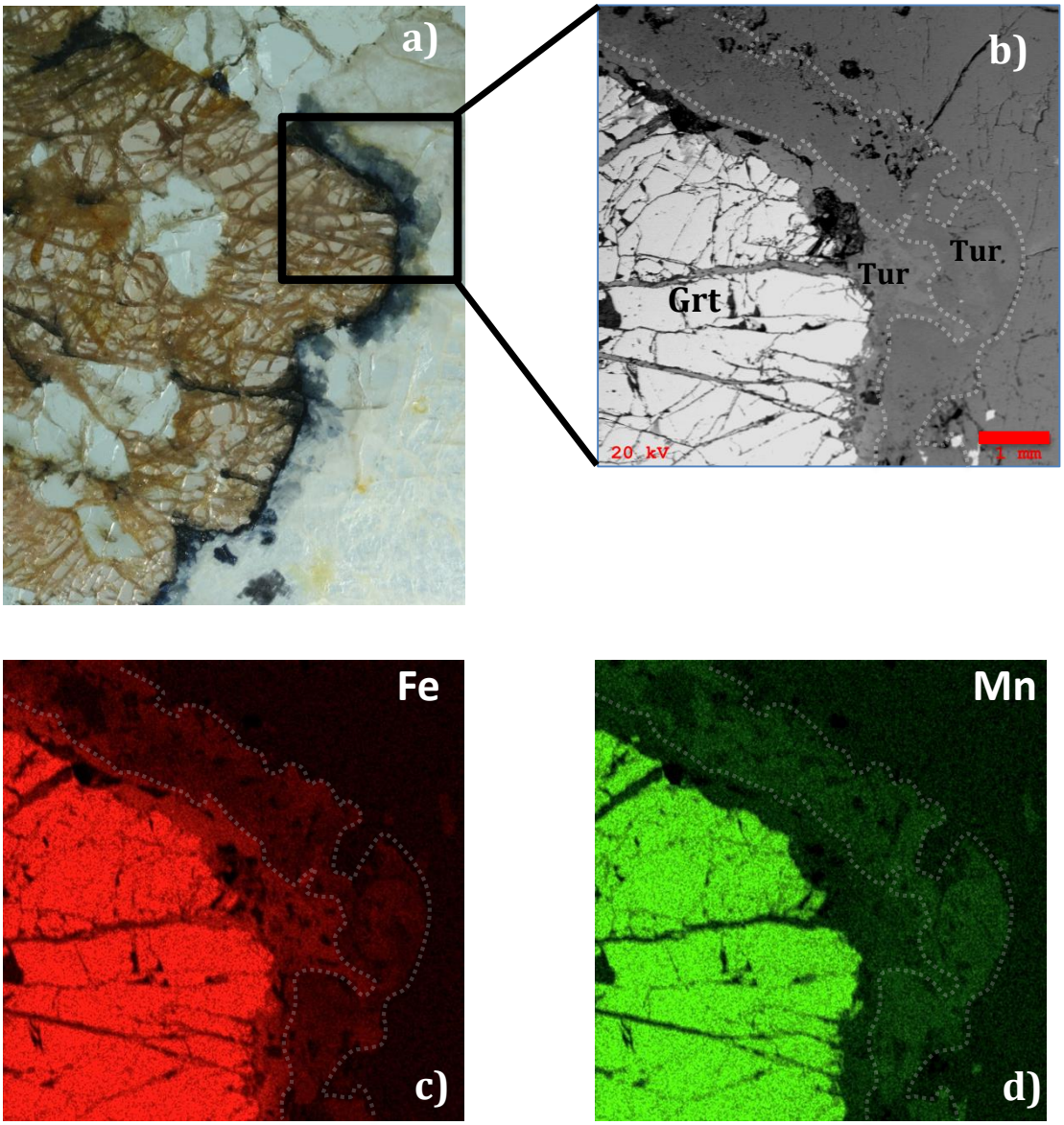

Figure 17: (a) Photomicrograph of a tourmaline halo along garnet crystal margin, note color zonation with black portions occurring closer to garnet crystal edge. Also note tourmaline filling fractured garnet along the margin. (b) Backscattered electron image of tourmaline (Tur) zonation (a division of two zones is outlined). (c) X-ray map of Fe content in red, note strikingly higher concentration in proximal tourmaline rim (zones from original image (b) are highlighted). (d) X-ray map of Mn content in green, note enrichment in distal tourmaline rim. (Zones from original image (b) are highlighted in (c) and (d)).

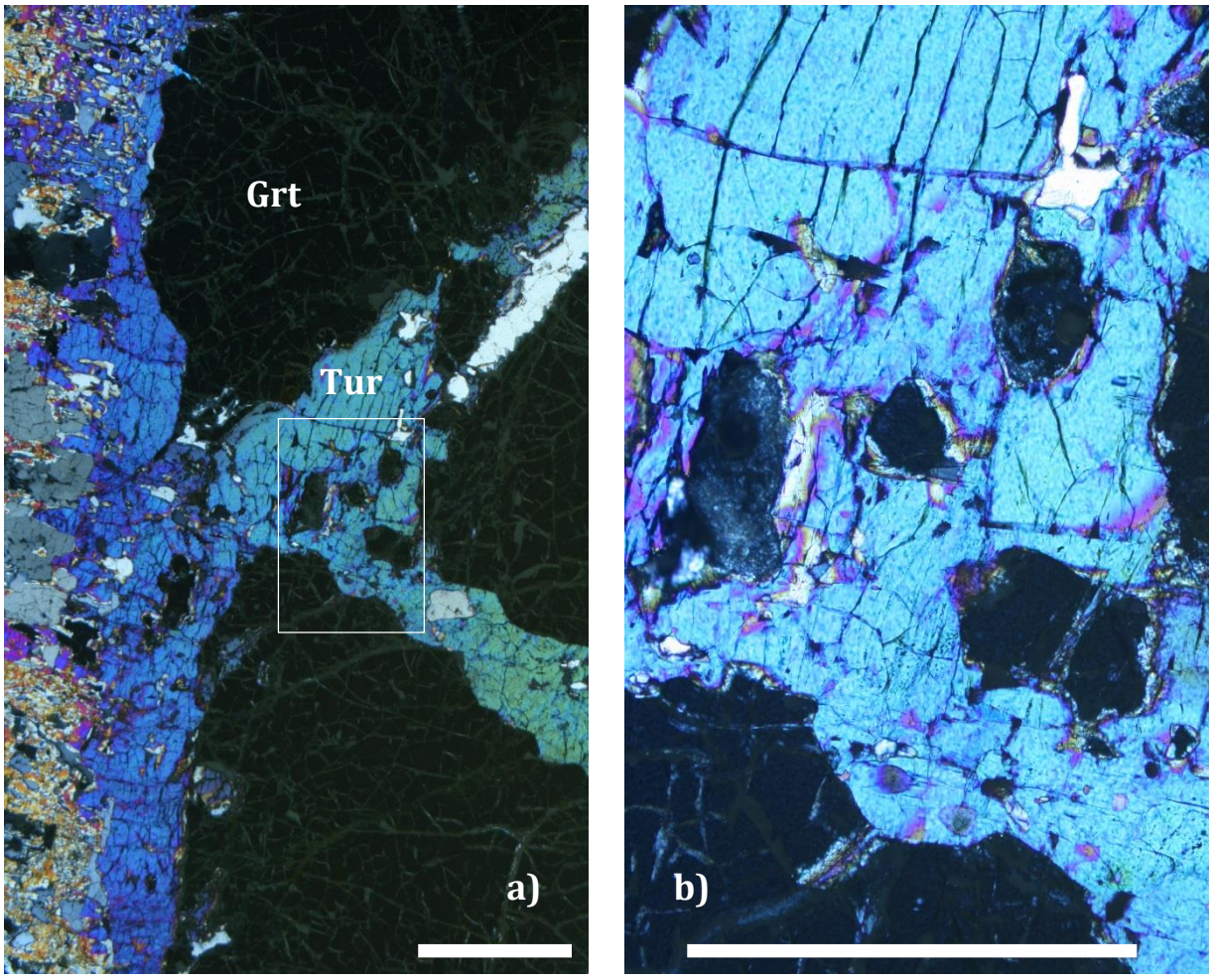

Figure 18: (a) Cross-polarized photomicrograph of a corroded garnet crystal margin with tourmaline rim and fracture filling 2.5x (white line is 1mm). Note the encapsulated, rounded garnet crystal fragments in host tourmaline. (b) Zoomed image of rounded garnet fragments in tourmaline 10x (white line is 1mm, area highlighted in previous image).

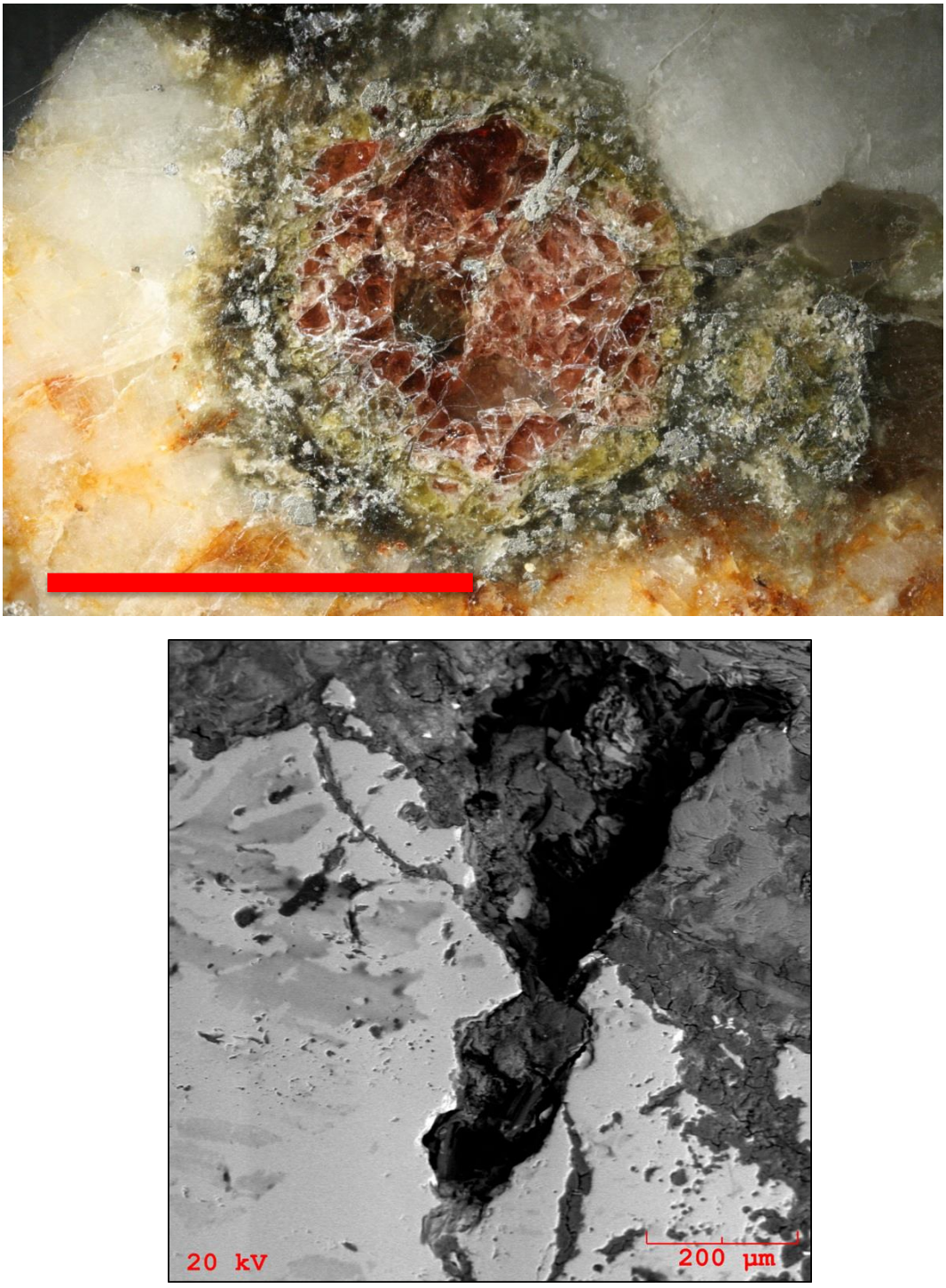

Figure 19: (a) Green/yellow muscovite and pyrite reaction rim around garnet, red line is 1cm. (b) Backscattered electron image of corroded garnet crystal margin.

Mica is also seen rimming the garnets with cleavage planes oriented parallel to the garnet crystal margin or as plumose/comb textures extending out from the garnet. At times the mica has appears to have replaced the albite matrix surrounding the garnet (Fig. 20). Similar zinnwaldite reaction rims have been described from lithian pegmatites in the Czech Republic (Němec 1983).

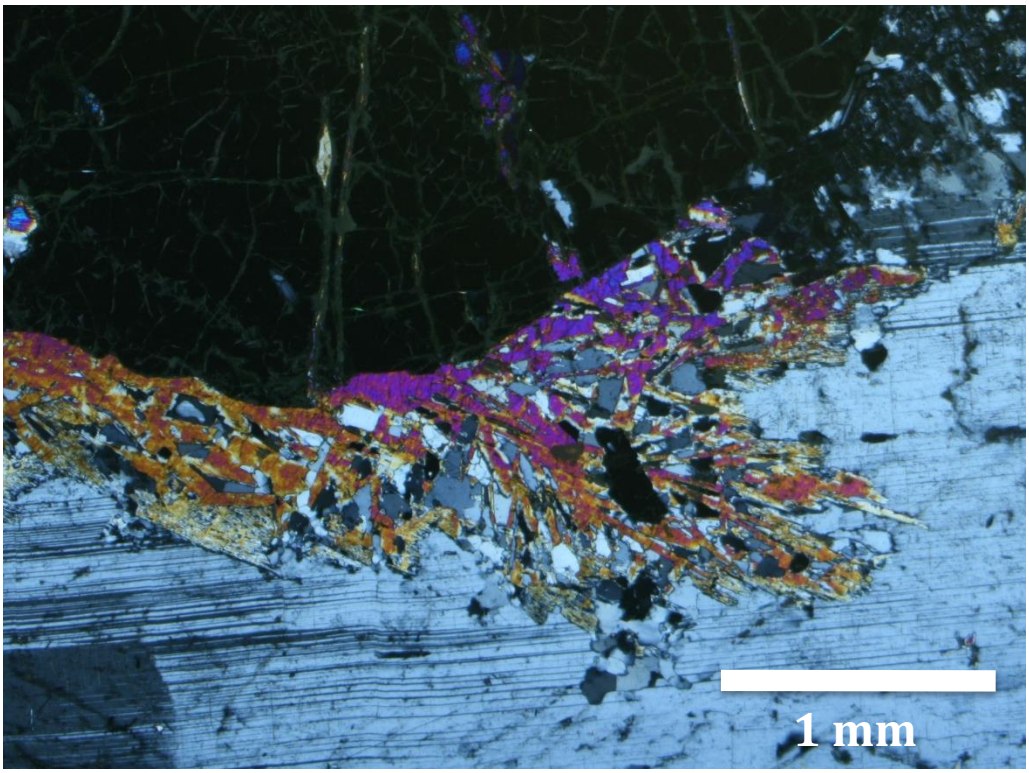

Figure 20: Cross-polarized photomicrograph at 5x. Digestion of albite by mica along garnet crystal margin. Quartz crystals entrapped in mica. Note kink banding in albite.

Garnet is characteristically highly fractured in these pegmatites. These fractures are mostly filled by quartz, mica or tourmaline, but combinations of these phases in a single fracture is not uncommon. When muscovite is present in the fractures, pollucite may occur. Pollucite crystallizes along mica cleavage planes (Fig. 21a & b), but may also be found as anhedral inclusions in garnet and as fracture fillings (Fig. 21c).

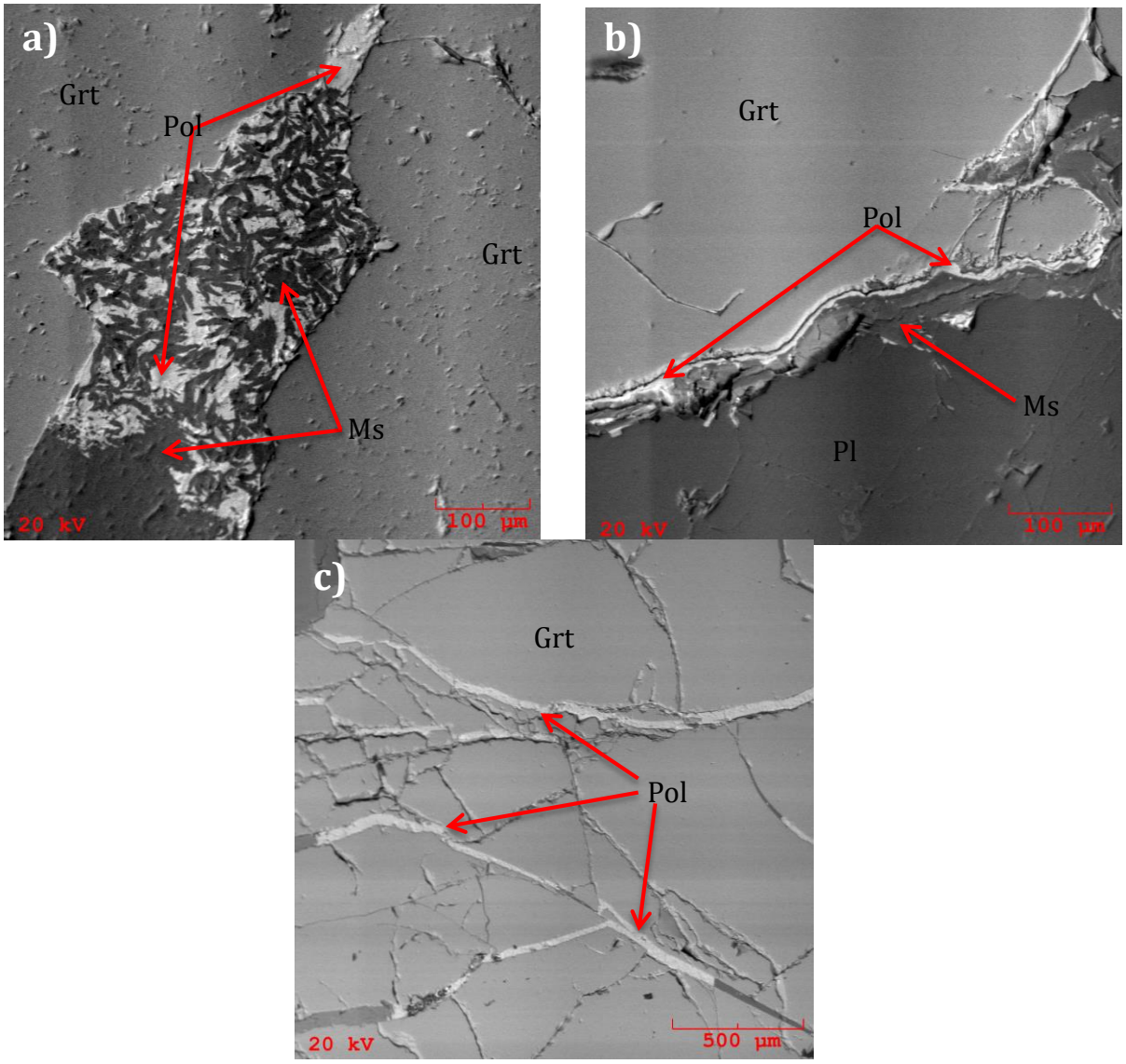

Figure 21: (a) Backscattered electron image of Pollucite (Pol) and muscovite (Ms) inclusion in garnet (Grt). (b) Pollucite following garnet crystal margin, muscovite is also present along rim of garnet. (c) Pollucite filling fractures in garnet.

Micrographic/myrmekitic intergrowths of quartz and garnet are common within single garnet crystals. The intergrowths generally show no preferred orientation; however, there are cases where the quartz does follow fractures. Macroscopically, some garnets appear to be zoned, but closer imaging revealed it to simply be an overgrowth of myrmekitic quartz and garnet surrounding a homogeneous garnet core (Fig. 22). Tourmaline intergrowths often mimic the myrmekitic texture just described. There appears to be a relation with Mn-enrichment in garnet near these Fe-dominant tourmaline inclusions, much like depletion halos. The mosaic (Fig. 23) of false color imagery clearly show the patterns of Mn-enrichment near the inclusions and homogeneity where they are absent. BSE did not reveal any compositional zoning between core and rim portions of single garnet crystals. The only example of noticeable heterogeneity is within the myrmekitic textures.

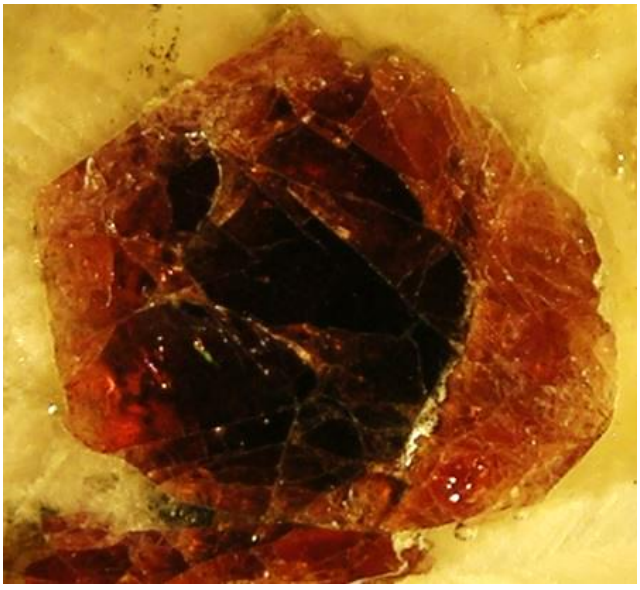

Figure 22: Micrographic quartz and garnet overgrowth on homogenous garnet core, field of view is 1 cm.

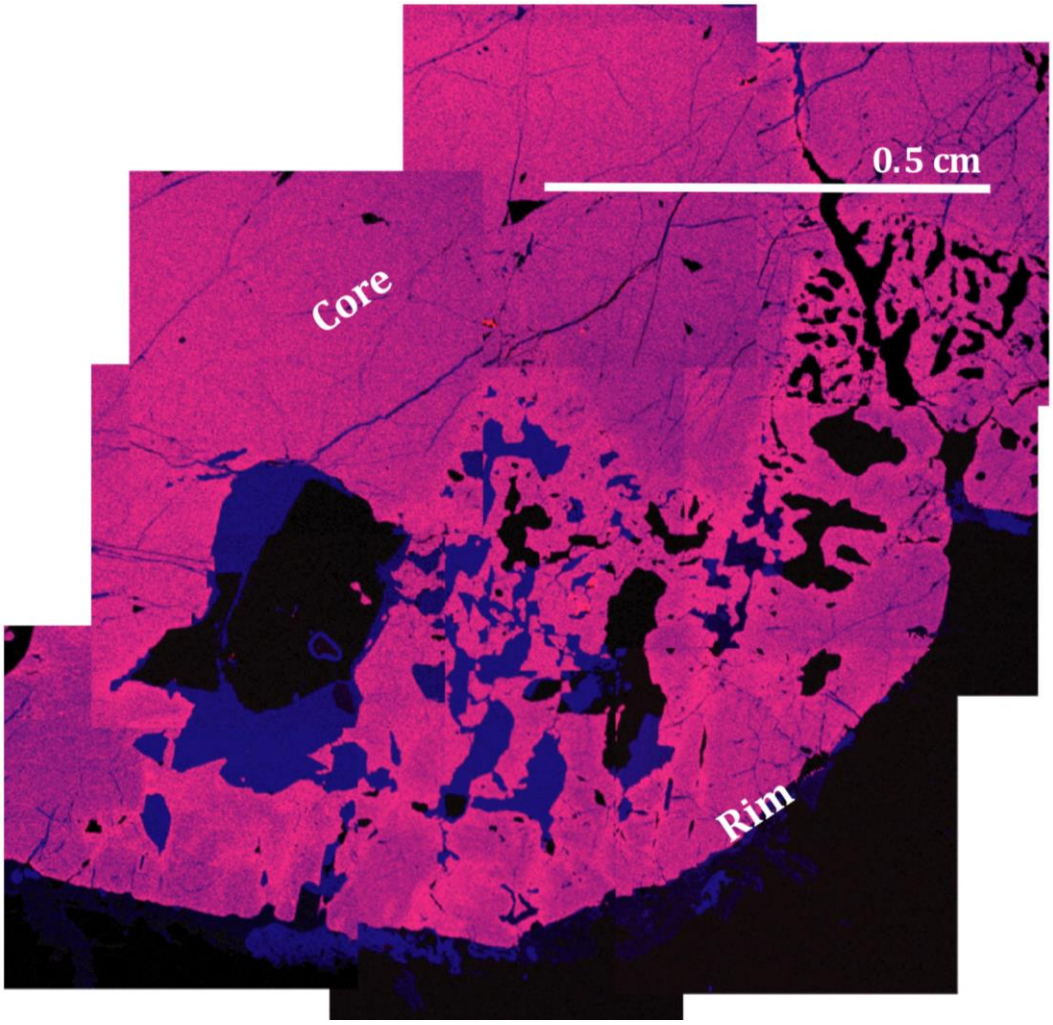

Figure 23: Mosaic of elemental X-ray maps of a garnet crystal from core (upper left) to margin (bottom of image). Mn-red, Fe-blue. Note increased Mn concentration near myrmekitic quartz (black portions within garnet) garnet intergrowth, whereas core is more homogenous with respect to Fe and Mn. Solid blue portions are schorl, note slight rimming in bottom of photo, as well as intergrowths within garnet crystal.

The garnets in the garnet line host a range of mineral inclusions. Quartz, schorl, muscovite, zircon, uraninite, xenotime, Nb/Ta oxides and löllingite are the most abundant species with rare biotite, cassiterite and wodginite. Occurrence and abundance of any inclusion(s) varies with each sample along strike of the pegmatite. Because these are interpreted as co-crystallizing phases, the presence or lack of a particular mineral phase is a potential indicator of localized melt enrichment in a micro-environment.

Zircon is found as inclusions in the garnets, feldspars and tourmaline. It is commonly associated with uranium phases (uraninite and other unidentified uranium minerals), which have either crystallized adjacent to or are present as inclusions in the zircon host. The zircons range in size (≤4 mm) and are concentrically zoned, with highly chaotic metamict cores and the prominent radial fracturing in the host mineral (Fig. 25a-c). Some zircons, however, show no zoning. Uraninite range in size from 0.1 to 0.5mm and occasionally display complex compositional internal heterogeneity in BSE and often coinciding with fracturing cracks and corroded crystal margins (Fig. 24). Microlite is rare (≤20 μm), but found in muscovite and feldspar.

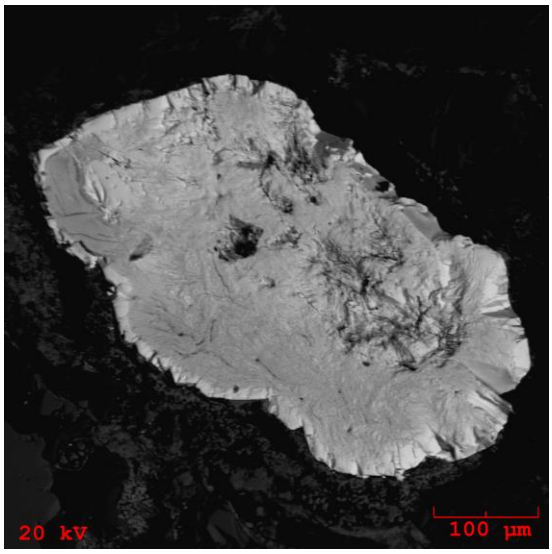

Figure 24: Backscattered electron imaged of zoned uraninite crystal, note corroded crystal margin and core.

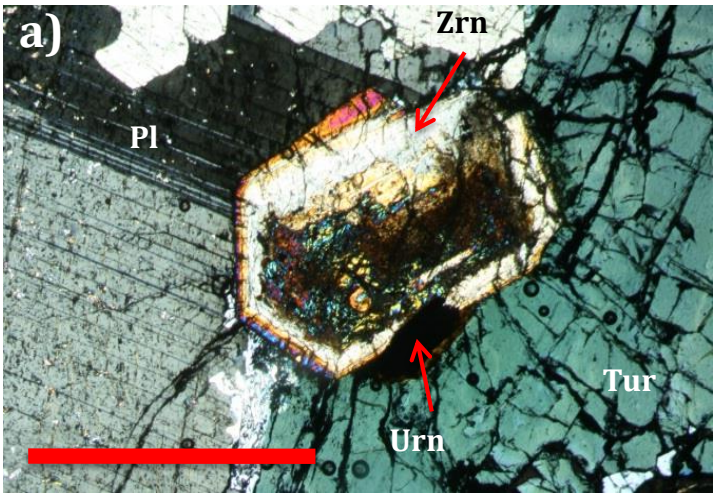

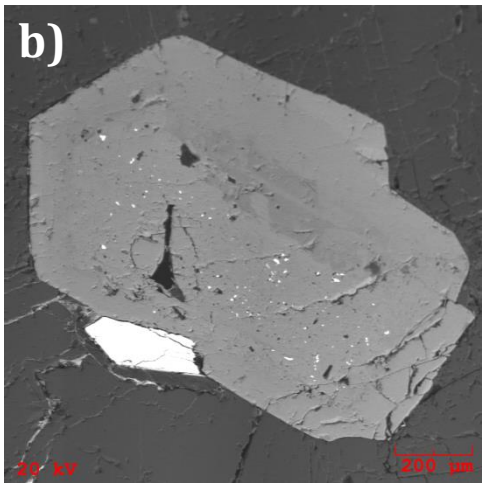

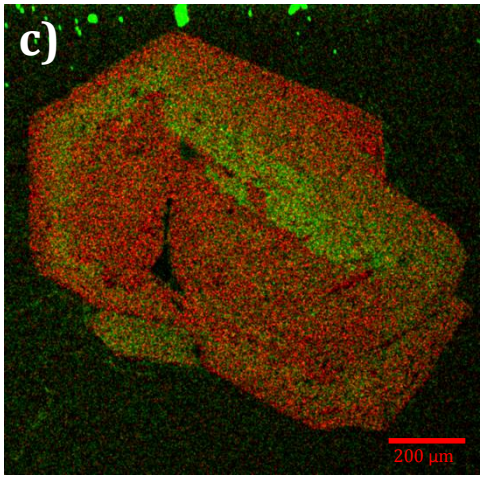

Figure 25: (a) Cross-polarized photomicrograph of a zoned, metamict zircon (Zrn) (left, red line is 1mm). Matrix is plagioclase (Pl) feldspar and tourmaline (Tur), the opaque in cpx is uraninite. (b) The same crystal in backscatter electron imaging, (c) SEM X-ray map; red-Zr_{Ka}, green-Ca_{Ka} (Ca appears in uraninite (Urn) due to U_{La} overlap with Ca_{Ka}). Note in (b) radial fracturing in outer zone of zircon and in (a) fractures extend out into surrounding matrix.

Other minerals found in the garnet line are: apatite inclusions (≤250 µm) within the blocky plagioclase feldspar, rare-cookeite among cleavelandite blades and apatite inclusions (≤60 µm). Monazite is extremely rare, but when present, it is green with a vitreous luster (Fig. 26a & b), the largest crystal being 0.5mm was rimmed by pyrite. Xenotime inclusions (≤90 µm) are found in garnet, tourmaline and feldspar and may host uranium-bearing species.

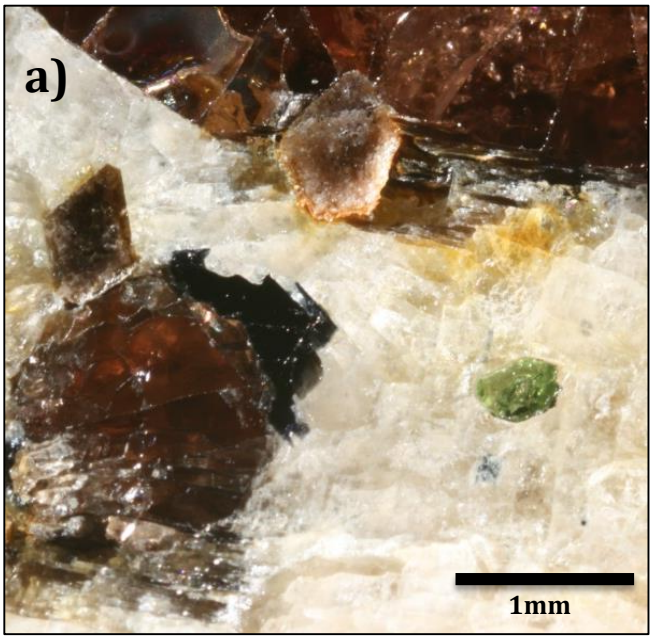

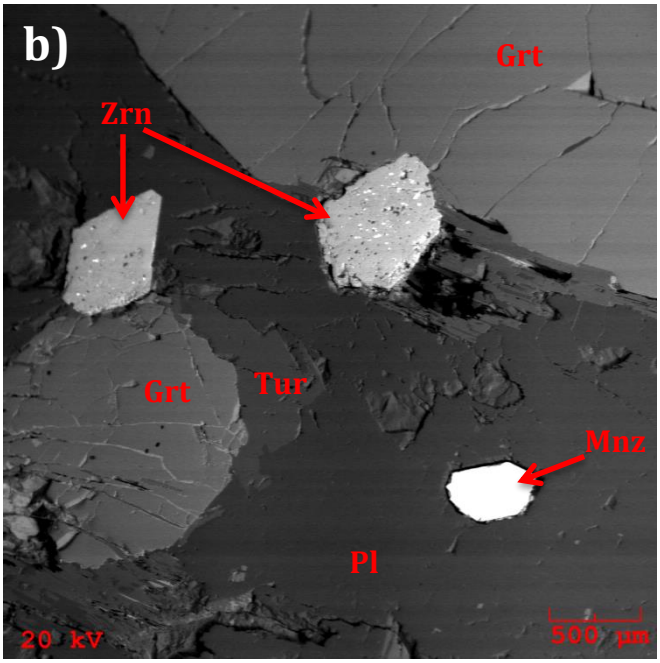

Figure 26: (a) Green monazite crystal in plane light, note translucent green mineral. Zoned and metamict zircons also field of view. (b) Same image in backscatter, high-Z elements in the monazite give it the white appearance. Zircons contain small uraninite inclusions, and pollucite fills some fractures within the smaller garnet crystal (lower left of image, pollucite fills are the white veinlets).

Mt. Apatite:

BSE imaging and photomicrographs reveal a range of fracture fillings and inclusions found within the garnets in all sample areas at Mt. Apatite. Muscovite and quartz are the dominant examples of fillings. Prismatic euhedral zircon (≤1 mm) grains are commonly encountered in garnet, often hosting uranium inclusions. Micro-inclusions of xenotime (≤30 μm) can be found in garnets and feldspar. Thorite is also commonly encountered inclusions.

Monazite (≤1.25 mm), when present, is metamict with radial fracture patterns and corroded crystal margins. The internal portions of crystals may also appear porous and commonly host Th-bearing species and apatite inclusions (Figs. 27a, b, c and d). Subhedral monazite is found in the hanging wall of the T.H.I.T.G as corroded, ≤700 μm grains. In the core zone of T.H.I.T.G it is found within the massive apatite pod as ≤30 μm grains and in Columbite as (≤5 μm) grains. Columbite from the core zone is homogeneous in BSE while the apatite is quite porous.

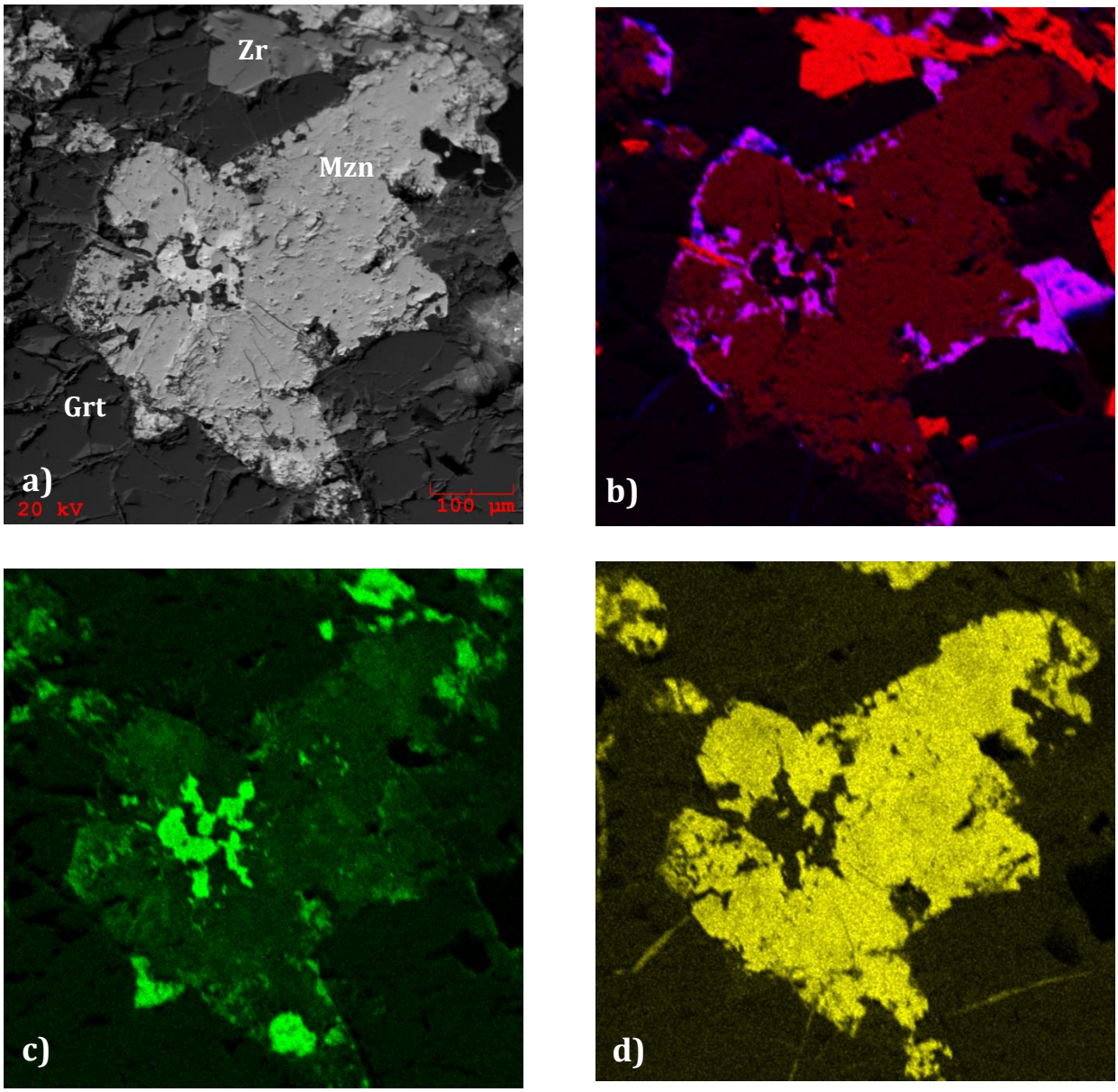

Figure 27: (a) Backscattered electron image of a metamict monazite (Mzn) in garnet (Grt) matrix. Thorite and apatite occupy the core portion of the radial fractures; apatite overgrowth along the monazite rim. (b) X-ray map: dark red-phosphorus and zirconium due to overlap of P_{Ka} and Zr_{La} spectral lines, blue- calcium (apatite in purple), zircons (Zrn) appear brighter red. (c) Green-Th showing where thorite is present. (d) yellow-Ce to highlight the monazite, note veins extending into the garnet matrix.

Bennett:

Garnets (≤750 μm) grains in the aplite are subhedral and show no compositional zoning in BSE. The aplite unit hosts few exotic accessory minerals. Euhedral zircon (≤40 μm) grains, löllingite (≤230 μm), apatite (≤200 μm) and monazite (≤175 μm) are the few examples.

Emmons:

Garnets and schorl show no compositional zoning in BSE images. Complexly zoned Nb-Ta oxides (≤60 μm) are occur as micro inclusions within the matrix hosting the garnet (Fig. 28a); cassiterite (≤120 μm) is associated with these species (Fig. 28b). Euhedral metamict zircon (≤375 μm) and subhedral monazite (≤70 μm) grains are present in the samples as well. The feldspar matrix displays an antiperthitic texture.

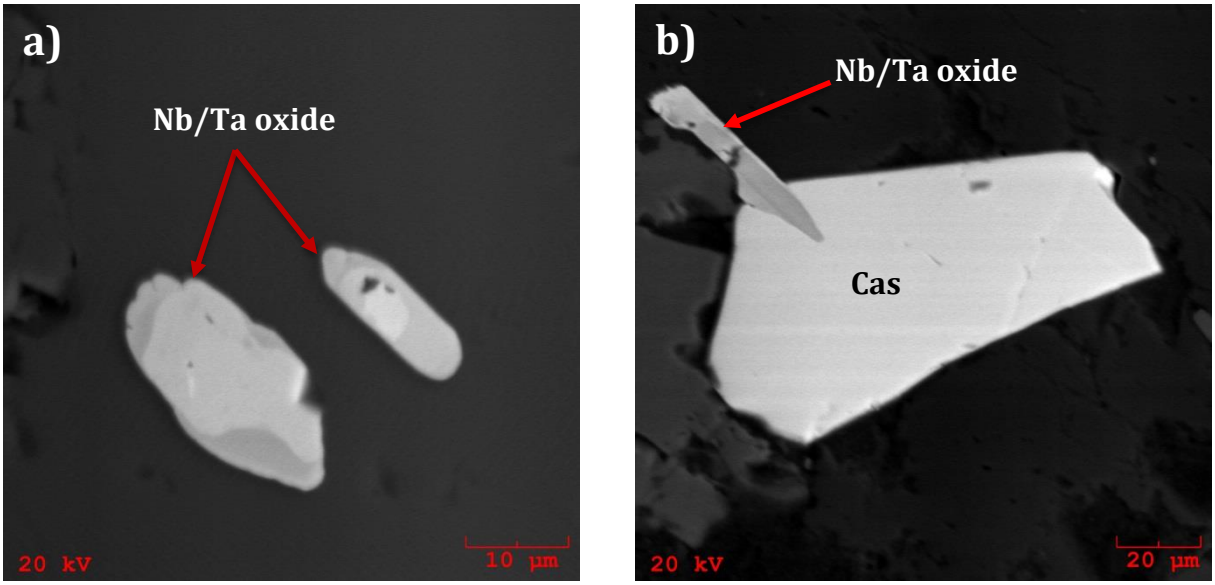

Figure 28: (a) Backscattered electron image of two zoned Nb/Ta crystals from the Emmons. (b) Zoned Nb/Ta crystal penetrating a cassiterite (Cas) from the Emmons.

Havey

Garnets do not display compositional zoning in BSE imaging. Pollucite is associated with the garnet and muscovite, similar to the occurrences found in the Mt Mica garnet line (Figs. 29a, b and c). Elongated blebs of pollucite predominantly occur within the mica following along the cleavage planes, but it is also seen crystallized within the nearby garnet (see image). Euhedral metamict zircon (≤3 mm) grains are found in garnet, feldspar and quartz. Biotite (≤50 µm) and prismatic, subhedral xenotime (≤50 µm) crystals are also present as micro inclusions within the Havey garnets. Anhedral apatite grains (≤125 µm) also occur in the feldspar.

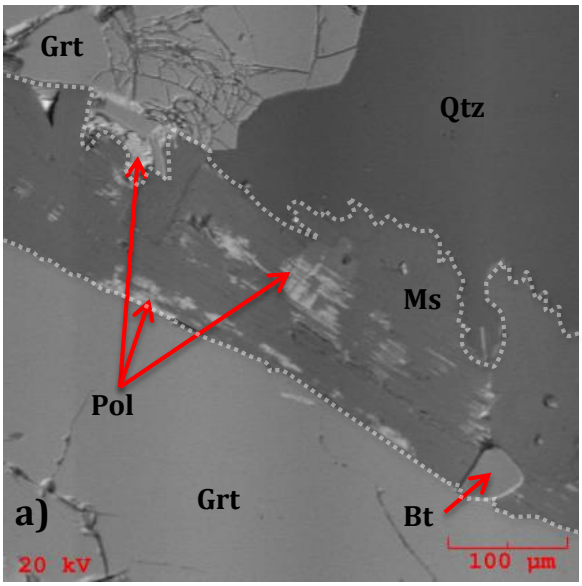

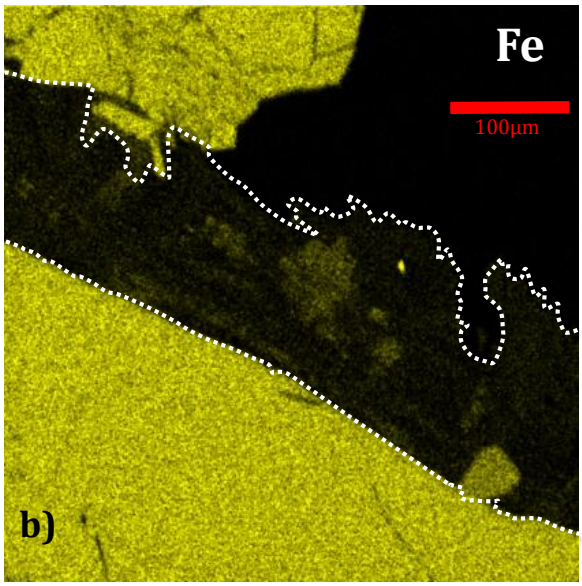

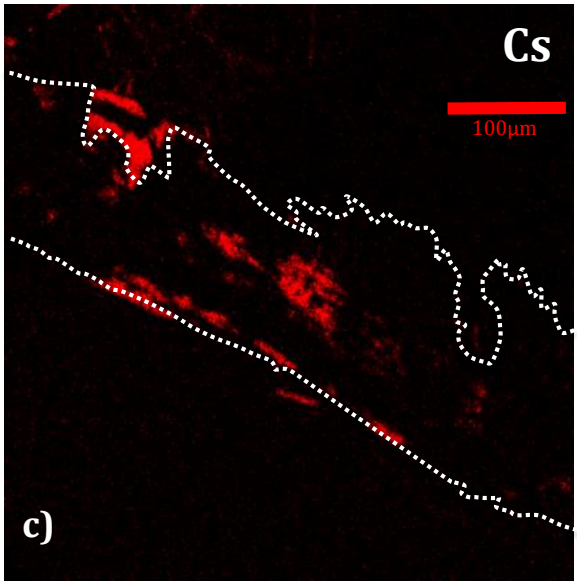

Figure 29: (a) Backscatter electron image of a sample from the Havey quarry, garnet (Grt), quartz (Qtz), muscovite (Ms), biotite (Bt), pollucite (Pol). Note the muscovite area highlighted by the white dotted lines, and their correlation with (b) and (c). (b) False color X-ray map image showing relative Fe content in yellow. Note the presence of Fe in pollucite. (c) False color X-ray map of Cs in red, note the abundance in the mica with minor occurrences in the garnet and quartz.

Tamminen:

Subhedral monazite (≤260 μm) grains are common micro inclusions. They are commonly corroded and highly porous, hosting Th-bearing species (≤15 μm) and apatite (≤25 μm) and are at times rimmed by iron oxides. Anhedral xenotime (≤325 μm) grains are frequently porous and fractured and host apatite (≤5 μm) inclusions. Multiphase inclusions are not uncommon and host xenotime, monazite, thorite/thorogummite (?) and iron oxides (Fig. 30). Bastnäsite inclusions were also found within the garnet line boundary layer.

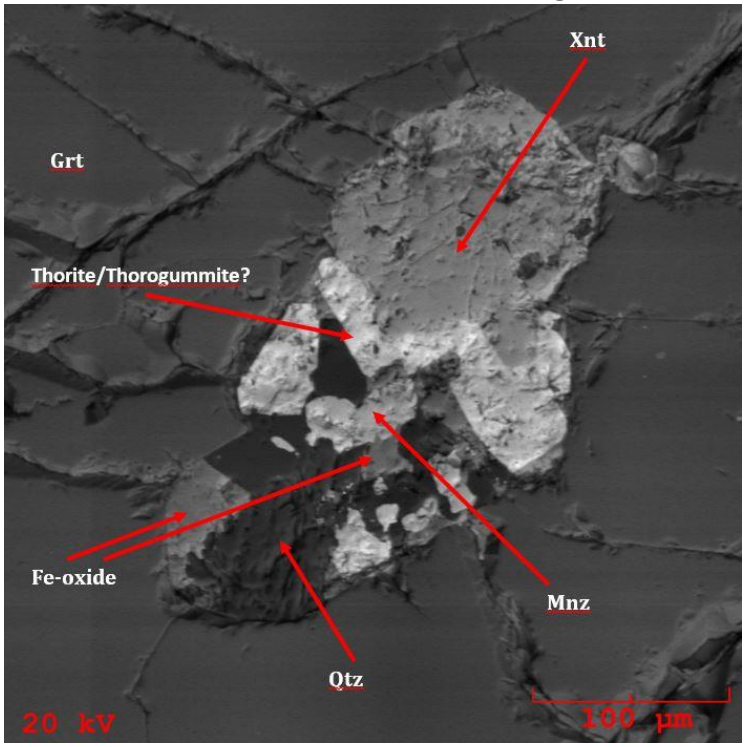

Figure 30: Backscattered photomicrograph of a multiphase inclusion from the Tamminen Quarry; Xnt-xenotime, Mnz-monazite, Grt-garnet, Qtz-quartz.

Results:

The following section is a report on the compositional characteristics of the associated minerals of the garnet line boundary layers within each pegmatite and was acquired by EMP and DCP analysis.

Garnet compositions fall within the almandine (Fe)-spessartine (Mn) series (Fig. 31 & 32 and Tables 1 & 2). The garnets from the garnet line in Mt. Mica show the greatest range within this solid solution (spess. 66.07- 38.12%) (Fig. 31). The most evolved compositions for garnets from within the Mt. Mica garnet line (i.e. those with the highest spessartine component) are found in garnet crystal fragments hosted by a secondary mineral phase within fractures of garnet crystals or along their intercrystalline boundaries (e.g. tourmaline rims).

Garnets from the line rock in the Bennett aplite also have a fairly wide range, 31.39-40.28% spess., whereas garnets from the garnet lines at the Mt. Apatite and Emmons quarries have tightly spaced compositions of 30.98-27.03 and 47.58-49.42% spessartine, respectively. Phosphorus and fluorine in garnets from the Mt. Mica garnet line reach 0.323 wt% P_2O_5 and 0.87 wt% F. Garnets from the garnet line at Mt. Apatite reach 0.948 wt% P_2O_5, whereas F is less than 0.023 wt%. Garnets from the lines rock in the Bennett aplite and garnets from the localized garnet boundary layer in the Emmons have the lowest concentrations; <0.126 wt% P_2O_5 and 0.35 wt% F.

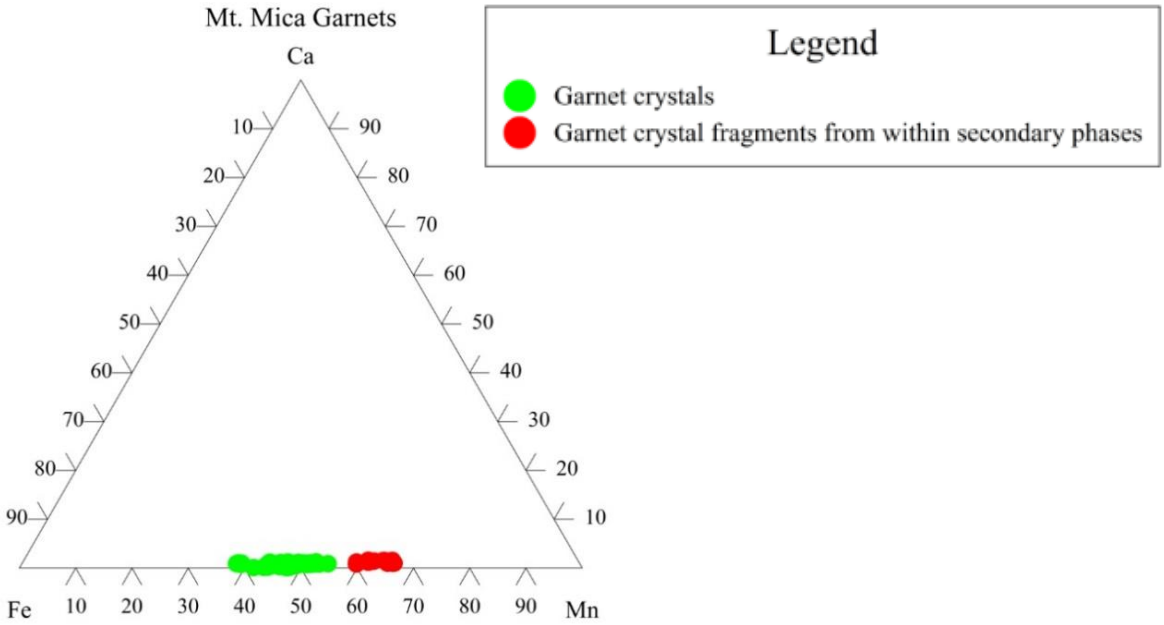

Figure 31: Almandine-Grossular-Spessartine ternary of garnets from the garnet line at Mt. Mica. The most spessartine-rich come from crystal fragments in secondary phases, i.e. tourmaline rims.

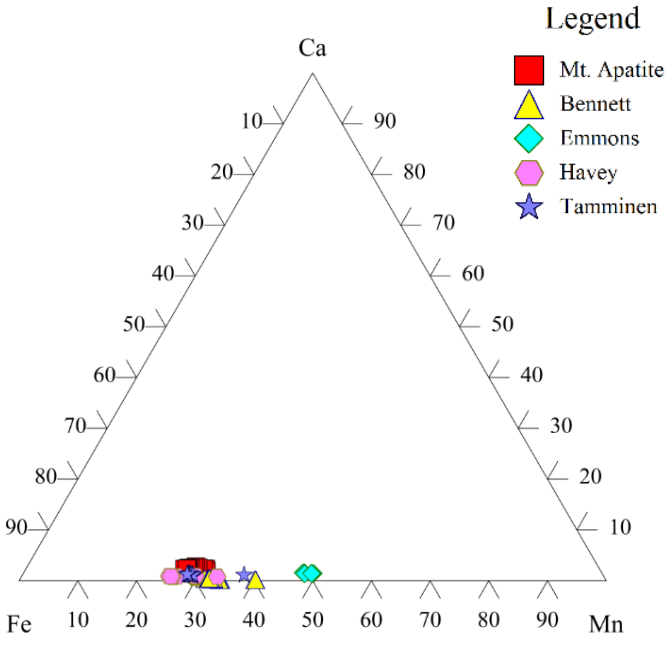

Figure 32: Almandine-Grossular-Spessartine ternary diagram, samples of garnet from garnet line boundary layers in each pegmatite are plotted based on atomic proportions.

Sample	MT2-3-a-2-2	MT2-3-a-2-3	MT6-1-a-4	MT6-1-a-5	MT1-2a-1	MT1-2a-2
P_2O_5	0.08	0.09	0.10	0.09	0.08	0.08
SiO_2	36.41	36.39	36.40	36.41	36.34	36.34
TiO_2	0.00	0.00	0.01	0.00	0.00	0.01
Al_2O_3	20.59	20.60	20.61	20.63	20.60	20.60
FeO	14.44	14.62	26.13	26.29	21.68	21.78
MnO	28.32	28.10	16.45	16.22	21.14	20.92
CaO	0.33	0.35	0.28	0.31	0.27	0.34
MgO	0.00	0.01	0.20	0.25	0.06	0.05
F	0.23	0.22	0.00	0.00	0.04	0.04
Subtotal	100.41	100.39	100.18	100.21	100.20	100.15
O=F	0.10	0.09	0.00	0.00	0.02	0.02
Total	100.31	100.29	100.18	100.21	100.18	100.14
X-site						
Fe	0.992	1.004	1.798	1.808	1.493	1.500
Mn	1.969	1.954	1.146	1.130	1.475	1.460
Ca	0.029	0.031	0.025	0.027	0.023	0.030
Mg	0.000	0.001	0.024	0.031	0.007	0.006
X-total	2.990	2.990	2.993	2.996	2.998	2.995
Y-site						
Cr	0.000	0.000	0.000	0.000	0.000	0.000
Al	1.992	1.993	1.999	2.000	1.999	1.999
Y-total	1.992	1.993	1.999	2.000	1.999	1.999
Z-site						
Si	2.989	2.988	2.995	2.994	2.992	2.993
Ti	0.000	0.000	0.001	0.000	0.000	0.001
Z-total	2.989	2.988	2.995	2.994	2.992	2.994
spss.%	65.868	65.375	38.613	38.117	49.308	48.819
grss.%	0.965	1.033	0.843	0.907	0.782	1.015
alm.%	33.167	33.592	60.544	60.976	49.910	50.166

Table 1: Representative microprobe analyses of garnet from the garnet line in Mt. Mica. Normalized to 12 oxygens

Sample	MA-14-1j-1	MA13-1-c-5	BT2-a-3	EM2-1a-4	HVY3-2-8	TM1-k-1
P_2O_5	0.08	0.95	0.02	0.10	0.04	0.07
SiO_2	36.82	36.71	36.48	36.45	36.30	36.27
TiO_2	0.01	0.02	0.00	0.00	0.00	0.00
Al_2O_3	21.18	21.20	20.41	20.98	20.46	20.50
FeO	28.75	28.30	28.19	21.75	30.28	30.78
MnO	11.80	11.98	14.57	20.82	12.73	12.11
CaO	0.57	0.82	0.06	0.38	0.32	0.43
MgO	0.45	0.41	0.12	0.21	0.03	0.02
F	0.00	0.00	0.00	0.02	0.03	0.02
Subtotal	99.65	100.38	99.85	100.72	100.19	100.21
O=F	0.00	0.00	0.00	0.01	0.01	0.01
Total	99.65	100.38	99.85	100.71	100.18	100.20
X-site						
Fe	1.969	1.916	1.948	1.487	2.090	2.124
Mn	0.818	0.821	1.019	1.442	0.890	0.846
Ca	0.050	0.071	0.005	0.034	0.028	0.038
Mg	0.054	0.049	0.015	0.026	0.003	0.003
X-total	2.891	2.858	2.987	2.988	3.012	3.011
Y-site						
Cr	0.000	0.000	0.000	0.000	0.000	0.000
Al	2.043	2.023	1.988	2.022	1.990	1.993
Y-total	2.043	2.023	1.988	2.022	1.990	1.993
Z-site						
Si	3.015	2.972	3.014	2.980	2.996	2.992
Ti	0.000	0.001	0.000	0.000	0.000	0.000
Z-total	3.015	2.973	3.014	2.980	2.996	2.992
spss.%	28.842	29.240	34.297	48.676	29.583	28.132
grss.%	1.753	2.539	0.167	1.133	0.938	1.275
alm.%	69.404	68.222	65.537	50.192	69.480	70.593

Table 2: Representative microprobe analyses of garnet from the garnet line boundary layer in Mt. Apatite, Bennett, Emmons, Havey and Tamminen quarries. Normalized to 12 oxygens.

There is a wide range of mica types within the garnet line at Mt. Mica. Micas present as fracture fillings within the garnets appear to be the most evolved types; F (0.44-0.62 apfu), Rb+Cs (0.09-0.153 apfu). Marchal *et al.* 2014 reported concentrations of Cs+Rb- <0.1 apfu and F content below detection limits from micas near the garnet line. The high F, Cs and Rb proportions recorded in this study were only reported from micas from the core regions in their study.

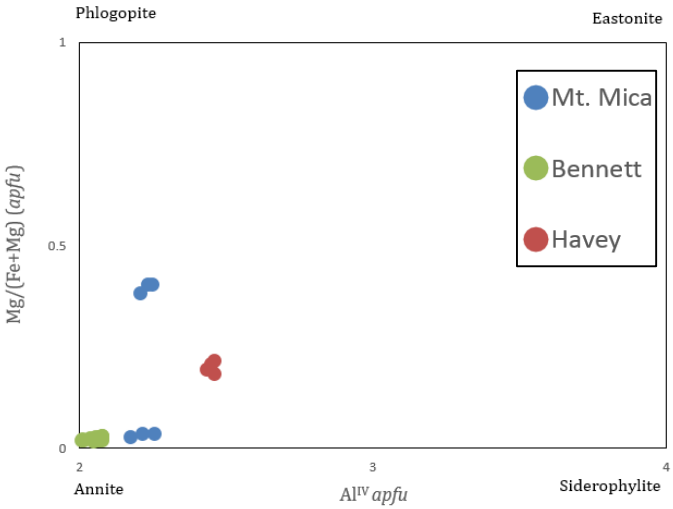

Figure 33: Biotite from the garnet boundary layers in Mt. Mica and the Bennett aplite and the schorl pod line at the Havey, from Deer *et al.* 1992

Mafic micas from the garnet line at Mt. Mica, the schorl pod line from the Havey and the garnet layers in line rock from the Bennett aplite plot within the annite/phlogopite field described by Deer *et al.* 1992 (Fig. 33). The biotites from the garnet line in Mt. Mica plot within two different areas, one with a higher phlogopite component. Whereas biotites from the intermediate zone hosting the schorl pod line in the Havey have the highest siderophyllite component.

DCP analysis provided a bulk Li analysis for dark micas (found within the fractures of garnets from the garnet line at Mt. Mica) of 2.62 wt% Li_2O, confirming the presence of Li in some of the Mt. Mica samples. This bulk analysis was used for Li content in all related EMPA samples of fracture filling micas within garnets from the garnet line at Mt. Mica (Figs. 34 & 35). Water (H_2O) was calculated based on ideal stoichiometry.

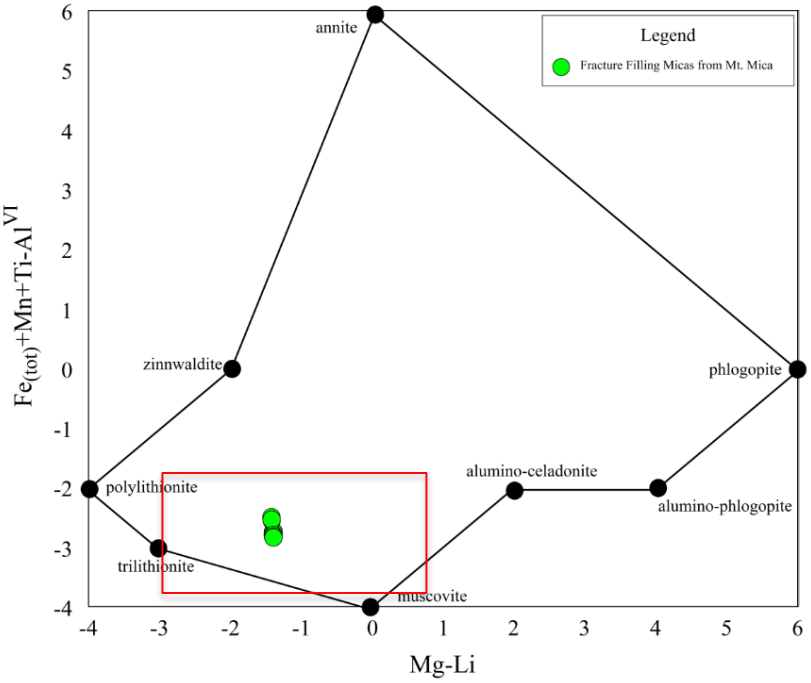

Figure 34: Compositional field of natural trioctahedral and dioctahedral micas with fracture filling micas from within garnets at Mt. Mica plotted. Red box highlights the field expanded in the next figure Tischendorf (1997).

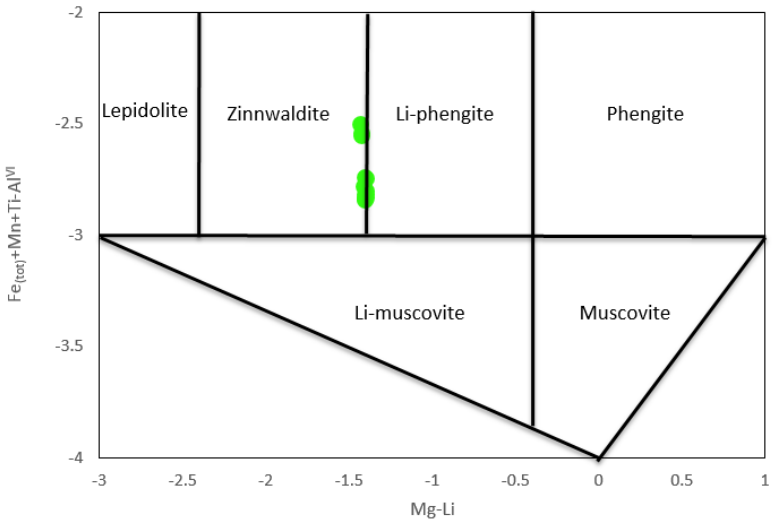

Figure 35: Expanded region (highlighted in red) from previous image of the fracture filling micas from within garnets in the Mt. Mica garnet line, plotting in the zinnwaldite field.

sample	MT4-1-b-1	MT1-1-f-2	MT1-1-h-3
SiO_2	45.21	45.39	45.39
TiO_2	0.17	0.11	0.08
Al_2O_3	32.46	32.68	32.90
FeO	3.87	3.56	3.63
MnO	0.32	0.32	0.34
MgO	0.10	0.09	0.08
CaO	0.03	0.04	0.03
Rb_2O	1.43	1.30	1.20
Cs_2O	0.44	0.24	0.38
Li_2O calc.	2.62	2.62	2.62
Na_2O	0.54	0.60	0.59
K_2O	8.34	8.56	8.60
H_2O calc	3.88	3.77	3.73
F	1.22	1.43	1.28
Subtotal	100.64	100.69	100.86
O=F	0.51	0.60	0.54
Total	100.13	100.09	100.32
apfu			
Si	6.086	6.094	6.093
Ti	0.017	0.011	0.008
Al	5.149	5.171	5.205
Fe	0.436	0.399	0.408
Mn	0.037	0.036	0.039
Mg	0.020	0.018	0.015
Ca	0.005	0.006	0.004
Rb	0.124	0.112	0.104
Cs	0.025	0.013	0.022
Li	1.418	1.415	1.414
Na	0.142	0.155	0.152
K	1.433	1.466	1.473
OH	3.481	3.379	3.338
F	0.521	0.607	0.544
^{IV}Al	1.914	1.906	1.907
^{VI}Al	3.236	3.265	3.298
Sum Tetrahedral	8.000	8.000	8.000
Sum Octahedral	5.164	5.144	5.183
Sum x-site	1.729	1.752	1.755
Sum w-site	4.001	3.986	3.882
Fe+Mn+Ti-VIAl	-2.746	-2.819	-2.843
Mg-Li	-1.398	-1.397	-1.399

Table 3: Representative microprobe analyses of Li-rich micas and biotites from the garnet line at Mt. Mica. Formulas calculated on the basis of 24 oxygens.

Table 3 cont.

sample	MT2-3-m-2	MT2-3-m-1	MT6-4-b-3
SiO_2	37.56	37.75	38.11
TiO_2	0.50	0.48	0.49
Al_2O_3	20.99	21.01	27.21
FeO	17.43	17.40	17.20
MnO	0.07	0.07	0.08
MgO	6.54	6.57	0.34
CaO	0.08	0.10	0.10
Rb_2O	0.12	0.14	0.20
Cs_2O	0.02	0.02	0.03
Na_2O	0.56	0.48	0.61
K_2O	8.11	8.20	8.14
H_2O calc	3.74	3.76	3.82
F	0.35	0.33	0.34
Subtotal	96.06	96.30	96.69
O=F	0.15	0.14	0.14
Total	95.92	96.16	96.55
apfu			
Si	5.769	5.782	5.743
Ti	0.058	0.055	0.056
Al	3.801	3.794	4.833
Fe	2.239	2.229	2.167
Mn	0.009	0.009	0.011
Mg	1.498	1.500	0.077
Ca	0.013	0.016	0.017
Rb	0.012	0.014	0.019
Cs	0.001	0.001	0.002
Na	0.166	0.142	0.179
K	1.590	1.603	1.565
OH	3.832	3.839	3.836
F	0.168	0.161	0.163
^{IV}Al	2.231	2.218	2.257
^{VI}Al	1.571	1.577	2.575
Sum Tetrahedral	8.000	8.000	8.000
Sum Octahedral	5.375	5.369	4.886
Sum x-site	1.782	1.776	1.782
Sum w-site	4.000	4.000	4.000
Fe/(Fe+Mg)	0.599	0.598	0.966

sample	BT2-a-1	BT2-a-2	BT3-g-2	BT3-g-3
SiO_2	36.43	36.36	37.89	37.88
TiO_2	1.39	1.87	2.11	2.13
Al_2O_3	18.92	18.97	18.90	18.86
FeO	20.89	20.92	23.76	23.73
MnO	1.00	1.06	0.97	0.94
MgO	0.23	0.21	0.38	0.35
CaO	0.98	0.09	0.19	0.21
Rb_2O	0.04	0.03	0.02	0.02
Cs_2O	0.00	0.00	0.00	0.00
Na_2O	0.50	0.52	0.57	0.54
K_2O	9.54	9.49	10.10	10.09
H_2O calc	3.07	2.99	3.30	3.31
F	1.27	1.43	1.14	1.11
Subtotal	94.27	93.94	99.34	99.18
O=F	0.53	0.60	0.48	0.47
Total	93.73	93.33	98.86	98.72
apfu				
Si	5.950	5.949	5.919	5.924
Ti	0.171	0.230	0.248	0.251
Al	3.642	3.658	3.480	3.476
Fe	2.853	2.863	3.104	3.104
Mn	0.138	0.146	0.129	0.125
Mg	0.057	0.052	0.089	0.083
Ca	0.172	0.016	0.032	0.036
Rb	0.004	0.003	0.002	0.002
Cs	0.000	0.000	0.000	0.000
Na	0.158	0.166	0.172	0.163
K	1.988	1.982	2.013	2.013
OH	3.346	3.260	3.435	3.453
F	0.654	0.740	0.565	0.546
^{IV}Al	2.050	2.051	2.081	2.076
^{VI}Al	1.592	1.608	1.398	1.400
Sum Tetrahedral	8.000	8.000	8.000	8.000
Sum Octahedral	4.811	4.900	4.968	4.962
Sum x-site	2.322	2.167	2.219	2.214
Sum w-site	4.000	4.000	4.000	4.000
Fe/(Fe+Mg)	0.980	0.982	0.972	0.974

Table 4: Representative microprobe analyses of biotites from the line rock in the Bennett quarry. Formulas calculated on the basis of 24 oxygens.

K-feldspar (Table 5) and Albite (Table 6) compositions are found in each of the garnet line boundary layers from the sampled quarries (Fig. 35). The Emmons quarry is the only location with an antiperthitic texture.

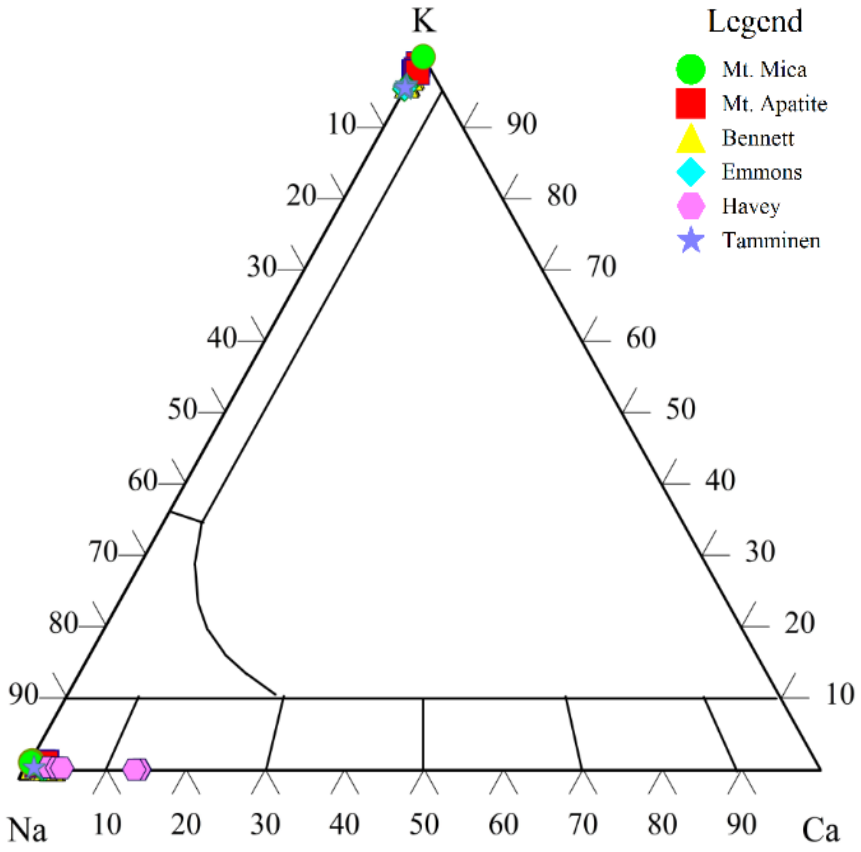

Figure 36: Feldspar ternary of plagioclase and K-feldspar from garnet line boundary layers in the Bennett, Emmons, Mt. Apatite and Mt. Mica quarries.

Sample	MA14-1-d-9	MT4-1-a-3	MT4-1-a-2	EM1-1-6	EM1-1-7	BT2-a-2	BT2-a-5
SiO_2	64.41	64.40	64.43	65.44	65.38	65.33	65.41
TiO_2	0.01	0.00	0.01	0.00	0.01	0.01	0.01
Al_2O_3	18.30	18.32	18.30	18.16	18.20	18.17	18.17
FeO	0.32	0.73	0.58	0.00	0.00	0.00	0.00
CaO	0.01	0.01	0.01	0.01	0.00	0.01	0.00
Cs_2O	0.00	0.00	0.00	0.00	0.00	0.00	0.00
Rb_2O	0.20	0.32	0.30	0.11	0.11	0.09	0.08
K_2O	15.51	15.56	15.51	16.06	15.90	16.12	16.08
Na_2O	0.19	0.00	0.00	0.45	0.51	0.29	0.46
Total	98.96	99.35	99.14	100.22	100.11	100.03	100.21
apfu							
Si	3.003	2.998	3.001	3.014	3.013	3.014	3.013
Ti	0.000	0.000	0.000	0.000	0.000	0.000	0.000
Al	1.005	1.005	1.005	0.986	0.988	0.988	0.986
Fe	0.013	0.029	0.023	0.000	0.000	0.000	0.000
Ca	0.001	0.000	0.000	0.000	0.000	0.001	0.000
Cs	0.000	0.000	0.000	0.000	0.000	0.000	0.000
Rb	0.006	0.010	0.009	0.003	0.003	0.003	0.002
K	0.923	0.924	0.922	0.943	0.935	0.949	0.945
Na	0.017	0.000	0.000	0.041	0.046	0.026	0.041
Ab	1.836	0.000	0.000	4.118	4.648	2.677	4.124
An	0.064	0.043	0.049	0.045	0.000	0.056	0.000
Or	98.101	99.957	99.951	95.837	95.352	97.267	95.876

Table 5: Representative microprobe analyses of K-feldspar from garnet line boundary layers in the Bennett, Mt. Apatite, Emmons and Mt. Mica quarries. Formulas calculated on the basis of 8 oxygens.

Sample	MA14-1-d-9	MT4-1-a-3	MT4-1-a-2	EM1-1-6	EM1-1-7	BT2-a-2	BT2-a-5
SiO_2	64.41	64.40	64.43	65.44	65.38	65.33	65.41
TiO_2	0.01	0.00	0.01	0.00	0.01	0.01	0.01
Al_2O_3	18.30	18.32	18.30	18.16	18.20	18.17	18.17
FeO	0.32	0.73	0.58	0.00	0.00	0.00	0.00
CaO	0.01	0.01	0.01	0.01	0.00	0.01	0.00
Cs_2O	0.00	0.00	0.00	0.00	0.00	0.00	0.00
Rb_2O	0.20	0.32	0.30	0.11	0.11	0.09	0.08
K_2O	15.51	15.56	15.51	16.06	15.90	16.12	16.08
Na_2O	0.19	0.00	0.00	0.45	0.51	0.29	0.46
Total	98.96	99.35	99.14	100.22	100.11	100.03	100.21
apfu							
Si	3.003	2.998	3.001	3.014	3.013	3.014	3.013
Ti	0.000	0.000	0.000	0.000	0.000	0.000	0.000
Al	1.005	1.005	1.005	0.986	0.988	0.988	0.986
Fe	0.013	0.029	0.023	0.000	0.000	0.000	0.000
Ca	0.001	0.000	0.000	0.000	0.000	0.001	0.000
Cs	0.000	0.000	0.000	0.000	0.000	0.000	0.000
Rb	0.006	0.010	0.009	0.003	0.003	0.003	0.002
K	0.923	0.924	0.922	0.943	0.935	0.949	0.945
Na	0.017	0.000	0.000	0.041	0.046	0.026	0.041
Ab	1.836	0.000	0.000	4.118	4.648	2.677	4.124
An	0.064	0.043	0.049	0.045	0.000	0.056	0.000
Or	98.101	99.957	99.951	95.837	95.352	97.267	95.876

Table 6: Representative microprobe analyses of plagioclase feldspar from the garnet line boundary layers in the Bennett, Mt. Apatite, Emmons and Mt. Mica quarries. Formulas calculated on the basis of 8 oxygens.

All tourmaline associated with a garnet line boundary layer from the sampled locations belong to the alkali group, where Na is the predominant alkali found in the X-site in these tourmalines (Figs. 37 & 39, Tables 7 & 8). Tourmaline in the Mt. Mica garnet line has a range of compositions dependent on the manner of occurrence. Compositional differences are related to the color zoned rims in (Fig. 17**)**, the two alkali subgroups found in the rims are schorl and elbaite (Figs. 37 & 38).

Tourmalines from the garnet line boundary layers of the Bennett, Emmons, Tamminen and the schorl pod layer in the Havey all plot within the alkali group (Fig. 39). The alkali group is subdivided further, Fig. 40, Fig. 41, where the tourmalines are found to plot within the schorl and elbaite fields. There is minor variation within the elbaite field in terms of Na and vacancy in the X-site and over all there is a high Fe content in the elbaite (Fig. 41), up to 6.117 wt% FeO and 0.835 apfu Fe. The tourmaline occurring within the Bennett aplite plot within the elbaite field in both the binary and ternary subgroup diagrams. Tourmaline from the garnet boundary layer in the Emmons quarry shows some variation between the Selway and Henry *et al.* plots. This is likely due to the calculated estimation of Li in the samples. The tourmaline samples associated with garnets from the schorl pod layer in an intermediate zone in the Havey quarry have the greatest dravitic component compared to all other locations.

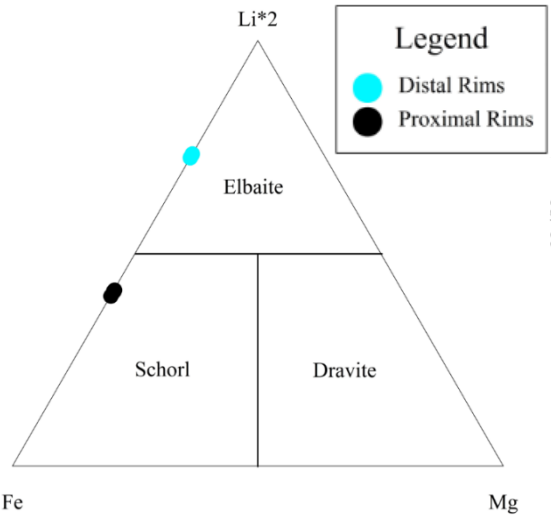

Figure 37: Tourmaline alkali subgroup ternary with data from distal and proximal portions of tourmaline rims around garnets from the garnet line in Mt. Mica, after Henry *et al.* 2011.

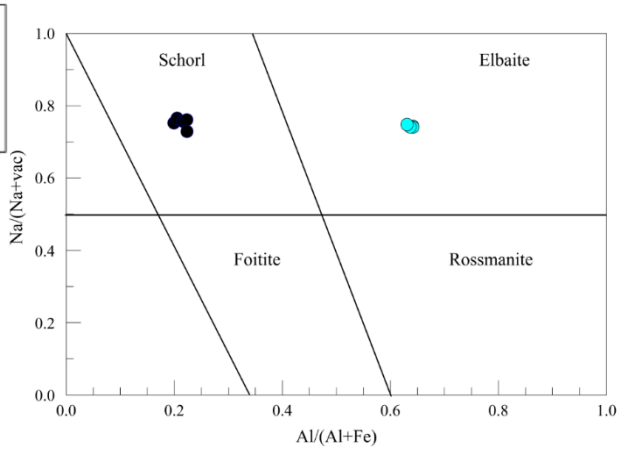

Figure 38: Tourmaline discrimination diagram of X vs Y-site components differentiating different compositions in tourmaline rims around garnet crystals in the Mt. Mica garnet line. (Selway *et al.* 1999).

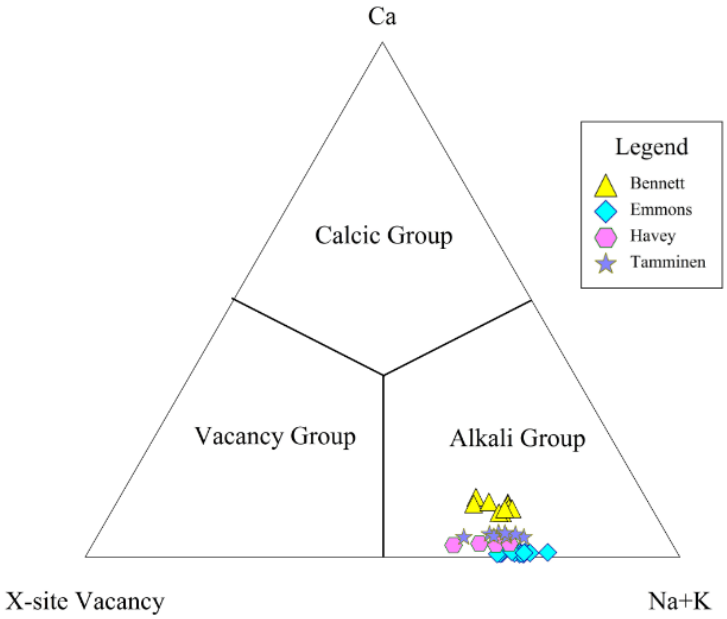

Figure 39: Ternary of primary tourmaline groups based on X-site occupancy, based on atomic proportions (Henry *et al.* 2011).

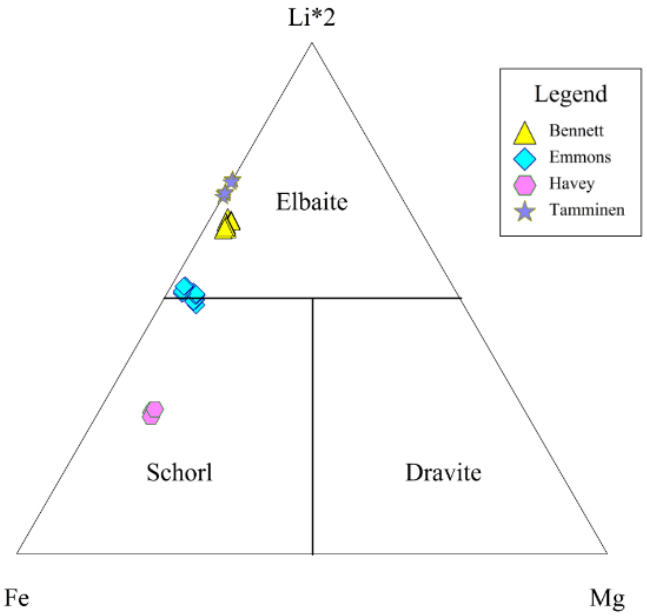

Figure 40: Ternary of alkali subgroups based on Y-site occupancy, based on atomic proportions (Henry *et al.* 2011).

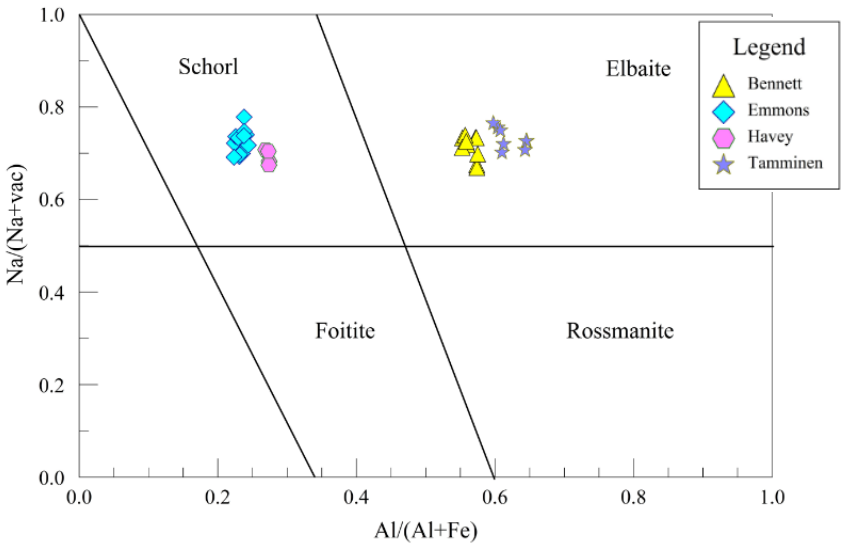

Figure 41: Tourmaline discrimination diagram of X vs Y-site components (Selway *et al.* 1999).

Sample	MT2-3-d-2	MT1-2-b-1	MT1-2-d-1	MT6-1-7-1	MT6-1-t-3	MT1-1A-1
SiO_2	36.50	36.58	36.57	35.21	35.99	36.68
TiO_2	0.01	0.01	0.01	0.01	0.01	0.01
B_2O_3 calc.	10.73	10.82	10.82	10.34	10.63	10.79
Al_2O_3	38.22	39.50	39.32	34.46	37.80	38.78
FeO	5.56	4.65	3.78	13.11	6.09	4.99
MnO	1.10	1.12	1.57	0.34	0.86	0.98
MgO						
CaO	0.48	0.12	0.43	0.09	0.59	0.53
Li_2O calc.	1.39	1.37	1.52	0.56	1.37	1.46
Na_2O	2.09	2.10	2.22	2.21	2.20	2.00
K_2O	0.03	0.02	0.02	0.02	0.02	0.02
H_2O calc.	3.21	3.27	3.27	3.18	3.25	3.21
F	1.04	0.99	0.98	0.83	0.89	1.10
Subtotal	100.37	100.55	100.52	100.38	99.70	100.55
O=F	0.44	0.42	0.41	0.35	0.37	0.46
Total	99.93	100.13	100.11	100.02	99.33	100.08
apfu						
Si	5.902	5.867	5.863	5.910	5.873	5.898
Ti	0.002	0.001	0.001	0.002	0.001	0.001
B	2.997	2.996	2.996	2.996	2.995	2.996
Al	7.285	7.468	7.431	6.817	7.271	7.351
Fe	0.752	0.624	0.507	1.841	0.832	0.671
Mn	0.151	0.152	0.213	0.049	0.119	0.134
Mg	0.000	0.000	0.000	0.000	0.000	0.000
Ca	0.083	0.021	0.074	0.017	0.103	0.092
Li	0.905	0.884	0.981	0.378	0.899	0.942
Na	0.656	0.653	0.689	0.720	0.696	0.623
K	0.006	0.004	0.004	0.005	0.005	0.004
H	3.467	3.499	3.502	3.557	3.542	3.440
F	0.533	0.501	0.498	0.443	0.458	0.560

Table 7: Representative Microprobe analyses of tourmaline from within the garnet line at Mt. Mica. Formulas calculated on the basis of 31 oxygens.

Sample	EM1-1-d-4	EM2-2-f-1	EM2-2-f-2	TM3-1-c-3	BT3-e-2	HVY1-d-1
SiO_2	36.51	36.48	36.42	36.40	36.55	35.60
TiO_2	0.88	0.21	0.23	0.03	0.04	0.13
B_2O_3 calc.	10.38	10.31	10.30	10.69	10.79	10.36
Al_2O_3	32.60	32.66	32.68	37.79	38.33	33.65
FeO	10.42	10.81	10.87	5.72	6.40	12.22
MnO	0.19	0.12	0.12	1.21	0.20	0.02
MgO	0.71	0.32	0.34		0.33	1.00
CaO	0.03	0.06	0.06	0.26	0.60	0.16
Li_2O calc.	1.19	1.28	1.24	1.37	1.35	0.57
Na_2O	2.24	2.22	2.15	2.31	1.91	2.10
K_2O	0.04	0.04	0.04	0.01	0.02	0.03
H_2O calc.	3.17	3.19	3.17	3.26	3.25	3.30
F	0.88	0.78	0.81	0.90	0.99	0.58
Subtotal	99.23	98.48	98.42	99.98	100.76	99.72
O=F	0.37	0.33	0.34	0.38	0.42	0.24
Total	98.86	98.15	98.08	99.60	100.35	99.47
apfu						
Si	6.106	6.146	6.141	5.915	5.884	5.974
Ti	0.110	0.027	0.029	0.004	0.005	0.017
B	2.998	2.998	2.998	3.000	3.000	3.000
Al	6.425	6.484	6.495	7.239	7.276	6.657
Fe	1.457	1.523	1.533	0.777	0.862	1.716
Mn	0.027	0.018	0.017	0.167	0.027	0.003
Mg	0.177	0.081	0.084	0.000	0.079	0.250
Ca	0.006	0.010	0.010	0.046	0.103	0.028
Li	0.802	0.865	0.839	0.898	0.871	0.384
Na	0.725	0.726	0.704	0.728	0.597	0.683
K	0.009	0.009	0.008	0.003	0.005	0.007
H	3.536	3.583	3.571	3.536	3.496	3.694
F	0.464	0.417	0.429	0.464	0.503	0.306

Table 8: Representative microprobe analyses of tourmaline from garnet line boundary layer in the Emmons, Bennett aplite and Tamminen quarries and from the schorl pod layer in the Havey quarry. Formulas calculated on the basis of 31

Niobium-Ta oxides from the garnet line boundary layer in the Emmons are often concentrically zoned and plot within two fields in the columbite-group quadrilateral (Fig. 42). The two groups of data points represent the different zones (see Fig. 28). Those plotting within the ferrocolumbite field are core regions of crystals, whereas the manganocolumbite group represents the rims of these crystals. Examples of columbite-group minerals from within the garnet line boundary layer at Mt. Mica, where no zoning is observed, fall into two fields on the quadrilateral; manganocolumbite and manganotantalite.

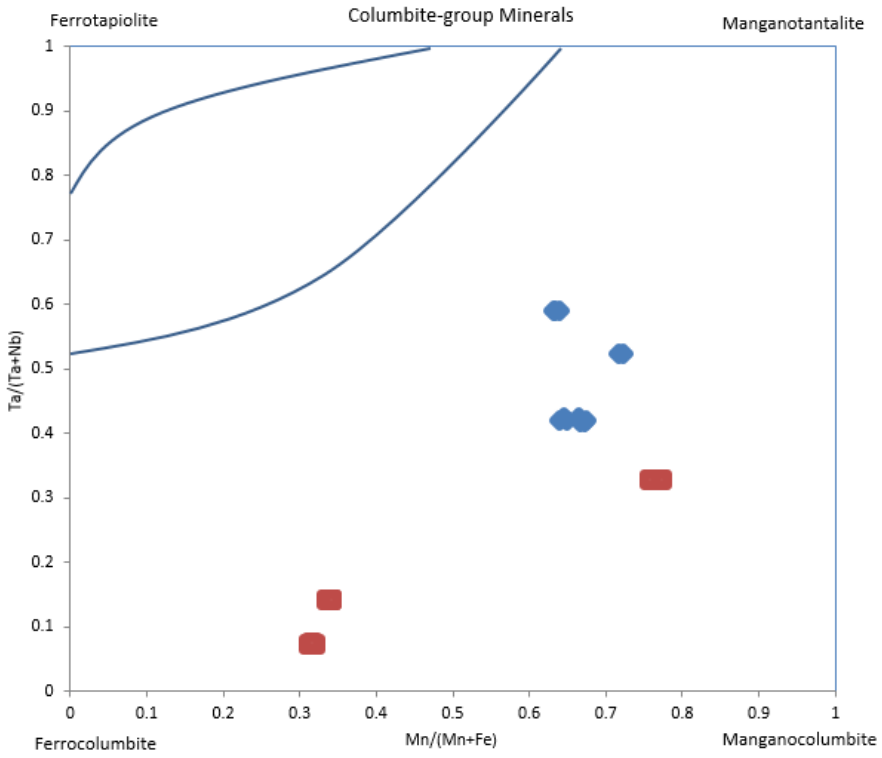

Figure 42: Columbite group minerals from within garnet boundary layers in the Emmons and Mt. Mica quarries plotted in the columbite quadrilateral. Dashed lines are boundaries of columbite-tantalite-tapiolite miscibility gap, Černý and Ercit (1989).

Sample	MT2-3-f-3	MT2-3-f-5	MT1-2-f-2	EM1-1-f-1	EM1-1-f-3	EM1-1-f-8
Nb_2O_5	29.44	24.90	37.56	71.34	71.43	44.96
Ta_2O_5	53.67	59.41	45.23	8.99	9.56	35.94
UO_2	0.00	0.00	0.02	0.02	0.03	0.66
SiO_2	0.09	0.06	0.01	0.03	0.03	0.06
TiO_2	0.00	0.00	0.00	0.27	0.27	0.10
SnO_2	0.14	0.14	0.01	0.12	0.13	0.18
Al_2O_3	0.00	0.00	0.00	0.23	0.01	0.03
FeO	4.76	5.99	6.22	12.90	12.78	4.10
MnO	11.89	10.21	11.34	5.78	5.84	13.80
CaO	0.00	0.00	0.00	0.00	0.00	0.01
Total	99.99	100.71	100.40	99.68	100.08	99.83
A-site						
Fe	1.136	1.458	1.419	2.503	2.479	0.902
Mn	2.874	2.519	2.619	1.136	1.148	3.078
Mg	0.000	0.000	0.000	0.000	0.000	0.000
A-total	4.010	3.976	4.037	3.640	3.627	3.980
B-site						
Sn	0.016	0.017	0.001	0.011	0.012	0.019
Ta	4.165	4.705	3.353	0.567	0.603	2.574
Nb	3.798	3.278	4.628	7.486	7.491	5.352
B-total	7.979	8.000	7.982	8.064	8.106	7.945
Mn/(Mn+Fe)	0.717	0.633	0.649	0.312	0.317	0.773
Ta/(Ta+Nb)	0.523	0.589	0.420	0.070	0.074	0.325

Table 9: Representative microprobe analyses of columbite-group minerals found in the garnet boundary layers in the Mt. Mica and the Emmons quarries. Formulas calculated on the basis of 24 oxygens.

Zircons from garnet line boundary layers at all locations show low Hf, Th and U content. The highest Hf and U concentrations, up to 4.11 wt% HfO_2 and 0.873 wt% UO_2 are at the Emmons. The highest Th enrichment is at Mt. Apatite, 0.393 wt% ThO_2; where there are more Th-rich mineral species present in these samples. A comparison of Hf concentration between all quarries except the Havey is provided in (Fig. 43).

Sample	BT3-e-1	EM2-2-7-3	MA2-1-4-1	MT6-1-a-1
ZrO_2	64.22	63.80	64.22	64.23
SiO_2	32.40	32.24	32.46	32.33
HfO_2	3.19	3.57	3.03	3.40
UO_2	0.02	0.15	0.07	0.02
FeO	0.05	0.14	0.45	0.02
CaO	0.06	0.13	0.03	0.03
Al_2O_3	0.04	0.06	0.03	0.03
MnO	0.05	0.09	0.09	0.04
ThO_2	0.09	0.20	0.21	0.10
Total	100.11	100.37	100.60	100.20
apfu				
Zr	0.967	0.962	0.964	0.968
Si	1.001	0.997	0.999	0.999
Hf	0.028	0.032	0.027	0.030
U	0.000	0.001	0.000	0.000
Fe	0.001	0.004	0.012	0.000
Ca	0.002	0.004	0.001	0.001
Al	0.002	0.002	0.001	0.001
Mn	0.001	0.002	0.002	0.001
Th	0.001	0.001	0.001	0.001
X-site	0.996	0.996	0.993	0.999
Y-site	1.001	0.997	0.999	0.999

Table 10: Representative microprobe analyses of zircon from garnet line boundary layers of the Bennett, Emmons, Mt. Apatite and Mt. Mica quarries. Formulas calculated on the basis of oxygens

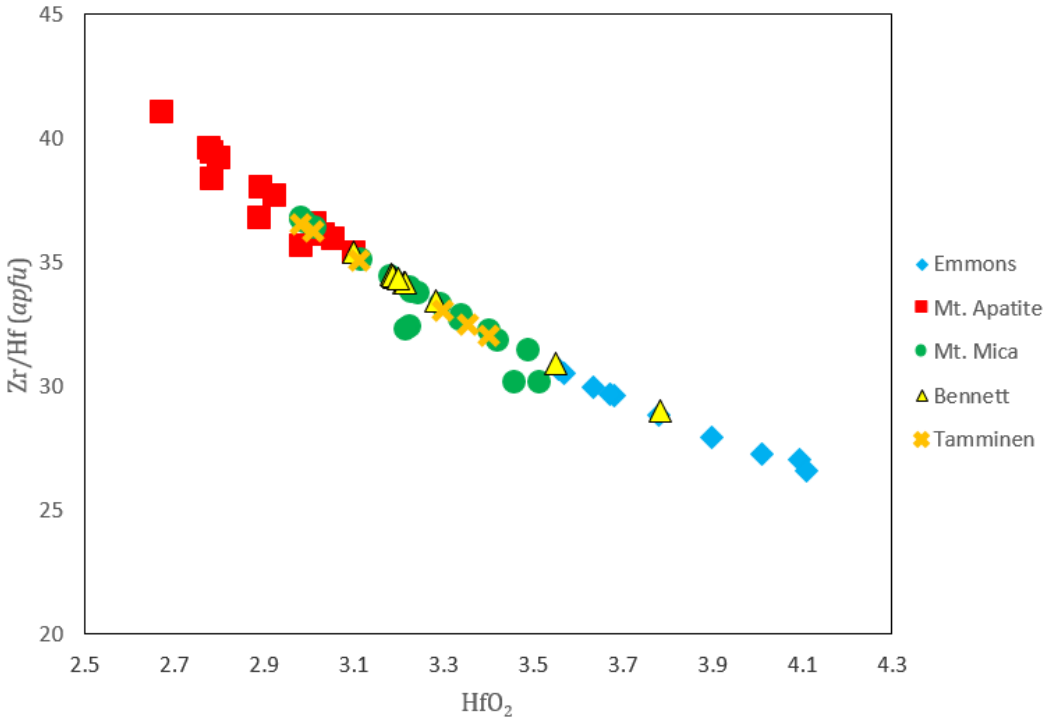

Figure 43: Comparisons of Hf enrichment from zircons from the garnet boundary layers in this study.

There is considerable diversity of X-site replacement between fluorapatites from the garnet boundary layers in the Bennett, Mt. Apatite and Mt. Mica quarries. Calcium is the dominant ion in this site, however, substitution of Fe, Mg, Mn and Sr can occur (Fig. 44).

Strontium enrichment is highest within the Mt. Apatite garnet line samples, up to 0.31 wt% SrO (0.014 apfu), although Sr content from apatites in the schorl pod line at the Havey is similar. Manganese proportions are highest in the Bennett aplite samples up to 1.44 wt% MnO (0.102 apfu), though there is a noticeable shift into the more Sr-rich field, up to 0.121 wt% SrO (0.006 apfu), this is also comparable to the apatites from the garnet boundary layer in the Tamminen quarry. Apatites from within the garnet line at Mt. Mica trend towards Mn-enrichment up to 0.232 wt% MnO (0.017 apfu), but still have a substantial Sr component up to 0.92 wt% SrO (0.45 apfu). Iron concentration is minimal in all samples, average between locations 0.01 wt% FeO (0.001 apfu).

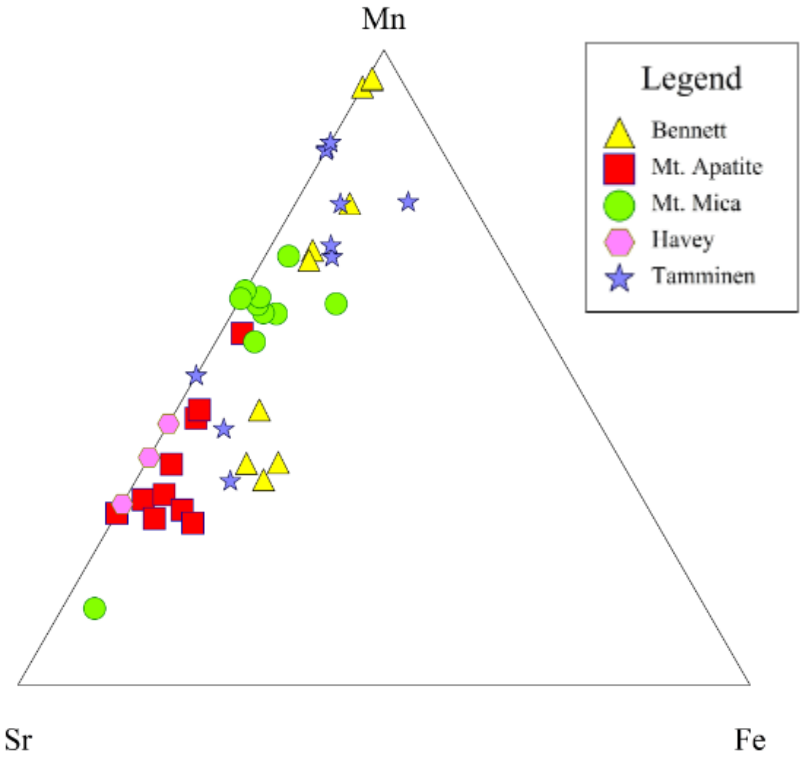

Figure 44: Fluorapatites from garnet line boundary layers in a Mn-Fe-Sr ternary showing the dominant substitutions in the X-site, based on atomic proportions.

Sample	BT1-a-1-1	BT2-a-2	MA13-1-h-4	MA13-1-h-1	TM2-b-2	MT2-3-d-2	MT6-1-c-2	MT1-2-h-2
SiO_2	0.06	0.06	0.07	0.11	0.11	0.08	0.07	0.05
Al_2O_3	0.02	0.00	0.00	0.00	0.00	0.02	0.03	0.03
FeO	0.01	0.01	0.01	0.01	0.00	0.03	0.00	0.01
MnO	0.12	0.02	0.11	0.06	0.11	0.14	0.20	0.17
MgO	0.00	0.00	0.00	0.01	0.00	0.01	0.00	0.00
SrO	0.07	0.05	0.21	0.21	0.03	0.09	0.17	0.11
CaO	0.00	0.00	55.11	54.94	55.41	55.41	55.48	55.33
P_2O_5	42.33	42.33	42.01	42.00	42.33	42.01	42.11	42.01
H_2O calc.	0.23	0.23	0.30	0.36	0.31	0.32	0.27	0.36
Cl	0.00	0.00	0.28	0.11		0.00	0.00	0.00
F	3.29	3.29	3.12	2.99	3.12	3.08	3.19	3.01
subtotal	101.75	101.60	101.23	100.81	101.42	101.20	101.53	101.07
O=F+Cl	1.39	1.39	1.37	1.29	1.31	1.30	1.34	1.27
Total	100.36	100.22	99.85	99.53	100.11	99.90	100.18	99.80
apfu								
Si	0.005	0.005	0.006	0.009	0.009	0.006	0.006	0.005
Al	0.002	0.000	0.000	0.000	0.000	0.002	0.003	0.003
Fe	0.001	0.001	0.001	0.001	0.000	0.002	0.000	0.001
Mn	0.009	0.002	0.008	0.004	0.008	0.010	0.014	0.012
Mg	0.000	0.000	0.000	0.001	0.000	0.001	0.000	0.000
Sr	0.003	0.002	0.010	0.010	0.001	0.004	0.008	0.005
Ca	4.982	4.987	4.968	4.963	4.971	4.991	4.986	4.988
P	2.997	3.000	2.992	2.998	3.001	2.990	2.990	2.992
H	0.129	0.128	0.171	0.202	0.173	0.180	0.153	0.200
Cl	0.000	0.000	0.039	0.016	0.000	0.000	0.000	0.000
F	0.871	0.871	0.829	0.798	0.826	0.820	0.847	0.800
X-site	4.997	4.992	4.968	4.963	4.980	5.011	5.011	5.008
Y-site	2.997	3.000	2.992	2.998	3.001	2.990	2.990	2.992
Z-site	1.000	1.000	1.000	1.000	0.999	1.000	1.000	1.000

Table 11: Representative microprobe analyses of apatite from the Mt. Apatite, Mt. Mica, Bennett and Tamminen quarries. Formulas calculated on the basis of 13 oxygens.

The pollucite fracture fillings in the garnets of the garnet line at Mt. Mica and from the garnets found within the schorl pods in the intermediate zone from the Havey have a high Fe content. Total Fe content was measured with the EMP as FeO, however, the proportion has been converted to Fe_2O_3 and is displayed in Table 12. The Fe_2O_3 content for pollucite associated with the garnets in the schorl pods is highest in the Havey, reaching 6.07 wt%, whereas pollucite in the Mt. Mica garnet line ranges from 0.12 to 5.69 wt%. Ratios for Si/Al for pollucite in the Havey range from 2.8 to 2.91, whereas the $Si/Al+Fe^{3+}$ ranges from 2.22 to 2.28.Silicon/Al ratios from the Mt. Mica pollucite in the garnet line range from 2.4 to 2.97, whereas $Si/Al+Fe^{3+}$ ratios range from 2.25 to 2.45. Cesium-Rb-K (CRK) values are as high as 85.28 in the pollucite associated with the garnets in the schorl pods form the Havey quarry and are as high as 88.7 in the pollucite from the garnet line at Mt. Mica (Fig. 45).

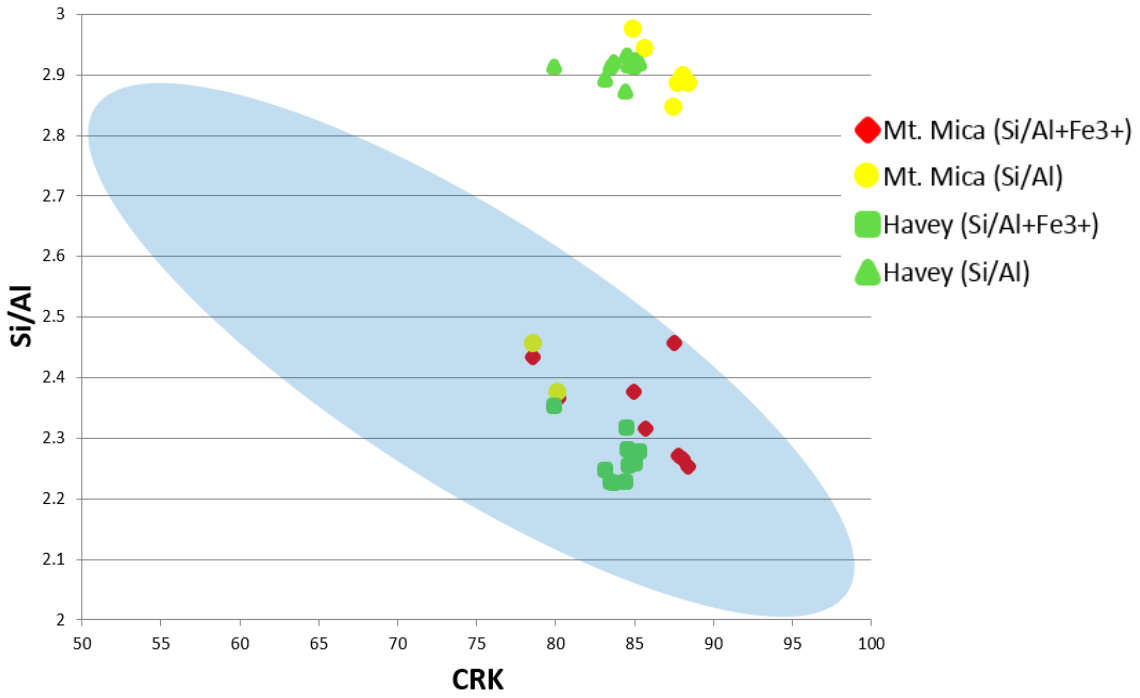

Figure 45: Compositional trends of pollucite the garnet line from Mt. Mica and from the schorl pods at the Havey quarry. Note the field plotting to the top right of the graph utilizes the standard Si/Al ratio, but with the incorporation of Fe^{3+} in the octahedral site these data groups fall within the field of commonly encountered pollucite compositions. The shaded oval represents a range of pollucite compositions from pegmatites around the world Černý *et al.* (2012), Teertstra *et al.* (1992), Teertstra and Černý (1997) and Wang *et al.* (2004).

Sample	MT4-1-b-2	MT6-1-c-2	MT4-1-A-2	MT4-1-b-1	HVY1-1-a-3	HVY1-1-c-2	HVY1-1-k-2
SiO2	43.98	43.893	46.99	43.98	43.31	43.32	43.42
Al2O3	12.68	12.9	16.78	12.54	12.61	12.61	12.57
Fe2O3	5.39	5.6897	0.12	4.95	6.07	5.55	5.20
MnO	0.25	0.292	0.30	0.27	0.19	0.20	0.22
Na2O	1.54	0.892	1.89	1.46	1.78	1.60	1.71
K2O	5.50	0.675	1.11	3.45	4.11	4.22	4.67
Rb2O	1.09	1.234	1.09	1.12	1.02	1.33	1.10
Cs2O	29.09	31.114	32.66	30.00	29.89	30.56	29.74
CaO	0.35	0.213	0.29	0.33	0.22	0.28	0.21
Total	99.879	96.9027	101.22143	98.109	99.214302	99.663079	98.842162
Si	2.052	2.093167	2.101	2.083	2.043	2.049	2.056
Al	0.697	0.7251019	0.884	0.700	0.701	0.703	0.702
Fe	0.189	0.2041827	0.004	0.177	0.215	0.197	0.185
Mn	0.010	0.0117949	0.011	0.011	0.008	0.008	0.009
Na	0.140	0.0824796	0.164	0.134	0.163	0.147	0.157
K	0.327	0.0410701	0.063	0.208	0.247	0.255	0.282
Rb	0.033	0.0378305	0.031	0.034	0.031	0.040	0.033
Cs	0.579	0.6327408	0.623	0.606	0.601	0.616	0.601
Ca	0.017	0.0108837	0.014	0.017	0.011	0.014	0.011
Si/Al	2.944	2.8867213	2.376	2.976	2.914	2.914	2.931
$Al+Fe^{3+}$	0.886	0.9292846	0.888	0.877	0.916	0.900	0.887
$Si/Al+Fe^{3+}$	2.315	2.25245	2.365	2.376	2.229	2.275	2.318
CRK	85.668	88.402141	80.168	84.924	83.481	84.986	84.501

Table 12: Representative microprobe analyses of pollucite from within the Mt. Mica garnet line and schorl pod line in the Havey. Formulas calculated on the basis of 6 oxygens and did not include any hydrous component.

Xenotime from the garnet boundary layers in Mt. Mica and Tamminen and from the schorl pod boundary layer in the Havey quarries is characterized by low UO_2 (0.0089 avg. wt%), ThO_2 (0.0115 avg. wt%) and low SiO_2 content (< 0.055 wt%), a part from the Tamminen where it is as high as 0.266 wt% SiO_2. The HREE concentrations are given in ppm in (Fig. 46). There are some differences in the HREE content between locations, where Dy_2O_3 is highest in the Tamminen (up to 4.33 wt%); see Table 13, Y_2O_3 is highest at Mt. Mica (up to 4.51 wt%), the Havey has the lowest concentrations of Er_2O_3 (as low as 1.91 wt%).

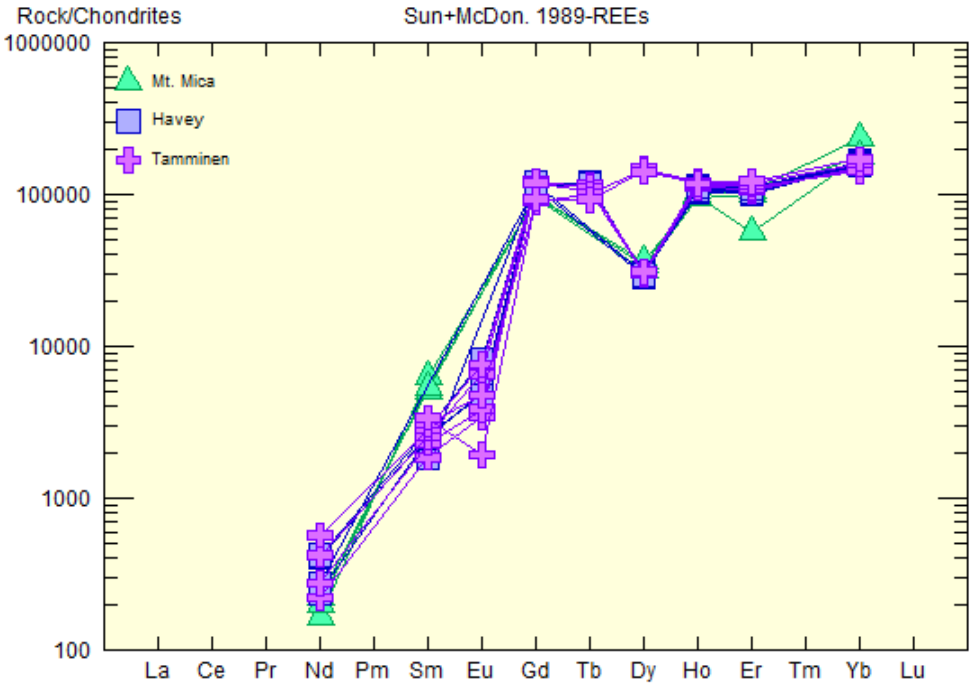

Figure 46: Chondrite normalized rare earth element plot of Xenotime from the garnet boundary layers in Mt. Mica and Tamminen and from the schorl pod layer in the Havey quarries.

Sample	TM3-1-e-1	TM3-1-e-2
P_2O_5	37.31	37.22
SiO_2	0.21	0.27
ThO_2	0.02	0.02
UO_2	0.01	0.01
Al_2O_3		
Y_2O_3	50.02	50.12
Nd_2O_3		
Sm_2O_3	0.06	0.06
Gd_2O_3	2.13	2.21
Dy_2O_3	4.33	4.12
Ho_2O_3	0.79	0.76
Er_2O_3	2.21	2.31
Yb_2O_3	3.11	3.31
FeO	0.04	0.04
MnO	0.03	0.04
CaO	0.12	0.11
Total	100.39	100.59
apfu		
P	1.006	1.004
Si	0.007	0.008
Th	0.000	0.000
U	0.000	0.000
Al	0.000	0.000
Y	0.848	0.849
Nd	0.000	0.000
Sm	0.001	0.001
Gd	0.023	0.023
Dy	0.044	0.042
Ho	0.008	0.008
Er	0.022	0.023
Yb	0.030	0.032
Fe	0.001	0.001
Mn	0.001	0.001
Ca	0.004	0.004

Monazite from the garnet boundary layers in the Bennett, Mt. Apatite, Mt. Mica and Tamminen quarries are relatively uniform in terms of REE concentrations, see Fig 47 and Table 14. The Tamminen has the lowest ThO_2 content (6.45 wt%), whereas concentrations in Mt. Mica are up to 10.45 wt%. The Y2O3 concentrations are also highest in Mt. Mica (up to 2.7 wt%), whereas the Tamminen accounts for the lowest (0.873 wt%). Uranium-Pb age dates were determined by averaging three spot analyses from monazites from Mt. Mica and Mt. Apatite, which yielded ages of 255.45 Ma and 258.73 Ma respectively. The standard deviation for the Mt. Mica age date is 3.71 Ma and 2.21 Ma for Mt. Apatite.

Table 13: Representative microprobe analyses of xenotime from garnet boundary layers in the Tamminen quarry. Formulas calculated on the basis of 4 oxygens, bdl is below detection limit.

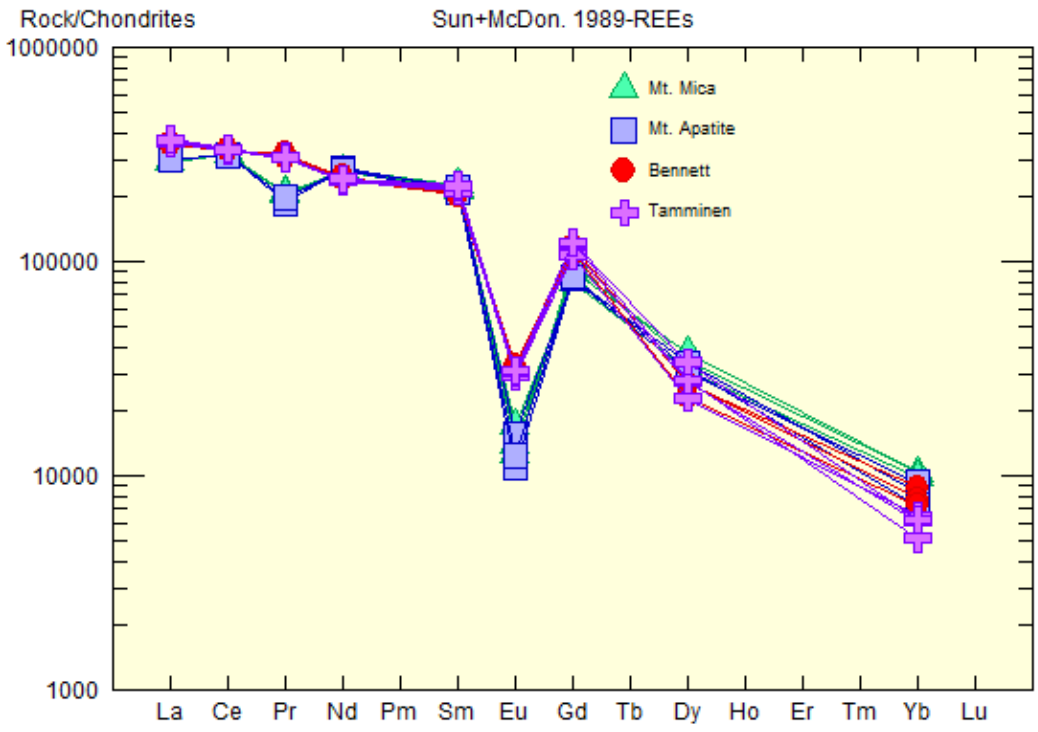

Figure 47: Chondrite normalized rare earth element plot of monazites from the garnet boundary layers in Mt. Mica, Mt. Apatite, Bennett and Tamminen quarries.

Sample	TM3-1-c-1	TM3-1-c-2	BT-3-2	BT-3-3	MA2-1-2	MA2-1-3	MT6-2-2	MT6-2-3
P_2O_5	29.982	30.091	30.044	29.880	29.630	29.777	29.567	29.555
SiO_2	0.983	0.975	1.090	1.000	1.500	1.610	1.650	1.670
ThO_2	7.233	7.191	8.020	8.100	10.240	10.210	10.430	10.450
UO_2	0.412	0.393	0.330	0.340	0.840	0.820	0.850	0.880
Al_2O_3	0.043	0.050	0.050	0.050	0.080	0.070	0.070	0.080
Y_2O_3	0.873	0.921	1.220	1.200	1.910	1.810	2.640	2.700
La_2O_3	10.345	10.292	9.830	9.870	8.290	8.330	8.090	8.120
Ce_2O_3	23.872	24.009	23.880	23.780	22.620	22.550	22.720	22.670
Pr_2O_3	3.412	3.399	3.550	3.430	2.090	2.200	2.280	2.300
Nd_2O_3	13.211	13.266	13.340	13.560	14.640	14.560	14.510	14.520
Sm_2O_3	3.983	4.007	3.730	3.630	3.930	3.710	4.030	3.780
Eu_2O_3	0.204	0.208	0.210	0.210	0.073	0.084	0.094	0.115
Gd_2O_3	2.882	2.911	2.780	2.620	1.980	2.010	2.120	1.890
Tb_2O_3	bdl	bdl	bdl	bdl	bdl	bdl	bdl	bdl
Dy_2O_3	0.812	0.990	0.780	0.680	0.880	0.920	1.090	0.910
Yb_2O_3	0.099	0.121	0.150	0.140	0.180	0.140	0.200	0.190
FeO	0.233	0.255	0.220	0.240	0.190	0.180	0.090	0.100
MnO	0.032	0.041	bdl	bdl	bdl	bdl	bdl	bdl
MgO	0.019	0.034	0.060	0.070	0.090	0.090	0.100	0.090
CaO	0.411	0.398	0.560	0.560	1.220	1.210	0.900	0.920
PbO	0.356	0.411	0.440	0.440	0.140	0.140	0.140	0.140
total	99.388	99.954	100.274	99.790	100.520	100.417	101.567	101.075
apfu								
A-site								
Th	0.064	0.064	0.071	0.072	0.090	0.089	0.091	0.091
U	0.004	0.003	0.003	0.003	0.007	0.007	0.007	0.008
Al	0.002	0.002	0.002	0.002	0.004	0.003	0.003	0.004
Y	0.018	0.019	0.025	0.025	0.039	0.037	0.054	0.055
La	0.149	0.148	0.141	0.142	0.118	0.118	0.115	0.115
Ce	0.342	0.342	0.339	0.340	0.320	0.318	0.319	0.319
Pr	0.049	0.048	0.050	0.049	0.029	0.031	0.032	0.032
Nd	0.185	0.185	0.185	0.189	0.202	0.200	0.199	0.199
Sm	0.054	0.054	0.050	0.049	0.052	0.049	0.053	0.050
Eu	0.003	0.003	0.003	0.003	0.001	0.001	0.001	0.002
Gd	0.037	0.038	0.036	0.034	0.025	0.026	0.027	0.024
Tb	bdl	bdl	bdl	bdl	bdl	bdl	bdl	bdl
Dy	0.010	0.012	0.010	0.009	0.011	0.011	0.013	0.011
Yb	0.001	0.001	0.002	0.002	0.002	0.002	0.002	0.002
Fe	0.008	0.008	0.007	0.008	0.006	0.006	0.003	0.003
Mn	0.001	0.001	bdl	bdl	bdl	bdl	bdl	bdl
Mg	0.001	0.002	0.003	0.004	0.005	0.005	0.006	0.005
Ca	0.017	0.017	0.023	0.023	0.050	0.050	0.037	0.038
Pb	0.004	0.004	0.005	0.005	0.001	0.001	0.001	0.001
A-total	0.949	0.952	0.955	0.958	0.964	0.955	0.964	0.961
B-site								
P	0.993	0.992	0.987	0.988	0.969	0.971	0.961	0.962
Si	0.038	0.038	0.042	0.039	0.058	0.062	0.063	0.064
B-total	1.032	1.030	1.029	1.027	1.027	1.033	1.024	1.026

Table 14: Representative microprobe analyses of monazite from the garnet boundary layers in the Tamminen, Bennett, Mt. Apatite and Mt. Mica quarries. Formulas calculated on the basis of 4 oxygens, bdl is below detection limit.

Discussion:

Garnet line paragenesis:

In all garnet samples there is no evidence of compositional zoning. However, there is compositional variation between quarry locations and there is minor compositional variation among individual garnet samples taken along strike at Mt. Apatite (27-30.9 % spss.) whereas variation is more prominent at Mt. Mica (38.1-66 % spss.). Despite the range of compositions there is no recognizable zoning within crystals. The intracrystalline, chemical homogeneity displayed by the garnets is characteristic of equilibrium crystallization with a melt equally saturated in almandine-spessartine components. The only instance where heterogeneity occurs is near fractures and inclusions (Fig. 23) in the Mt. Mica garnet, where Fe depletion halos surround the features. This is evidence of a localized depletion of material that likely occurred, as the garnet was co-crystallizing with the inclusions, which are dominantly quartz and tourmaline; the latter being a competing mafic phase.

A relationship between garnet chemistry and pegmatite zones was demonstrated from numerous Li-rich and –deficient pegmatites in Africa by Selway and Von Knorring 1983 (Fig. 49). Their results have an interesting comparison with the garnets in this study, which all came from lithium-rich pegmatites. Garnet samples from the garnet line at Mt. Mica are from the core zone of the pegmatite. The garnet samples from the Mt. Apatite (Rose *et al.* 1997), Emmons and Havey (Roda-Robles *et al.* 2011) quarries are from intermediate zones. The garnets from the Bennett pegmatite come from an aplite unit (Wise and Rose 2000). The Emmons and Bennett garnets fall into the determined fields,

apart from a single outlier in the Bennett plotting in the intermediate zone field. Mt. Mica samples show a well-defined trend have the largest spread from contact zone, intermediate zones and core and replacement zones (lithium-deficient pegmatites) compositions. There is a recognizable gap along the trend-line between the core-replacement zone and intermediate zone fields for the Mt. Mica garnet line samples. The nature and reason for this division is unknown. The most intriguing aspect of this plot is the position of the Mt. Apatite, Havey and Tamminen garnets, which all plot well into the contact zone field of Baldwin (1983). The garnets from these quarries are all from well-defined intermediate zones.

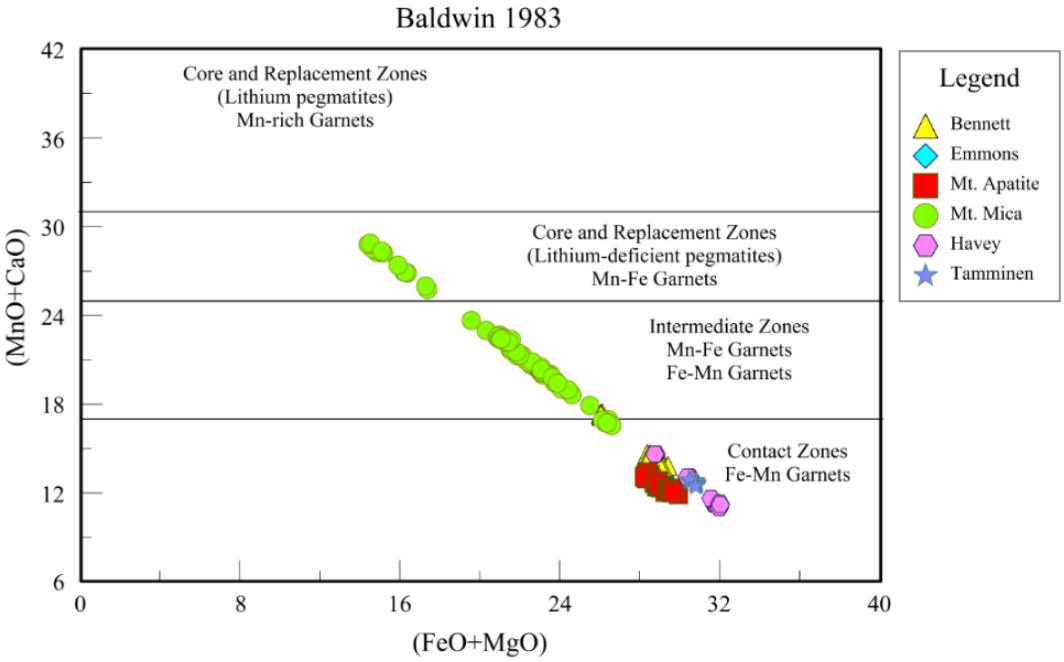

Figure 48: Chemical composition of garnets related to pegmatite zones, based on analyses by Baldwin and Von Knorring (1983). Plotted here are samples from the garnet boundary layers in Oxford County, Maine pegmatites.

The large sizes of the garnets at Mt. Mica, Mt. Apatite (T.H.I.T.G and T.H.I.T.G prospect) and the Havey suggest high crystal growth rates and low nucleation rates. Garnets from the Emmons and Tamminen quarries are smaller and not as abundant. They

infer low nucleation rates coupled with crystal growth rates that may be less than the other quarries. An alternative and equally likely interpretation is that the dissolved garnet components were less abundant in the melts during the onset of garnet crystallization.

In the previously mentioned cases the diffusion rate within the magma was likely higher than what occurred in the Bennett aplite, which would have also experienced higher nucleation rates and lower crystal growth rates. An intriguing compositional comparison is that the aplite garnets have a higher average spessartine component (34.3% spss.) than the Mt. Apatite garnets (28.4% spss.), which occur in the intermediate zones. The aplite unit at the Bennett is assumed to have developed earlier than its intermediate and core zone portions. The higher Mn/Fe ratio within the aplite garnets suggests that the melt that formed the Bennett pegmatite was more evolved even in the earliest stages of pegmatite consolidation than the intermediate and core zones of the Mt. Apatite pegmatite.

Interestingly, the thickness and occurrence of the garnet line at Mt. Apatite differs along dip. The Pulisifer has two monomineralic layers (garnet lines) that are bound together by graphic granite. These are similar to the unidirectional solidification textures seen in the aplite in the Little Three mine, San Diego, California (Webber et *al.* 1997, London, 2009), which represent distinct changes in melt chemistry and low diffusion rates of components along a crystallization front. The melt which generated the Little Three pegmatite experienced a high degree of undercooling while it produced the aplite and was initially oversaturated in components that are essential to crystallizing quartzofeldspathic minerals. However, along the crystallization front nonessential components (Mn and Fe) were continually partitioned into the melt (because they are incompatible in the quartzofeldspathic phases) until enough of these components became available to

crystallize a new phase (garnet). A similar rhythmic layering is encountered in the Pulsifer quarry (Figs. 6a and b), albeit there are some textural differences. The quartzofeldspathic phases take the form of graphic granite, which crystallize from a dehydrated melt in disequilibrium, which existed far below the desired solidus. When nucleation began the melt began to crystallize somewhat differently than an aplite where the inward advance of the crystallization front was met with a sufficient amount of lateral diffusion of components. Elongated, unidirectional graphic crystals and lack of hydrous mineral phases illustrate this affect. In comparison to T.H.I.T.G and T.H.I.T.G prospect, the Pulsifer had much lower concentrations of Mn and Fe in the melt. Consequently the garnet lines are significantly thinner and the garnets are also smaller.

The existence of a schorl boundary line layer at Mt. Mica is an interesting feature that should be thoroughly investigated in the future. Without any available research the author infers, based on textural and mineralogical occurrences, that it represents a chemical transition in the melt. Iron preferentially partitions into schorl whereas Mn partitions into garnet preferentially (Wolf and London 1997). The sequestration of Fe into the schorl boundary layer would raise the Mn/Fe ratio of the melt. The subsequent crystallization of the garnet line marks the increase in the ratio. As the melt became super saturated in Mn garnet became available to partition the component out of the melt and at a much more efficient rate that any other co-crystallizing mineral phase. However, the required melt saturation of garnet components did not develop initially after the formation of the schorl line, but came later after a sequence of very coarse graphic granite. The schorl line also reflects significant boron enrichment early in the crystallization history, which still existed while the garnet line formed; schorl is a co-crystallizing phase in this layer.

A puzzling aspect of the garnet line from Mt. Apatite and Mt. Mica is its position within the pegmatite body. The fabric forms along the footwall wall zone portion of the dike and may develop from issues dealing with thermal gradient, much like the aplite portions of pegmatites are commonly observed in the footwall sections of zoned pegmatites, which represent the most undercooled portion of the pegmatite (London 2008). This is not to suggest that the garnet line crystallized under the same parameters. Garnet in T.H.I.T.G is observed in multiple zones; hangingwall wall zone, core, footwall wall zone, so it is evident that the garnet phase was able to crystallize through a range of zones. The question arises, why did the melt become significantly oversaturated in these essential structural components along the footwall portions of the dike? Unfortunately this paper is constrained to chemical interpretation, which is inadequate for a full interpretation of the reason for the garnet line position in the pegmatite. However, if a correlation can be made to what is known about line-rock aplite formation, then the garnet line boundary layer is the result of the oversaturation of garnet components in the melt. Lastly, it is necessary to mention that the two most well developed garnet lines occur in shallowly dipping (avg. 20-30°), but a structural correlation with the development of the garnet line is beyond the scope of this paper.

Pollucite occurrence:

Pollucite is one of the last minerals to crystallize in highly evolved granitic pegmatites (Teertstra and Černý 1997, London et *al.* 1998). This is due to Cs' highly incompatible nature in major rock forming minerals, e.g. feldspar (partition coefficient of 0.13, Icenhower and London 1996) and mica (partition coefficients of 0.16-0.24, London 2008). However, there are multiple examples of Cs-rich micas in granitic pegmatites and highly fractionated granites (Wang 2004), which suggest the mica species can be a reservoir for the alkali element.

Pollucite in the garnet line at Mt. Mica occurs within fractures and almost always occurs with mica (apart from some inclusions found in garnet). In these instances the mica is volumetrically of greater proportion (60-90%). The micas in these fracture fillings have a Cs_2O component up to 0.484 wt% Cs_2O, unlike the compositions reported of the mica crystals within the garnet line from Marchal *et al.* (2014) and more than any other micas analyzed in this study. Cesium is not an element that is readily incorporated in the mica structure so the nature of the late stage residual fluid must have been considerably enriched in this component. Furthermore, the pollucite reported in this study is unique due to the high Fe (up to 5.11 wt% Fe_{tot}) component. There is no documentation of Fe content this high in pollucite, reports generally fall below detection limits and the highest concentration known to the author are 0.11 wt% FeO from the Yichun topaz-lepidolite granite in southern, China (Wang *et al.* 2004) . It is evident that the residual melt that made the Cs-enriched micas and Fe-rich pollucite was fracture controlled and crystallized in a hydrous disequilibrium state.

Conversely, the abundance of Fe may be a consequence of microbeam analysis technique and the fact that these veinlets of pollucite are very small and very close to iron-bearing mineral phases: mica, garnet and tourmaline, though careful precautions are taken to prevent this. The EMPA calculate the total iron in the sample without differentiating FeO from Fe_2O_3. Within the Si/Al versus CRK plot, the majority of the samples plot outside the projected field of the data sets found in the literature (Fig 42). However, if assumed that Fe^{3+} is present in the EMPA calculations then it could satisfy the charge in the Y-site in place of Al, which on average is low in these samples (0.765 apfu). With Fe^{3+} correction to the EMPA analysis the Y-site totals average 0.894 apfu and fall into the ranges reported by Černý *et al.* 2012, Wang *et al.* 2004 and references therein. Iron and Al substitution has been reported in synthesized pollucite and the product is found to be a stable compound (Kume and Koizumi 1965, Brovetto *et al.* 1995, Rodriguez *et al.* 2013). However, no naturally occurring examples have been reported. Furthermore, the problem remains that all magmatic Fe-bearing mineral species in association with the garnet line at Mt. Mica contain Fe^{+2}. Why would this one particular phase have Fe^{+3}? Perhaps the hydrothermal conditions that produced the late stage fluid had some impact on the oxidation of iron.

London (1998) proposes that high concentrations of Cs coupled with other fluxing components (B, F and P) could produce an immiscible two-phase melt, he has suggested that this may be responsible for some of the zoning in the Tanco pegmatite in Manitoba, Canada. The pollucite in the Mt. Mica garnet line occurs with mica in fracture fillings and can be interpreted to have crystallized after the mica, once the concentration of Cs reached saturation to begin precipitating pollucite. However, the author suggests that the two species may have crystallized simultaneously. Textural observations indicate that the two

phases have sharp contacts with one another and do not appear as mixing. There is potential a case for mingling between the two phases (see Fig. 21a), which may be a dissolution texture of the preexisting phase, here the mica is interpreted to have crystallized first. However, even with the latest example the grain boundaries between the two phases are sharp and well defined.

REE phosphates:

Xenotime is a common HREE-bearing accessory phosphate mineral found in igneous rocks, particularly in peraluminous granites (Hetherington et *al.* 2008, Förster 1998). It is also found in many granitic pegmatites worldwide (Hetherington et *al.* 2008, Masau et *al.* 2000, Åmli 1975). However, until now its occurrence have never been reported before from any of the Oxford County pegmatites.

Monazite is a Ce, LREE bearing accessory phosphate that commonly occurs in a range of rock types (Hetherington and Harlov 2008) and this thesis reports the first occurrence in Oxford County pegmatites. The examples from Mt. Apatite and the Tamminen display dissolution- reprecipitation textures (Figs. 27a and 30). Without any evidence of post-pegmatite deformation these textures and inclusions likely developed from the presence of a reactive fluid, which developed within the pegmatite. The fluid partially dissolved the preexisting phosphate and reprecipitated a new mineral assemblage of apatite and Th-inclusions.

The monazites in the sampled locations are generally metamict, which is a common occurrence in minerals that contain radiogenic elements. Thorium and U are the two radiogenic elements found in monazite and xenotime. Metamictization affects the structural integrity of the mineral by damaging the crystallographic lattice and effectively creating pore space within the crystal. The pores serve as channels and nucleation and growth sites for metasomatized fluids (Hetherington and Harlov 2008).

Tourmaline rims at Mt. Mica

The tourmaline rims along the garnet crystal margins are an intriguing texture. Buřival and Novák (2014) describe an occurrence from the Sahatany Valley, Madagascar and claim that such growth is potentially the result of hydrothermal alteration of the garnet by late stage fluids that developed in the final stages of pegmatite crystallization and base their estimation with a potential replacement reaction:

$$24NaAlSi_3O_8 + 3\ (Mn_{1.6}Fe_1Ca_{0.4})Al_2Si_3O_{12} + 12\ H_3BO_3 + 2\ LiF \Rightarrow 4(Na_{0.5}Ca_{0.3}\square_{0.2})(Al_{1.5}Fe_{0.75}Li_{0.5}Mn_{0.25})Al_6(Si_6O_{18})(BO_3)_3(OH_{3.5}F_{0.5}) + 46SiO_2 + 11Na_2SiO_3 + 3.8MnO_2 + 0.4O + 9H_2O + 4H^+$$

Texturally, the results in this thesis may support their claim. Where the tourmaline rims are present, the garnet crystal margins are corroded. Sub-rounded fragments of garnet are often entrapped in the tourmaline rims and appear as though they have been partially dissolved. This is undeniably a dissolution texture postdating the crystallization of the garnet. There are two possible origins for the formation of this unique texture. (1) The

formation of garnet would have forced the non-essential components away from the crystallizing surface. This action could eventually oversaturate the melt with fluids rich in volatiles and other incompatible elements (F, B, H_2O, P, Li, Rb, Cs) that do not fit in the garnet structure or any other co-crystallizing mineral phases like quartz and feldspar. Apart from mica and schorl there are no other reservoirs to remove these components from the melt. The resulting composition of the melt at the boundary between crystals and melt, produced by crystal fractionation, would be capable of reacting with preexisting mineral phases if the melt became enriched in the previously mentioned volatile components. It is obvious that the melt, which favored the dissolution of the garnet, was saturated in these components given that these precipitated phases are enriched in these components. Furthermore, tourmaline fracture fillings are commonly seen connected to the tourmaline rims. A substance capable of migrating into those micron-sized fractures would need to have an extremely low viscosity, which melts with high concentrations of volatiles can achieve. (2) The reactive fluid may have migrated from a nearby source within the dike and the highly fractured garnets provided the proper conduit for such transport. 'Secondary' quartz, tourmaline and micas alike are not only restricted to the intercrystalline margins as rims around garnet, but are commonly found within the fractured core regions of garnet crystals. Therefore, these secondary phases were injected and proceeded to nucleate much later, after the magmatic garnet had crystallized and most likely reacted with the garnet for entirety of their residence within the fractures (note the dissolved crystal surfaces and entrapped garnet crystal fragments in Fig 17). Furthermore, field investigations suggest that the tourmaline rimming texture is localized, occurring near Li-rich/pocket zones. These areas within the pegmatite are far more enriched in

incompatible elements capable of producing a hydrothermal phase. The idealized interpretation of fluid migration is illustrated in Fig. 50.

The color zones seen with some tourmaline overgrowths, is a consequence of garnet dissolution and a result of preferential accommodation of Fe over Mn in the tourmaline (London *et al.* 2001). Tourmaline chemistry changes from a Fe-dominant species (proximal), to a Mn-Fe (distal). X-ray map (Fig. 17c & d) and EPMA are evidence for this; black (proximal) rim: FeO= 12.665 wt%, MnO= 0.870wt%, blue (distal) rim: FeO= 5.082 wt%, MnO= 1.279 wt%. The proximal rim plots in the schorl field, while the distal rim falls into the elbaite, which allows for the accommodation of Mn (London *et al.* 2001, London 2008).

Recent field investigations by the author have uncovered the presence of a garnet line beneath the pocket zone at the Havey quarry. These garnets have bi-colored tourmaline rims. Unfortunately due to time constraints these examples are not detailed in this study as it only includes garnet analysis from a schorl line at the Havey quarry. If researched in the future they will add to the knowledge of this unique texture and the capabilities of highly reactive fluids on primary mineral phases.

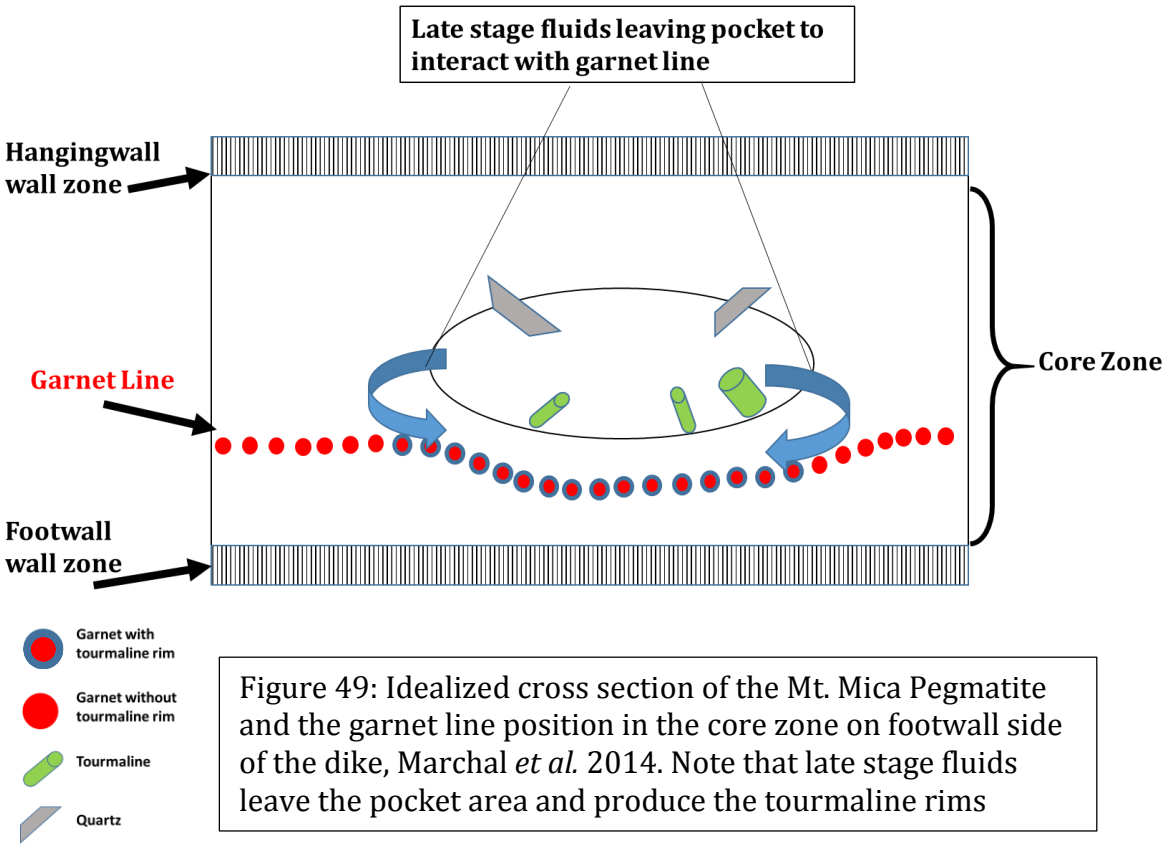

Figure 49: Idealized cross section of the Mt. Mica Pegmatite and the garnet line position in the core zone on footwall side of the dike, Marchal *et al.* 2014. Note that late stage fluids leave the pocket area and produce the tourmaline rims

Localized replacement textures in the garnet line at Mt. Mica:

The peculiar, unique and localized yellow-green muscovite and sulfide rims around garnet tell an interesting story. The presence of this assemblage is an indication of post-crystallization hydrothermal replacement in strongly reducing conditions. The highly reactive fluid partially dissolved the garnets in the garnet line (see corroded crystal margin, Fig. 18) and what may have been tourmaline rims; tourmaline rims are not found in this

region of the garnet line. The fluid phase responsible for this is a result of prolonged differentiation in the melt and is not meteoric, most importantly this occurs in only one region of the dike. Therefore, it is another example of the extreme chemical heterogeneity found along dip within the Mt. Mica pegmatite.

Conclusions

In each case where a well-developed garnet boundary layer (Mt. Mica and Mt. Apatite) or discontinuous garnet 'stringers' (Emmons, Tamminen) are found in the Oxford County pegmatites, HFSE-bearing micro-inclusions and one or more REE-bearing phosphate(s) exist in close relation to the garnets. It is unknown at this time if similar examples of these micro inclusions exist in other areas of the pegmatite, but their presence in these zones suggest that during the formation of the boundary layer the melts were highly evolved and that the garnet line is far more complex than previously assumed.

The garnet line at Mt. Mica and Mt. Apatite show a range of chemical and physical variation. At Mt. Mica chemical heterogeneity is prevalent within the garnet line. Along the fabric, garnets occur with no tourmaline rims, mono-colored (black) or bi-colored rims (black/blue) and rims with pyrite and muscovite. Miners have noted that areas where pockets develop and there is Li-mineralization, there is a tendency for garnets to have tourmaline rims (often bi-colored), whereas in barren (pocket-free) zones garnets do not display this texture (Gary Freeman person comm. 2014). The occurrence of these textures and assemblages suggest a late stage metasomatic fluid, enriched in Cs, F, Rb, H_2O, replaced

preexisting mineral phases within the garnet line at Mt. Mica. At Mt. Apatite the greatest difference is the range in thickness of the garnet line from different portions along the pegmatite. Each of these pegmatites reflect the extreme chemical heterogeneity associated with highly evolved melts. The smaller discontinuous garnet 'stringers' also show this process as they are restricted to single portions of the dike.

References:

ÅMLI, R. (1975) Mineralogy and rare earth geochemistry of apatite and xenotime from the Gloserheia granite pegmatite, Froland, Southern Norway. *American Mineralogist*, **60**, 607-620.

BALDWIN, J. R., VON KNORRING, O. (1983) Compositional range of Mn-garnet in zoned granitic pegmatites. *Canadian Mineralogist*. **21**, 683-688.

BASTIN, E. S. (1911) Geology of the pegmatites and associated rocks of Maine including feldspar, quartz, mica, and gem deposits. *United States Geological Survey Bulletin 445*.

BITNER, J., HEIMANN, A., WISE, M. A., RODRIGUES SOARES, D., & MOUSINHO FERREIRA, A. (2011) Garnet and gahnite from the Borborema pegmatite province, northeastern Brazil, as indicators of pegmatite evolution and potential for rare-metal mineralization. Abstracts With Programs - Geological Society Of America, **43**(5), 413.

BRADLEY, D.C., BUCHWALDT, R., SHEA, E., BOWRING, S., O'SULLIVAN, P., BENOWITZ, J., MCCAULEY, A., & BRADLEY, L.M. (2013): Geochronology and orogenic context of Northern Appalachian lithium-cesium-tantalum pegmatites: *Geological Society of America* Abstracts 45(1), 108.

BROVETTO, P., MAXIA, V., SALIS, M., BORLERA, M.L., MAZZA, D. (1995) A study by Mössbauer spectroscopy of iron-pollucite. *Il Nuovo Cimento D* **17**(9), 1079-1082.

BUŘIVAL, Z., NOVÁK, M. (2014) Hydrothermal replacement of garnet by tourmaline-an example from LCT pegmatites in the Sahatany Valley, Madagascar. *4th Central European Mineralogical Conference Skalský Dv**ůr**, Czech Republic: Book of Abstracts*. 17-18.

CAMERON, E. N. LARRABEE, D. M., MCNAIR, A. H., PAGE, J. J., STEWART, G. W., SHAININ, V. E. (1954) Pegmatites investigations 1942-45, in New England. *U.S. Geological Survey Professional Paper 225*.

ČERNÝ, P., ERCIT, T.S. (1989) Mineralogy of niobium and tantalum: crystal chemical relationships, paragenetic aspects and their economic implications. Lanthanides, Tantalum and Niobium: Special Publication No. 7 of the Society of Geological Applied to Mineral Deposits **7**, 27-79.

ČERNÝ, P., ERCIT, T.S. (2005) The classification of granitic pegmatites revisited. *The Canadian Mineralogist* **43**, 2005-2026.

ČERNÝ, P., LONDON, D., NOVÁK, M. (2012) Granitic pegmatites as reflections of their sources. *Elements* **8**(4), 289-294.

ČERNÝ, P., TEERTSTRA, D.K., CHAPMAN, R., SELWAY, J.B., HAWTHORNE F.C., FERREIRA, K., CHACKOWSKY, L.E., WANG, X., MEINTZER, R.E. (2012) Extreme fractionation and deformation of the leucogranite-pegmatite suite at red cross lake, Manitoba, Canada. IV. Mineralogy. *The Canadian Mineralogist* **50**, 1839-1875.

CREASY, J. W. (1979) Reconnaissance bedrock geology of the Poland quadrangle, Maine. Maine Geological Survey Department of Conservation. Open File No. 79-15.

DEER, W.A., HOWIE, R.A., ZUSSMAN, J. (1992) *An introduction to the rock-forming minerals*- 2nd ed. 549.

Dunn, P. J. (1975) Personality Sketch: Frank Perham pegmatite miner, geologist and humorist. *The Mineralogical Record* **6**(3): 105.

FOORD, E. E. (1997) The Himalaya dike system, Mesa Grande district, San Diego County, California. *Mineralogical Record* **8**, 461-474.

FÖRSTER, H. J. (1998) The chemical composition of REE-Y-Th-U-rich accessory minerals in peraluminous granites of the Erzgebirge-Fichtelgebirge region, Germany. Part II: xenotime. *American Mineralogist* **83**, 1302-1315.

FRANCIS, C.A., WISE, M.A., KAMPF, A.R., BROWN, C.D. & WHITMORE, R.W. (1993) Granitic pegmatites in northern New England. Field Trip Guidebook or the Northeastern United States: 1993 Boston GSA, E1- E24.

GADAS, P., NOVÁK, M., TALLA, D., GALIOVÁ, M. V. (2013) Compositional evolution of grossular garnet from leucotonalitic pegmatite at Ruda nad Moravou, Czech Republic; a complex EMPA, LA-ICP-MS, IR and CL study. *Mineralogy and Petrology* **107** (2) 311-326.

GREW, E. S., CARSON, C. J., & YATES, M. G. (2004) Diverse borosilicate assemblages in anatectic granitic pegmatites cutting boron-rich granulite-facies rocks of the Larsemann Hills, Prydz Bay, East Antarctica. *Abstracts With Programs - Geological Society Of America* **36**(5), 115.

GUIDOTTI, C. V., JOHNSON, S. E. (2002) Pseudomorphs and associated microstructures of western Maine, USA. *Journal of Structural Geology* **24**, 1139-1156.

HAMLIN, A. (1895) The history of Mount Mica of Maine, U.S.A., and its wonderful deposits of matchless tourmalines. United States: Publisher unknown : Bangor, ME, United States.

HENRY, D.J., NOVÁK, M., HAWTHORNE, F.C., ERTL, A., DUTROW, B.L., UHER, P., PEZZOTTA, F. (2011) Nomenclature of the tourmaline-supergroup minerals. *American Mineralogist* **96**, 895-913.

HETHERINGTON, C. J., HARLOV, D.E. (2008) Metasomatic thorite and uraninite inclusions in xenotime and monazite from granitic pegmatites, Hindra anorthosite massif, southwestern Norway: Mechanics and fluid chemistry. *American Mineralogist* **93**, 806-820.

HETHERINGTON, C. J., JERCINOVIC, M. J., WILLIAMS, M. L., MAHAN, K. (2008) Understanding geologic processes with xenotime: Composition, chronology, and a protocol for electron probe microanalysis. *Chemical Geology* **254**, 133-147.

HOLDAWAY, M. J., DUTROW, B.L., HINTON, R.W. (1988) Devonian and Carboniferous metamorphism in west-central Maine: The muscovite-almandine geobarometer and the staurolite problem revisited. *American Mineralogist* **73**, 20-47.

HÖNIG, S., LEICHMANN, J., NOVÁK, M. (2011) Magmatic layering (unidirectional solidification textures and Y-enriched garnet train textures) in aplite- pegmaties of the Cadomian Brno Batholith, Czech Republic. *Asociación Geológica Argentina: Contributions to the 5th International Symposium on Granitic Pegmatites, Mendoza Argentina.*

HÖNIG, S., LEICHMANN, J., NOVÁK, M. (2010) Unidirectional solidification textures and garnet layering in the Y-enriched aplite-pegmatites in Cadomian Brno Batholith, Czech Republic. *Journal of Geosciences* **55**, 113-129.

HUBERTY, J., BROWN, P. (2007) A fluid inclusion study of Mt. Apatite, Maine: implications for pematite formation. Pan-American Conference on Fluid Inclusions (PACROFI) IX program abstracts 9:32, Reston, VA.

ICENHOWER, J., LONDON, D. (1996) Experimental partitioning of Rb, Cs, Sr, and Ba between alkali feldspar and peraluminous melt. *American Mineralogist* **81**, 719-734.

JAFFE, H.W. (1951) The role of yttrium and other minor elements in the garnet group. *American Mineralogist* **36**, 133-155.

JOHNSON, C.M. (2013) A study of heavy minerals found in a unique carbonate assemblage from the Mt. Mica pegmatite, Oxford County, Maine. *Senior Honors Theses.* Paper 36.

KUME, S., KOIZUMI, M. (1965) Synthetic pollucites in the system $Cs_2O{\cdot}Al_2O_3{\cdot}4SiO_2{\cdot}Fe_2O_3{\cdot}4SiO_2$-$H_2O$- Their phase relationship and physical properties. *American Mineralogist* **50**, 587-592.

LAURS, B.M., KNOX, K. (2001) Spessartine garnet from Ramona, San Diego County, California. *Gems & Geology* **34**(4), 278-295.

LONDON, D. (2008) *Pegmatites*: The Canadian Mineralogist Special Publication 10, 347.

LONDON, D., EVENSEN, J.M., FRITZ, E., ICENHOWER, J.P., MORGAN, G.B., WOLF, M.B. (2001) Enrichement and accommodation of manganese in granite-pegmatite systems. Eleventh Annual V. M. Goldschmidt Conference, Abstract #3369.

LONDON, D., MORGAN, G.B., ICENHOWER, J. (1998) Stability and solubility of pollucite in the granite system at 200 MPa H_2O. *The Canadian Mineralogist* **36**(2), 497-510.

MACLEOD, G. (1992) Zoned Manganiferous garnets of magmatic origin from the Southern Uplands of Scotland. *Mineralogical Magazine* **56**, 115-116.

MARCHAL, K.L., SIMMONS, W.B., FALSTER, A.U., WEBBER, K.L. (2014) Geochemistry, mineralogy, and evolution of Li-Al micas and feldspars from the Mount Mica pegmatite, Maine, USA. *The Canadian Mineralogist* **52**: 2, 221-233.

MARTIN, R.F., DE VITO, C. (2005) The pattern of enrichment in felsic pegmatites ultimately depend on tectonic setting. *The Canadian Mineralogist* **43**, 2027-2048.

MASAU, M., ČERNÝ,, P., CHAPMAN, R. (2000) Dysprosian Xenotime-(Y) from the Annie Claim #3 granitic pegmatite, Southeastern Manitoba, Canada: Evidence of the tetrad effect?. *The Canadian Mineralogist* **38**, 899-905.

MCCAULEY, A., BRADLEY, D. (2013) The secular distribution of granitic pegmatites and rare-metal pegmatites. *PEG 2013: The 6th International Symposium on Granitic Pegmatites Abstracts*. 92-92.

MCCAULEY, A., BRADLEY, D. (2014) The global age distribution of granitic pegmatites. *The Canadian Mineralogist* **52**, 183-190.

MOENCH, R.H., ALEINIKOFF, J.N. (2003) Stratigraphy, geochronology, and accretionary terrane settings of two Bronson Hill arc sequences, northern New England. *USGS Staff—Published Research.* Paper 436.

MÜLLER, A., IHLEN, P. M., LARSEN, R. B., SPRATT, J., SELTMANN, R. (2009) Quartz and garnet chemistry of south Norwegian pegmatites and its implications for pegmatite genesis. *Estudos Geológicos* **19**, 20-24.

MÜLLER, A., KEARSLEY, A., SPRATT, J., SELTMANN, R. (2012) Petrogenetic implications of magmatic garnet in granitic pegmatites from southern Norway. *Canadian Mineralogist*. **50**, 1095-1115.

NĚMEC, D. (1983) Masutomilite in lithium pegmatites of West-Moravia, Czechoslovakia. *N. Jb. Miner. Mh. H.* **12**, 537-540.

PANKIWSKYJ, K. A. (1978) Reconnaissance bedrock geology of the Buckfield quadrangle, Maine. Maine. Maine Geological Survey Department of Conservation. Open File No. 78-18.

REUSCH, D. N., VAN STAAL, C. R. (2012) The Dog Bay-Liberty Line and its significance for Silurian tectonics of the Northern Appalachian Orogen. Canadian Journal of Earth Sciences **49**(1), 239-258.

ROCHESTER, N. (1997) Mt. Apatite Tourmalines. *Rock and Gem*, 28-31.

RODA-ROBLES, E., SIMMONS, W., NIZAMOFF, J., PESQUERA, A., GIL-CRESPO, P. P., TORRES-RUIZ, J. (2011) Chemical variation in tourmaline from the Berry-Havey pegmatite (Maine, USA), and implications for pegmatitic evolution. *Asociación Geológica Argentina: Contributions to the 5th International Symposium on Granitic Pegmatites, Mendoza Argentina. No. 14: 165-168.*

RODRIGUEZ, M.A., GARINO, T.J., RADEMACHER, D.X., ZHANG, X., NENOFF, T.M. (2013) The synthesis of Ba- and Fe- substituted $CsAlSi_2O_6$ pollucites. *Journal of the American Ceramic Society* **96**(9), 2966-2972.

ROSE, T. R., WISE, M., BROWN, C. (1997) Renewed mining at the Western quarries of Mount Apatite, Maine. *Rocks & Minerals*, **72**, January/February, 44-48.

SELWAY, J.B., NOVÁK, M., ČERNÝ, P., HAWTHORNE, F.C. (1999) Compositional evolution of tourmaline in lepidolite-subtype pegmatites. *European Journal of Mineralogy* **11**(3), 569-584

SIRBU, S., BUZGAR, N., & KASPER, H. (2010) Geochemistry of selected garnets in pegmatites from the Razoare Formation (Preluca Mountains, Romania). Analele Stiintifice Ale Universitati "Al.I.Cuza" Din Iasi. Sectiunea II B. Geologie **56**(2), 109-121.

SIMMONS, W.B. (2007) Pegmatite genesis: recent advances and areas for future research. *Granitic Pegmatites: The State of the Art – International Symposium. 06th-12th May 2007, Porto, Portugal.*

SIMMONS, W. B., LAURS, B. M., FALSTER, A. U., KOIVULA, J. I., WEBBER, K. L. (2006) Mt. Mica: A renaissance in Maine's gem tourmaline production. *Gems & Geology*.

SIMMONS, W.B., PEZZOTTA, F., SHIGLEY, J.E., BEURLEN, H. (2012) Granitic pegmatites as sources of colored gemstones. *Elements* **8**, 281-287.

SMITH, H. A. BARREIRO, B. (1990) Monazite U-Pb dating of staurolite grade metamorphism in pelitic schists. *Contributions to Mineralogy and Petrology* **105**, 602-615.

SOLOLOV, Y.M, KHLESTOV, V.V. (1990) Garnets as indicators of the physicochemical conditions of pegmatite formation. "Granaty-indikatory fiziko-khimicheskikh usloviy obrazovaniya pegmatitov," *Geologiya rudnykh mestorozhdeniy* **5**, 19-31.

SOLAR, G.S., BROWN, M. (2001) Petrogenesis of migmatites in Maine, USA: possible source of peraluminous leucogranite in plutons? *Journal of Petrology* **42**(4), 789-823.

SOLAR, G. S., PRESSLEY, R. A., BROWN, M., TUCKER, R. D. (1998) Granite ascent in convergent orogenic belts: testing a model. *Geology* **26**, 711-714.

SWANSON, S. E. (2012) Mineralogy of spodumene pegmatites and related rocks in the tin-spodumene belt of North Carolina and South Carolina, USA. *Canadian Mineralogist*. **50**, 1589-1608.

TEERTSTRA, D.K., ČERNÝ, P. (1997) The compositional evolution of pollucite from African granitic pegmatites. *Journal of African Earth Sciences* **25**(2), 317-331.

TEERTSTRA, D.K., ČERNÝ, P., CHAPMAN, R. (1992) Compositional heterogeneity of pollucite from high grade dyke, Maskwa Lake, Southeastern Manitoba. *The Canadian Mineralogist* **30**, 687-697.

TISCHENDORF, G (1997) On Li-bearing micas: estimating Li from electron microprobe analyses and an improved diagram for graphical representation. *Mineralogical Magazine* **61**, 809-834.

TOMASCAK, P. (1995) January 1. The petrogenesis of granitic rocks in southwestern Maine. PhD dissertation: University of Maryland.

TOMASCAK, P., KROGSTAD, E. J., WALKER, R. J. (1996) U-Pb monazite geochronology of granitic rocks from Maine: implications for late Paleozoic tectonics in the northern Appalachians. *Journal of Geology* **104**, 185-195.

TOMASCAK, P. B., BROWN, M., SOLAR, G. S., BECKER, H. J., CENTORBI, T. L., TIAN, J. (2005) Source contribution Devonian granite magmatism near the Laurentian border, New Hampshire and Western Maine, USA. *Lithos* **80**, 75-99.

TOMASCAK, P. B., SOLAR, G. S. (2013) Age distinctions among granites and migmatites in southwestern Maine. Geological Society of America *Abstracts with Programs* **45**(1), 96.

WANG, R.C., HU, H., ZHANG, A.C., HUANG, X.L., NI, P. (2004) Pollucite and the cesium-dominant analogue of polylithionite as expressions of extreme Cs enrichment in the Yichun topaz-lepidolite granite, southern China. *The Canadian Mineralogist* **42**, 883-896.

WEBBER, K. L., FALSTER, A. U., SIMMONS, W. B., FOORD, E. E. (1997) The role of diffusion-controlled oscillatory nucleation in the formation of line rock in pegmatite-aplite dikes. *Journal of Petrology* **38**(12), 1777-1791.

WISE, M., BROWN, C. E. (2010) Mineral chemistry, petrology and geochemistry of the Sebago granite-pegmatite system, southern Maine, USA. *Journal of Geosciences* **55**, 3-26.

WISE, M.A., FRANCIS, C.A. (1992) Distribution, classification and geological setting of granitic pegmatites in Maine. *Northeastern Geology* **14**(2&3), 82-93.

WISE, M. A., ROSE, T. R. (2000) The Bennett pegmatite, Oxford County, Maine. *Maine Geological Survey Mineralogy of Maine* **2**, 323-332.

WOLF, M.B., LONDON, D. (1997) Boron in granitic magmas: stability of tourmaline in equilibrium with biotite and cordierite. *Contributions to Mineralogy and Petrology* **130**, 12-30.

Appendix

Garnet analyses Table 15: Garnet compositions from all garnet line layer samples, Mt-Mt. Mica, MA-Mt. Apatite, Em-Emmons, HVY-Havey, BT-Bennett, TM-Tamminen

Sample	MT1-2a-1	MT1-2a-2	MT1-2a-3	MT1-2a-4	MT1-2-k-6-1	MT1-2-k-6-2	MT1-2-k-6-3	MT1-2-m-1-1	MT1-2-m-1-2	MT1-2-m-1-3	MT4-1-a-3-1
P_2O_5	0.08	0.08	0.07	0.08	0.07	0.07	0.09	0.10	0.04	0.07	0.11
SiO_2	36.34	36.34	36.39	36.43	36.44	36.41	36.39	36.40	36.39	36.41	36.34
TiO_2	0.00	0.01	0.02	0.00	0.01	0.00	0.00	0.00	0.00	0.01	0.00
Al_2O_3	20.60	20.60	20.54	20.61	20.56	20.56	20.61	20.52	20.43	20.63	20.50
FeO	21.68	21.78	21.44	22.68	22.78	22.82	22.78	24.51	24.22	25.40	22.87
MnO	21.14	20.92	21.26	20.57	20.44	20.36	20.41	18.57	18.89	17.85	20.22
CaO	0.27	0.34	0.37	0.04	0.03	0.03	0.04	0.05	0.06	0.03	0.07
MgO	0.06	0.05	0.03	0.03	0.03	0.03	0.03	0.04	0.03	0.04	0.03
F	0.04	0.04	0.04	0.04	0.03	0.02	0.03	0.00	0.00	0.00	0.01
Subtotal	100.20	100.15	100.18	100.46	100.39	100.31	100.38	100.19	100.07	100.44	100.16
O=F	0.02	0.02	0.02	0.01	0.01	0.01	0.01	0.00	0.00	0.00	0.01
Total	100.18	100.14	100.16	100.45	100.38	100.30	100.37	100.19	100.07	100.44	100.15
X-site											
Fe	1.493	1.500	1.477	1.559	1.567	1.571	1.567	1.689	1.672	1.747	1.577
Mn	1.475	1.460	1.483	1.432	1.424	1.419	1.422	1.296	1.321	1.243	1.412
Ca	0.023	0.030	0.032	0.004	0.003	0.003	0.003	0.004	0.006	0.003	0.006
Mg	0.007	0.006	0.004	0.003	0.004	0.004	0.004	0.005	0.004	0.005	0.003
X-total	2.998	2.995	2.996	2.997	2.998	2.997	2.996	2.994	3.003	2.998	2.998
Y-site											
Cr	0.000	0.000	0.000	0.000	0.000	0.000	0.000	0.000	0.000	0.000	0.000
Al	1.999	1.999	1.994	1.997	1.993	1.995	1.999	1.993	1.988	2.000	1.992
Y-total	1.999	1.999	1.994	1.997	1.993	1.995	1.999	1.993	1.988	2.000	1.992
Z-site											
Si	2.992	2.993	2.996	2.994	2.998	2.997	2.994	2.999	3.004	2.995	2.996
Ti	0.000	0.001	0.001	0.000	0.001	0.000	0.000	0.000	0.000	0.000	0.000
Z-total	2.992	2.994	2.998	2.994	2.998	2.997	2.994	2.999	3.004	2.995	2.996
spss.%	49.308	48.819	49.563	47.821	47.572	47.418	47.524	43.352	44.046	41.539	47.150
grss.%	0.782	1.015	1.082	0.118	0.097	0.091	0.106	0.133	0.189	0.100	0.198
alm.%	49.910	50.166	49.354	52.062	52.331	52.491	52.370	56.515	55.766	58.361	52.653

Table 15 cont.

Sample	MT4-1-a-3-2	MT4-1-a-3-3	MT4-1-a-3-4	MT4-1-f-1	MT4-1-f-2	MT4-1-f-3	MT4-1-f-4	MT4-1-f-5	MT4-1a-3-1	MT4-1a-3-2	MT4-1a-3-3
P_2O_5	0.13	0.13	0.13	0.13	0.14	0.12	0.09	0.09	0.06	0.08	0.08
SiO_2	36.41	36.37	36.38	36.43	36.44	36.41	36.42	36.51	36.44	36.46	36.51
TiO_2	0.00	0.00	0.00	0.01	0.01	0.01	0.01	0.01	0.01	0.00	0.00
Al_2O_3	20.49	20.52	20.60	20.52	20.58	20.57	20.60	20.69	20.62	20.61	20.59
FeO	22.91	22.82	22.95	22.67	22.22	22.45	22.71	23.43	23.28	23.34	23.29
MnO	20.12	20.37	20.12	20.46	20.82	20.56	20.33	19.89	19.89	19.77	19.81
CaO	0.08	0.11	0.11	0.12	0.14	0.09	0.14	0.10	0.14	0.11	0.16
MgO	0.03	0.02	0.02	0.02	0.01	0.03	0.03	0.04	0.02	0.05	0.04
F	0.03	0.03	0.03	0.06	0.06	0.05	0.05	0.00	0.04	0.05	0.09
Subtotal	100.20	100.36	100.35	100.41	100.42	100.29	100.38	100.77	100.51	100.46	100.57
O=F	0.01	0.01	0.01	0.02	0.02	0.02	0.02	0.00	0.02	0.02	0.04
Total	100.19	100.35	100.33	100.39	100.40	100.27	100.35	100.77	100.49	100.44	100.53
X-site											
Fe	1.578	1.571	1.579	1.559	1.526	1.544	1.562	1.606	1.600	1.604	1.599
Mn	1.404	1.420	1.402	1.424	1.449	1.433	1.416	1.381	1.384	1.376	1.377
Ca	0.007	0.010	0.010	0.011	0.013	0.008	0.013	0.009	0.013	0.010	0.014
Mg	0.004	0.002	0.003	0.003	0.002	0.004	0.003	0.005	0.003	0.006	0.005
X-total	2.992	3.003	2.993	2.996	2.990	2.989	2.993	3.001	3.000	2.995	2.994
Y-site											
Cr	0.000	0.000	0.000	0.000	0.000	0.000	0.000	0.000	0.000	0.000	0.000
Al	1.989	1.991	1.997	1.989	1.992	1.994	1.996	1.998	1.997	1.996	1.991
Y-total	1.989	1.991	1.997	1.989	1.992	1.994	1.996	1.998	1.997	1.996	1.991
Z-site											
Si	2.999	2.993	2.992	2.995	2.994	2.996	2.994	2.992	2.994	2.995	2.996
Ti	0.000	0.000	0.000	0.000	0.001	0.000	0.000	0.001	0.001	0.000	0.000
Z-total	2.999	2.993	2.992	2.996	2.995	2.996	2.995	2.993	2.995	2.995	2.996
spss.%	46.969	47.317	46.878	47.578	48.493	47.994	47.353	46.095	46.193	46.028	46.065
grss.%	0.224	0.326	0.321	0.359	0.424	0.275	0.421	0.296	0.423	0.333	0.459
alm.%	52.807	52.356	52.801	52.063	51.082	51.731	52.226	53.609	53.384	53.639	53.476

Table 15 cont.

Sample	MT2-3-a-2-1	MT2-3-a-2-2	MT2-3-a-2-3	MT2-3-a-2-4	MT2-3-a-2-5	MT2-3-a-2-6	MT6-1-a-1	MT6-1-a-2	MT6-1-a-3	MT6-1-a-4	MT6-1-a-5
P_2O_5	0.10	0.08	0.09	0.11	0.09	0.10	0.09	0.10	0.10	0.10	0.09
SiO_2	36.37	36.41	36.39	36.40	36.43	36.48	36.36	36.56	36.37	36.40	36.41
TiO_2	0.01	0.00	0.00	0.01	0.00	0.00	0.01	0.00	0.01	0.01	0.00
Al_2O_3	20.61	20.59	20.60	20.64	20.63	20.59	20.62	20.67	20.60	20.61	20.63
FeO	14.83	14.44	14.62	14.36	16.31	17.23	26.00	26.12	25.86	26.13	26.29
MnO	27.89	28.32	28.10	28.43	26.43	25.54	16.43	16.68	16.56	16.45	16.22
CaO	0.33	0.33	0.35	0.34	0.40	0.42	0.28	0.26	0.34	0.28	0.31
MgO	0.00	0.00	0.01	0.00	0.00	0.00	0.22	0.25	0.22	0.20	0.25
F	0.21	0.23	0.22	0.21	0.07	0.05	0.00	0.00	0.00	0.00	0.00
Subtotal	100.35	100.41	100.39	100.50	100.37	100.40	100.02	100.63	100.05	100.18	100.21
O=F	0.09	0.10	0.09	0.09	0.03	0.02	0.00	0.00	0.00	0.00	0.00
Total	100.26	100.31	100.29	100.41	100.34	100.38	100.02	100.63	100.05	100.18	100.21
X-site											
Fe	1.019	0.992	1.004	0.984	1.120	1.183	1.791	1.790	1.781	1.798	1.808
Mn	1.940	1.969	1.954	1.975	1.839	1.777	1.147	1.157	1.155	1.146	1.130
Ca	0.029	0.029	0.031	0.030	0.035	0.037	0.025	0.022	0.030	0.025	0.027
Mg	0.000	0.000	0.001	0.000	0.000	0.000	0.027	0.031	0.027	0.024	0.031
X-total	2.988	2.990	2.990	2.989	2.994	2.997	2.990	3.000	2.993	2.993	2.996
Y-site											
Cr	0.000	0.000	0.000	0.000	0.000	0.000	0.000	0.000	0.000	0.000	0.000
Al	1.995	1.992	1.993	1.995	1.997	1.992	2.002	1.996	1.999	1.999	2.000
Y-total	1.995	1.992	1.993	1.995	1.997	1.992	2.002	1.996	1.999	1.999	2.000
Z-site											
Si	2.987	2.989	2.988	2.985	2.992	2.995	2.995	2.995	2.995	2.995	2.994
Ti	0.001	0.000	0.000	0.001	0.000	0.000	0.001	0.000	0.001	0.001	0.000
Z-total	2.987	2.989	2.988	2.986	2.992	2.995	2.996	2.995	2.996	2.995	2.994
spss.%	64.922	65.868	65.375	66.072	61.411	59.280	38.705	38.973	38.941	38.613	38.117
grss.%	0.984	0.965	1.033	0.994	1.176	1.236	0.840	0.757	1.015	0.843	0.907
alm.%	34.094	33.167	33.592	32.934	37.414	39.484	60.455	60.270	60.045	60.544	60.976

Table 15 cont.

Sample	MT6-1-a-6	MT6-1-c-1	MT6-1-c-2	MT6-1-c-3	MT6-1-c-4	MT6-1-c-5	MT6-1-f-1	MT6-1-f-2	MT6-1-f-3	MT6-1-f-4	MT6-1-f-5
P_2O_5	0.11	0.15	0.09	0.07	0.11	0.11	0.12	0.09	0.08	0.07	0.10
SiO_2	36.35	36.37	36.40	36.41	36.39	36.33	36.41	36.36	36.33	36.41	36.45
TiO_2	0.00	0.00	0.00	0.00	0.01	0.01	0.00	0.00	0.00	0.00	0.00
Al_2O_3	20.59	20.59	20.61	20.61	20.62	20.60	20.66	20.66	20.57	20.67	20.69
FeO	26.07	24.00	23.73	22.90	23.54	23.82	22.60	23.66	17.22	19.43	22.87
MnO	16.35	18.67	18.75	19.56	19.11	18.77	20.22	19.23	25.45	23.33	20.22
CaO	0.37	0.28	0.41	0.39	0.31	0.22	0.31	0.29	0.28	0.30	0.29
MgO	0.24	0.18	0.20	0.20	0.13	0.21	0.10	0.09	0.11	0.09	0.11
F	0.00	0.03	0.04	0.05	0.00	0.00	0.05	0.03	0.00	0.05	0.02
Subtotal	100.07	100.27	100.23	100.17	100.24	100.08	100.47	100.41	100.05	100.34	100.75
O=F	0.00	0.01	0.02	0.02	0.00	0.00	0.02	0.01	0.00	0.02	0.01
Total	100.07	100.25	100.21	100.16	100.24	100.08	100.45	100.39	100.05	100.33	100.74
X-site											
Fe	1.795	1.650	1.632	1.575	1.619	1.641	1.552	1.626	1.187	1.335	1.567
Mn	1.140	1.300	1.305	1.362	1.331	1.309	1.406	1.339	1.776	1.624	1.404
Ca	0.032	0.025	0.036	0.034	0.027	0.020	0.027	0.026	0.025	0.026	0.025
Mg	0.030	0.022	0.025	0.024	0.016	0.026	0.012	0.011	0.014	0.011	0.014
X-total	2.998	2.997	2.998	2.996	2.995	2.995	2.997	3.002	3.002	2.997	3.010
Y-site											
Cr	0.000	0.000	0.000	0.000	0.000	0.000	0.000	0.000	0.000	0.000	0.000
Al	1.998	1.995	1.997	1.998	1.999	2.000	1.998	2.002	1.997	2.001	1.998
Y-total	1.998	1.995	1.997	1.998	1.999	2.000	1.998	2.002	1.997	2.001	1.998
Z-site											
Si	2.993	2.990	2.993	2.995	2.993	2.992	2.989	2.988	2.994	2.992	2.987
Ti	0.000	0.000	0.000	0.000	0.001	0.000	0.000	0.000	0.000	0.000	0.000
Z-total	2.993	2.990	2.993	2.995	2.994	2.993	2.989	2.988	2.994	2.992	2.987
spss.%	38.422	43.691	43.901	45.847	44.704	44.084	47.105	44.771	59.440	54.391	46.847
grss.%	1.085	0.835	1.221	1.151	0.923	0.663	0.919	0.860	0.839	0.885	0.844
alm.%	60.492	55.474	54.879	53.002	54.373	55.253	51.975	54.370	39.721	44.724	52.310

Table 15 cont.

Sample	MT6-1-f-6	MT6-1-h-1	MT6-1-h-2	MT6-1-h-3	MT6-1-h-4	MT6-1-h-5	MT6-1-h-6	MT6-1-h-7	MT6-1-h-8	MT6-1-h-9	MT6-1-i-1
P_2O_5	0.11	0.12	0.06	0.08	0.07	0.10	0.22	0.17	0.13	0.14	0.10
SiO_2	36.50	36.45	36.46	36.45	36.45	36.46	36.44	36.43	36.50	36.63	36.38
TiO_2	0.00	0.00	0.00	0.01	0.01	0.00	0.00	0.00	0.00	0.00	0.01
Al_2O_3	20.65	20.62	20.65	20.60	20.62	20.59	20.62	20.63	20.60	20.72	20.66
FeO	20.13	22.65	22.82	22.84	22.78	17.23	16.21	16.14	16.20	14.45	22.04
MnO	22.67	20.21	19.88	19.93	20.09	25.54	26.33	26.41	26.43	28.32	21.01
CaO	0.28	0.19	0.21	0.22	0.21	0.42	0.55	0.51	0.46	0.53	0.27
MgO	0.13	0.16	0.18	0.16	0.17	0.00	0.00	0.00	0.01	0.00	0.01
F	0.03	0.00	0.00	0.00	0.01	0.87	0.16	0.22	0.31	0.43	0.01
Subtotal	100.49	100.41	100.26	100.29	100.41	101.21	100.53	100.53	100.64	101.24	100.48
O=F	0.01	0.00	0.00	0.00	0.00	0.37	0.07	0.09	0.13	0.18	0.01
Total	100.48	100.41	100.26	100.29	100.41	100.85	100.47	100.43	100.51	101.06	100.48
X-site											
Fe	1.381	1.556	1.569	1.571	1.565	1.173	1.110	1.106	1.109	0.983	1.515
Mn	1.575	1.406	1.384	1.388	1.398	1.761	1.827	1.833	1.832	1.951	1.462
Ca	0.025	0.017	0.019	0.020	0.018	0.037	0.048	0.045	0.040	0.047	0.023
Mg	0.016	0.019	0.022	0.019	0.021	0.000	0.000	0.000	0.001	0.000	0.001
X-total	2.997	2.998	2.995	2.998	3.002	2.971	2.985	2.984	2.982	2.981	3.002
Y-site											
Cr	0.000	0.000	0.000	0.000	0.000	0.000	0.000	0.000	0.000	0.000	0.000
Al	1.996	1.996	2.001	1.996	1.997	1.975	1.991	1.992	1.987	1.987	2.000
Y-total	1.996	1.996	2.001	1.996	1.997	1.975	1.991	1.992	1.987	1.987	2.000
Z-site											
Si	2.994	2.994	2.997	2.997	2.994	2.968	2.985	2.985	2.987	2.980	2.989
Ti	0.000	0.000	0.000	0.000	0.000	0.000	0.000	0.000	0.000	0.000	0.000
Z-total	2.994	2.994	2.997	2.997	2.995	2.968	2.985	2.985	2.987	2.980	2.989
spss.%	52.835	47.201	46.578	46.608	46.895	59.280	61.200	61.424	61.466	65.455	48.734
grss.%	0.837	0.567	0.631	0.657	0.617	1.236	1.602	1.506	1.338	1.561	0.781
alm.%	46.327	52.232	52.791	52.735	52.488	39.484	37.197	37.069	37.195	32.984	50.485

Table 15 cont.

Sample	MT6-1-i-2	MT6-1-i-3	MT6-1-i-4	MT6-1-1-1	MT6-1-1-2	MT6-1-1-3	MT6-1-1-4	M T6-1-o-1	M T6-1-o-2	M T6-1-o-3	M T6-1-o-4
P_2O_5	0.09	0.14	0.13	0.20	0.14	0.16	0.14	0.11	0.19	0.21	0.19
SiO_2	36.40	36.41	36.45	36.51	36.45	36.41	36.44	36.50	36.49	36.52	36.49
TiO_2	0.00	0.00	0.01	0.01	0.01	0.00	0.00	0.00	0.00	0.00	0.00
Al_2O_3	20.62	20.65	20.66	20.64	20.63	20.57	20.65	20.68	20.70	20.66	20.68
FeO	22.57	22.57	22.45	22.57	22.55	21.91	22.98	21.46	21.22	21.76	20.81
MnO	20.21	20.40	20.31	20.56	20.61	21.09	20.11	21.45	21.81	21.09	22.09
CaO	0.41	0.28	0.41	0.22	0.21	0.20	0.20	0.37	0.35	0.40	0.38
MgO	0.00	0.00	0.01	0.02	0.02	0.02	0.02	0.00	0.00	0.02	0.00
F	0.00	0.00	0.00	0.00	0.02	0.03	0.01	0.04	0.05	0.04	0.05
Subtotal	100.30	100.46	100.42	100.73	100.64	100.39	100.57	100.59	100.82	100.70	100.68
O=F	0.00	0.00	0.00	0.00	0.01	0.01	0.01	0.01	0.02	0.02	0.02
Total	100.30	100.46	100.42	100.73	100.63	100.38	100.56	100.57	100.80	100.68	100.66
X-site											
Fe	1.552	1.550	1.542	1.546	1.547	1.506	1.577	1.471	1.452	1.490	1.425
Mn	1.408	1.419	1.413	1.426	1.432	1.468	1.398	1.489	1.512	1.463	1.532
Ca	0.036	0.025	0.036	0.019	0.018	0.017	0.018	0.032	0.031	0.035	0.033
Mg	0.000	0.000	0.001	0.003	0.002	0.003	0.003	0.000	0.000	0.002	0.000
X-total	2.997	2.994	2.992	2.994	3.000	2.994	2.996	2.993	2.995	2.989	2.991
Y-site											
Cr	0.000	0.000	0.000	0.000	0.000	0.000	0.000	0.000	0.000	0.000	0.000
Al	1.999	1.999	2.000	1.993	1.995	1.992	1.998	1.998	1.996	1.993	1.996
Y-total	1.999	1.999	2.000	1.993	1.995	1.992	1.998	1.998	1.996	1.993	1.996
Z-site											
Si	2.994	2.991	2.993	2.991	2.990	2.992	2.991	2.993	2.986	2.990	2.988
Ti	0.000	0.000	0.001	0.001	0.001	0.000	0.000	0.000	0.000	0.000	0.000
Z-total	2.994	2.991	2.993	2.991	2.990	2.992	2.991	2.993	2.986	2.990	2.988
spss.%	46.990	47.401	47.243	47.676	47.777	49.081	46.711	49.766	50.478	48.955	51.237
grss.%	1.212	0.829	1.209	0.651	0.613	0.574	0.588	1.074	1.036	1.174	1.106
alm.%	51.798	51.770	51.548	51.673	51.610	50.345	52.701	49.159	48.486	49.870	47.657

Table 15 cont.

Sample	MT-6-1-q-1	MT-6-1-q-2	MT-6-1-q-3	MT6-1-u-1	MT6-1-u-2	MT6-1-u-3	MT1-1-A-1	MT1-1-A-2	MT1-1-A-3	MT1-1-A-4	MT1-1-A-5
P_2O_5	0.19	0.32	0.23	0.09	0.17	0.21	0.10	0.08	0.06	0.08	0.08
SiO_2	36.34	36.40	36.38	36.50	36.48	36.54	36.40	36.41	36.38	36.41	36.38
TiO_2	0.01	0.01	0.01	0.00	0.00	0.00	0.00	0.01	0.00	0.00	0.02
Al_2O_3	20.62	20.60	20.64	20.70	20.67	20.68	20.60	20.58	20.52	20.43	20.51
FeO	23.54	24.34	23.78	15.11	15.85	15.03	20.89	20.82	21.09	21.34	21.09
MnO	19.57	18.76	19.22	27.66	26.89	27.79	22.34	22.23	22.19	21.90	22.09
CaO	0.21	0.19	0.18	0.53	0.48	0.52	0.30	0.31	0.30	0.28	0.32
MgO	0.02	0.02	0.04	0.01	0.00	0.00	0.04	0.03	0.03	0.03	0.03
F	0.01	0.00	0.00	0.28	0.31	0.26	0.03	0.05	0.03	0.03	0.03
Subtotal	100.52	100.64	100.48	100.88	100.85	101.04	100.71	100.52	100.60	100.50	100.56
O=F	0.01	0.00	0.00	0.12	0.13	0.11	0.01	0.02	0.01	0.01	0.01
Total	100.51	100.64	100.48	100.76	100.72	100.93	100.69	100.50	100.59	100.49	100.55
X-site											
Fe	1.617	1.668	1.633	1.033	1.082	1.025	1.433	1.430	1.450	1.468	1.450
Mn	1.361	1.302	1.337	1.914	1.860	1.919	1.553	1.547	1.545	1.526	1.538
Ca	0.019	0.017	0.016	0.047	0.042	0.046	0.026	0.027	0.026	0.025	0.028
Mg	0.003	0.003	0.005	0.001	0.000	0.000	0.005	0.004	0.004	0.004	0.003
X-total	3.000	2.990	2.990	2.994	2.985	2.990	3.018	3.009	3.024	3.022	3.019
Y-site											
Cr	0.000	0.000	0.000	0.000	0.000	0.000	0.000	0.000	0.000	0.000	0.000
Al	1.996	1.990	1.998	1.993	1.990	1.987	1.992	1.992	1.988	1.981	1.987
Y-total	1.996	1.990	1.998	1.993	1.990	1.987	1.992	1.992	1.988	1.981	1.987
Z-site											
Si	2.985	2.984	2.986	2.982	2.980	2.980	2.986	2.991	2.990	2.995	2.990
Ti	0.001	0.000	0.001	0.000	0.000	0.000	0.000	0.001	0.000	0.000	0.001
Z-total	2.986	2.984	2.987	2.982	2.980	2.980	2.986	2.992	2.990	2.995	2.991
spss.%	45.419	43.593	44.775	63.941	62.322	64.186	51.542	51.483	51.139	50.542	50.992
grss.%	0.620	0.562	0.522	1.562	1.419	1.528	0.875	0.914	0.872	0.823	0.943
alm.%	53.961	55.846	54.703	34.498	36.259	34.286	47.582	47.603	47.989	48.635	48.065

Table 15 cont.

Sample	MT1-1-F-1	MT1-1-F-2	MT1-1-F-3	MT1-1-F-4	MA-14-1a-1	MA-14-1a-2	MA-14-1a-3	MA-14-1a-4	MA-14-1a-5	MA-14-1a-6	MA-14-1j-1
P_2O_5	0.03	0.05	0.09	0.08	0.07	0.07	0.07	0.07	0.07	0.08	0.08
SiO_2	36.41	36.42	36.45	36.39	36.69	36.77	36.87	36.73	36.75	36.73	36.82
TiO_2	0.01	0.00	0.00	0.00	0.01	0.01	0.01	0.01	0.01	0.01	0.01
Al_2O_3	20.28	20.44	20.34	20.51	21.13	21.22	21.32	21.17	21.23	21.31	21.18
FeO	21.50	21.35	20.92	20.98	28.32	28.19	28.43	27.83	28.01	27.82	28.75
MnO	22.09	21.89	22.10	22.09	12.00	12.22	11.93	12.44	12.38	12.49	11.80
CaO	0.23	0.28	0.26	0.30	0.69	0.71	0.68	0.70	0.67	0.67	0.57
MgO	0.02	0.02	0.03	0.03	0.34	0.33	0.33	0.41	0.38	0.40	0.45
F	0.05	0.05	0.05	0.05	0.00	0.00	0.00	0.00	0.00	0.00	0.00
Subtotal	100.63	100.49	100.23	100.43	99.25	99.54	99.64	99.37	99.49	99.51	99.65
O=F	0.02	0.02	0.02	0.02	0.00	0.00	0.00	0.00	0.00	0.00	0.00
Total	100.61	100.47	100.21	100.41	99.25	99.54	99.64	99.37	99.49	99.51	99.65
X-site											
Fe	1.480	1.468	1.441	1.443	1.947	1.932	1.945	1.910	1.920	1.906	1.969
Mn	1.540	1.525	1.542	1.539	0.836	0.848	0.827	0.865	0.859	0.867	0.818
Ca	0.021	0.025	0.023	0.026	0.061	0.063	0.059	0.062	0.059	0.058	0.050
Mg	0.003	0.003	0.003	0.003	0.042	0.041	0.041	0.050	0.047	0.049	0.054
X-total	3.043	3.021	3.009	3.012	2.885	2.884	2.872	2.887	2.886	2.880	2.891
Y-site											
Cr	0.000	0.000	0.000	0.000	0.000	0.000	0.000	0.000	0.000	0.000	0.000
Al	1.967	1.982	1.976	1.988	2.047	2.050	2.056	2.047	2.051	2.058	2.043
Y-total	1.967	1.982	1.976	1.988	2.047	2.050	2.056	2.047	2.051	2.058	2.043
Z-site											
Si	2.996	2.996	3.003	2.993	3.016	3.013	3.016	3.014	3.013	3.009	3.015
Ti	0.001	0.000	0.000	0.000	0.001	0.001	0.001	0.000	0.001	0.001	0.000
Z-total	2.997	2.996	3.003	2.993	3.016	3.014	3.016	3.015	3.013	3.009	3.015
spss.%	50.653	50.530	51.301	51.153	29.393	29.841	29.205	30.492	30.275	30.607	28.842
grss.%	0.676	0.823	0.752	0.879	2.128	2.199	2.096	2.170	2.086	2.062	1.753
alm.%	48.671	48.646	47.947	47.968	68.478	67.960	68.699	67.338	67.640	67.331	69.404

Table 15 cont.

Sample	MA-14-1j-2	MA-14-1j-3	MA-14-1j-4	MA-14-1j-5	MA-14-1j-6	MA-14-1j-7	MA10-1-1	MA10-1-2	MA10-1-3	MA10-1-4	MA10-1-5	MA10-1-6
P_2O_5	0.08	0.07	0.08	0.07	0.08	0.08	0.08	0.08	0.08	0.09	0.07	0.06
SiO_2	36.72	36.72	36.83	36.75	36.77	36.73	36.56	36.70	36.85	36.67	36.73	36.84
TiO_2	0.01	0.01	0.01	0.02	0.01	0.01	0.01	0.01	0.01	0.01	0.02	0.01
Al_2O_3	21.23	21.20	21.31	21.21	21.20	21.22	21.17	21.20	21.18	21.18	21.23	21.21
FeO	28.75	28.64	28.45	28.36	28.46	28.51	28.02	27.89	28.00	27.89	27.80	28.55
MnO	11.76	11.78	11.81	12.01	11.89	11.80	12.44	12.25	12.65	12.70	12.32	11.67
CaO	0.62	0.57	0.57	0.60	0.60	0.56	0.77	0.69	0.75	0.60	0.73	0.65
MgO	0.39	0.43	0.34	0.34	0.34	0.42	0.43	0.39	0.35	0.40	0.38	0.46
F	0.00	0.00	0.00	0.02	0.01	0.01	0.00	0.00	0.02	0.00	0.00	0.00
Subtotal	99.57	99.42	99.41	99.36	99.37	99.34	99.48	99.21	99.89	99.53	99.29	99.45
O=F	0.00	0.00	0.00	0.01	0.00	0.01	0.00	0.00	0.01	0.00	0.00	0.00
Total	99.57	99.42	99.41	99.36	99.36	99.34	99.48	99.21	99.88	99.53	99.29	99.45
X-site												
Fe	1.970	1.965	1.950	1.946	1.952	1.956	1.924	1.916	1.914	1.913	1.908	1.956
Mn	0.816	0.819	0.820	0.835	0.826	0.820	0.865	0.852	0.876	0.882	0.856	0.810
Ca	0.055	0.050	0.050	0.052	0.053	0.049	0.067	0.061	0.065	0.053	0.065	0.057
Mg	0.047	0.053	0.042	0.042	0.042	0.052	0.053	0.048	0.042	0.049	0.046	0.056
X-total	2.889	2.887	2.862	2.875	2.874	2.877	2.910	2.876	2.897	2.897	2.875	2.879
Y-site												
Cr	0.000	0.000	0.000	0.000	0.000	0.000	0.000	0.000	0.000	0.000	0.000	0.000
Al	2.051	2.050	2.058	2.052	2.050	2.052	2.048	2.053	2.041	2.047	2.054	2.048
Y-total	2.051	2.050	2.058	2.052	2.050	2.052	2.048	2.053	2.041	2.047	2.054	2.048
Z-site												
Si	3.010	3.013	3.018	3.015	3.017	3.014	3.001	3.015	3.012	3.008	3.015	3.019
Ti	0.000	0.001	0.001	0.001	0.001	0.001	0.001	0.001	0.001	0.001	0.001	0.001
Z-total	3.010	3.013	3.019	3.016	3.018	3.014	3.002	3.015	3.013	3.008	3.016	3.019
spss.%	28.731	28.891	29.079	29.468	29.182	29.026	30.292	30.122	30.674	30.978	30.273	28.689
grss.%	1.925	1.756	1.772	1.847	1.872	1.730	2.359	2.141	2.285	1.848	2.281	2.021
alm.%	69.344	69.353	69.149	68.685	68.947	69.244	67.349	67.738	67.041	67.173	67.445	69.290

Table 15 cont.

Sample	MA10-1-7	MA13-1-c-1	MA13-1-c-2	MA13-1-c-3	MA13-1-c-4	MA13-1-c-5	MA13-1-c-6	MA13-1-c-7	MA2-1-c-1	MA2-1-c-2	MA2-1-c-3	MA2-1-c-4
P_2O_5	0.06	0.05	0.05	0.05	0.06	0.95	0.04	0.05	0.03	0.04	0.04	0.03
SiO_2	36.74	36.69	36.72	36.78	36.63	36.71	36.71	36.77	36.67	36.70	36.64	36.73
TiO_2	0.01	0.02	0.02	0.02	0.01	0.02	0.01	0.01	0.01	0.01	0.02	0.01
Al_2O_3	21.22	21.31	21.23	21.27	21.20	21.20	21.26	21.31	21.22	21.19	21.25	21.31
FeO	28.62	28.33	28.29	28.31	28.42	28.30	28.40	28.54	28.77	28.90	28.99	29.22
MnO	11.58	12.01	11.98	11.95	11.98	11.98	11.78	11.67	11.34	11.46	11.54	11.32
CaO	0.73	0.80	0.80	0.79	0.81	0.82	0.89	0.82	0.68	0.71	0.76	0.73
MgO	0.47	0.47	0.51	0.44	0.45	0.41	0.45	0.43	0.44	0.49	0.47	0.43
F	0.00	0.00	0.00	0.00	0.00	0.00	0.00	0.00	0.00	0.00	0.00	0.00
Subtotal	99.45	99.68	99.60	99.60	99.55	100.38	99.55	99.61	99.17	99.50	99.70	99.78
O=F	0.00	0.00	0.00	0.00	0.00	0.00	0.00	0.00	0.00	0.00	0.00	0.00
Total	99.45	99.68	99.60	99.60	99.55	100.38	99.55	99.61	99.17	99.50	99.70	99.78
X-site												
Fe	1.962	1.939	1.938	1.938	1.949	1.916	1.946	1.953	1.977	1.982	1.986	1.999
Mn	0.804	0.833	0.831	0.828	0.832	0.821	0.818	0.809	0.790	0.796	0.801	0.785
Ca	0.064	0.070	0.070	0.069	0.071	0.071	0.078	0.072	0.060	0.062	0.066	0.064
Mg	0.057	0.057	0.063	0.054	0.054	0.049	0.055	0.053	0.054	0.060	0.057	0.053
X-total	2.888	2.899	2.901	2.890	2.907	2.858	2.897	2.887	2.881	2.900	2.910	2.901
Y-site												
Cr	0.000	0.000	0.000	0.000	0.000	0.000	0.000	0.000	0.000	0.000	0.000	0.000
Al	2.051	2.056	2.049	2.052	2.049	2.023	2.053	2.056	2.056	2.048	2.052	2.055
Y-total	2.051	2.056	2.049	2.052	2.049	2.023	2.053	2.056	2.056	2.048	2.052	2.055
Z-site												
Si	3.012	3.003	3.007	3.011	3.004	2.972	3.008	3.009	3.014	3.009	3.002	3.005
Ti	0.001	0.001	0.001	0.001	0.001	0.001	0.001	0.001	0.001	0.001	0.001	0.001
Z-total	3.013	3.004	3.008	3.012	3.005	2.973	3.009	3.010	3.015	3.010	3.003	3.006
spss.%	28.407	29.295	29.277	29.209	29.180	29.240	28.769	28.542	27.940	28.019	28.076	27.550
grss.%	2.271	2.468	2.464	2.438	2.480	2.539	2.755	2.546	2.106	2.188	2.323	2.244
alm.%	69.321	68.236	68.259	68.353	68.340	68.222	68.475	68.912	69.954	69.793	69.601	70.206

Table 15 cont.

Sample	MA2-1-c-5	MA2-1-e-1	MA2-1-e-2	MA2-1-e-3	MA2-1-e-4	MA2-1-e-5	BT1-b-1-1	BT1-b-1-2	BT1-b-1-3	BT1-b-1-4	BT1-b-1-5
P_2O_5	0.03	0.04	0.04	0.04	0.04	0.04	0.02	0.02	0.04	0.04	0.04
SiO_2	36.71	36.60	36.63	36.66	36.70	36.67	36.43	36.42	36.38	36.39	36.46
TiO_2	0.01	0.01	0.01	0.01	0.01	0.01	0.01	0.01	0.01	0.00	0.01
Al_2O_3	21.26	21.31	21.28	21.22	21.30	21.23	20.40	20.41	20.50	20.45	20.46
FeO	29.43	29.23	29.13	29.09	29.24	29.19	25.89	25.93	25.93	25.96	25.90
MnO	11.11	11.44	11.31	11.21	11.33	11.27	17.12	17.22	17.12	17.31	17.29
CaO	0.74	0.82	0.76	0.76	0.77	0.75	0.05	0.06	0.05	0.05	0.05
MgO	0.45	0.40	0.38	0.44	0.39	0.38	0.12	0.11	0.11	0.11	0.09
F	0.00	0.00	0.00	0.00	0.00	0.01	0.00	0.00	0.00	0.00	0.00
Subtotal	99.74	99.85	99.56	99.44	99.78	99.56	100.05	100.18	100.15	100.33	100.29
O=F	0.00	0.00	0.00	0.00	0.00	0.01	0.00	0.00	0.00	0.00	0.00
Total	99.74	99.85	99.56	99.44	99.78	99.55	100.05	100.18	100.15	100.33	100.29
X-site											
Fe	2.015	2.001	1.998	1.996	2.001	2.002	1.787	1.789	1.789	1.789	1.784
Mn	0.771	0.794	0.786	0.779	0.785	0.783	1.197	1.203	1.196	1.208	1.206
Ca	0.065	0.072	0.067	0.067	0.068	0.066	0.004	0.005	0.004	0.005	0.004
Mg	0.054	0.049	0.047	0.054	0.048	0.046	0.015	0.014	0.013	0.014	0.011
X-total	2.905	2.915	2.897	2.897	2.902	2.897	3.004	3.011	3.002	3.016	3.006
Y-site											
Cr	0.000	0.000	0.000	0.000	0.000	0.000	0.000	0.000	0.000	0.000	0.000
Al	2.051	2.056	2.057	2.053	2.055	2.052	1.985	1.984	1.993	1.987	1.987
Y-total	2.051	2.056	2.057	2.053	2.055	2.052	1.985	1.984	1.993	1.987	1.987
Z-site											
Si	3.005	2.996	3.004	3.008	3.004	3.007	3.007	3.004	3.000	2.998	3.003
Ti	0.001	0.001	0.001	0.001	0.001	0.001	0.001	0.000	0.001	0.000	0.000
Z-total	3.006	2.997	3.005	3.009	3.004	3.008	3.008	3.004	3.001	2.998	3.004
spss.%	27.030	27.683	27.563	27.417	27.516	27.452	40.049	40.149	40.014	40.249	40.287
grss.%	2.289	2.515	2.349	2.357	2.372	2.324	0.148	0.162	0.145	0.159	0.133
alm.%	70.681	69.802	70.089	70.226	70.112	70.224	59.803	59.689	59.841	59.592	59.580

Table 15 cont.

Sample	BT1-b-1-6	BT2-a-1	BT2-a-2	BT2-a-3	BT3-d-1	BT3-d-2	BT3-d-3	BT3-d-B-1	BT3-d-B-2	BT3-d-B-3	BT3-d-C-1
P_2O_5	0.05	0.03	0.03	0.02	0.02	0.03	0.02	0.03	0.02	0.03	0.03
SiO_2	36.49	36.39	36.41	36.48	36.54	36.48	36.55	36.49	36.43	36.44	36.40
TiO_2	0.00	0.00	0.01	0.00	0.01	0.01	0.01	0.01	0.00	0.01	0.01
Al_2O_3	20.55	20.39	20.39	20.41	20.98	21.13	21.20	21.09	21.23	21.19	21.08
FeO	25.89	28.34	28.21	28.19	28.82	28.99	28.67	28.72	28.89	28.80	29.12
MnO	17.22	14.32	14.44	14.57	13.78	13.82	14.00	13.98	13.88	14.01	13.23
CaO	0.06	0.08	0.08	0.06	0.10	0.09	0.09	0.11	0.10	0.12	0.13
MgO	0.10	0.13	0.14	0.12	0.18	0.16	0.19	0.23	0.25	0.21	0.16
F	0.00	0.00	0.00	0.00	0.00	0.00	0.00	0.00	0.00	0.02	0.03
Subtotal	100.37	99.69	99.72	99.85	100.44	100.71	100.74	100.67	100.81	100.83	100.20
O=F	0.00	0.00	0.00	0.00	0.00	0.00	0.00	0.00	0.00	0.01	0.01
Total	100.37	99.69	99.72	99.85	100.44	100.71	100.74	100.67	100.81	100.82	100.19
X-site											
Fe	1.781	1.961	1.952	1.948	1.976	1.984	1.959	1.965	1.975	1.968	2.000
Mn	1.200	1.004	1.012	1.019	0.957	0.958	0.969	0.969	0.961	0.970	0.920
Ca	0.005	0.007	0.007	0.005	0.009	0.008	0.008	0.010	0.009	0.011	0.012
Mg	0.013	0.017	0.018	0.015	0.022	0.019	0.023	0.029	0.031	0.025	0.020
X-total	2.999	2.989	2.988	2.987	2.963	2.968	2.959	2.972	2.975	2.974	2.952
Y-site											
Cr	0.000	0.000	0.000	0.000	0.000	0.000	0.000	0.000	0.000	0.000	0.000
Al	1.993	1.989	1.988	1.988	2.027	2.038	2.042	2.034	2.045	2.041	2.040
Y-total	1.993	1.989	1.988	1.988	2.027	2.038	2.042	2.034	2.045	2.041	2.040
Z-site											
Si	3.002	3.011	3.012	3.014	2.995	2.985	2.987	2.986	2.977	2.978	2.989
Ti	0.000	0.000	0.001	0.000	0.001	0.000	0.000	0.001	0.000	0.000	0.000
Z-total	3.002	3.011	3.012	3.014	2.996	2.985	2.987	2.986	2.977	2.978	2.989
spss.%	40.185	33.774	34.069	34.297	32.524	32.472	33.007	32.917	32.630	32.886	31.392
grss.%	0.165	0.245	0.230	0.167	0.299	0.270	0.265	0.325	0.294	0.365	0.396
alm.%	59.650	65.981	65.701	65.537	67.177	67.258	66.728	66.758	67.075	66.749	68.212

Table 15 cont.

Sample	EM1-1-d	EM1-1-d	EM1-1-d	EM1-1-d	EM1-2-b-1	EM1-2-b-2	EM1-2-b-3	EM1-2-b-4	EM1-2-b-5	EM1-2-b-6	EM2-1a-1
P_2O_5	0.12	0.11	0.10	0.09	0.10	0.12	0.12	0.09	0.10	0.13	0.12
SiO_2	36.60	36.58	36.61	36.57	36.59	36.59	36.77	36.62	36.60	36.60	36.57
TiO_2	0.00	0.01	0.01	0.02	0.00	0.01	0.00	0.01	0.01	0.01	0.01
Al_2O_3	21.33	21.29	21.30	22.28	21.31	21.29	21.30	21.29	21.29	21.32	21.28
FeO	22.00	21.87	21.95	21.85	21.25	21.39	21.41	21.51	21.48	21.49	21.45
MnO	20.33	20.41	20.36	20.43	21.10	21.08	21.10	21.07	21.09	21.06	20.99
CaO	0.53	0.51	0.49	0.46	0.49	0.47	0.46	0.51	0.48	0.48	0.46
MgO	0.30	0.31	0.31	0.30	0.29	0.29	0.31	0.30	0.23	0.24	0.31
F	0.03	0.03	0.03	0.03	0.03	0.03	0.03	0.03	0.03	0.04	0.03
Subtotal	101.25	101.12	101.16	102.02	101.15	101.29	101.50	101.43	101.30	101.36	101.22
O=F	0.01	0.01	0.01	0.01	0.01	0.01	0.01	0.01	0.01	0.01	0.01
Total	101.24	101.11	101.15	102.01	101.14	101.27	101.49	101.42	101.29	101.35	101.20
X-site											
Fe	1.493	1.486	1.491	1.469	1.443	1.452	1.450	1.459	1.458	1.458	1.457
Mn	1.398	1.405	1.401	1.391	1.452	1.449	1.447	1.447	1.450	1.447	1.444
Ca	0.046	0.045	0.042	0.039	0.042	0.041	0.039	0.044	0.041	0.041	0.040
Mg	0.036	0.037	0.038	0.036	0.035	0.035	0.037	0.036	0.028	0.030	0.038
X-total	2.974	2.973	2.972	2.935	2.973	2.978	2.973	2.987	2.978	2.977	2.979
Y-site											
Cr	0.000	0.000	0.000	0.000	0.000	0.000	0.000	0.000	0.000	0.000	0.000
Al	2.041	2.039	2.039	2.110	2.041	2.037	2.032	2.035	2.038	2.038	2.037
Y-total	2.041	2.039	2.039	2.110	2.041	2.037	2.032	2.035	2.038	2.038	2.037
Z-site											
Si	2.970	2.972	2.974	2.939	2.972	2.970	2.977	2.970	2.972	2.969	2.970
Ti	0.000	0.000	0.001	0.001	0.000	0.001	0.000	0.001	0.000	0.001	0.001
Z-total	2.970	2.973	2.974	2.940	2.972	2.971	2.977	2.971	2.972	2.970	2.970
spss.%	47.582	47.855	47.747	47.984	49.424	49.252	49.279	49.054	49.160	49.113	49.107
grss.%	1.581	1.518	1.447	1.352	1.446	1.401	1.344	1.499	1.407	1.404	1.346
alm.%	50.838	50.626	50.805	50.664	49.131	49.348	49.377	49.447	49.433	49.483	49.547

Table 15 cont.

Sample	BT3-d-C-2	BT3-d-C-3	BT3-d-C-4	BT3-d-C-5	BT4-a-1	BT4-a-2	BT4-a-3	BT4-a-4	BT4-a-5	BT4-a-6	EM1-1-d
P_2O_5	0.04	0.04	0.04	0.03	0.03	0.03	0.03	0.04	0.03	0.03	0.10
SiO_2	36.40	36.44	36.45	36.50	36.61	36.59	36.60	36.56	36.51	36.61	36.56
TiO_2	0.00	0.00	0.01	0.01	0.01	0.01	0.01	0.01	0.01	0.01	0.01
Al_2O_3	21.16	21.17	21.09	21.31	21.00	21.23	21.22	21.10	20.98	21.23	21.23
FeO	28.78	29.21	28.69	28.79	28.76	28.83	28.78	28.88	28.78	28.81	21.90
MnO	13.44	13.65	14.01	13.77	13.56	13.59	13.60	13.54	13.56	13.60	20.42
CaO	0.14	0.13	0.15	0.15	0.15	0.15	0.15	0.15	0.14	0.14	0.53
MgO	0.16	0.14	0.12	0.13	0.13	0.14	0.16	0.22	0.12	0.17	0.35
F	0.00	0.01	0.00	0.00	0.00	0.00	0.00	0.00	0.01	0.00	0.02
Subtotal	100.12	100.80	100.56	100.70	100.25	100.58	100.55	100.50	100.14	100.61	101.12
O=F	0.00	0.01	0.00	0.00	0.00	0.00	0.00	0.00	0.01	0.00	0.01
Total	100.12	100.79	100.56	100.70	100.25	100.58	100.55	100.50	100.14	100.61	101.11
X-site											
Fe	1.976	1.998	1.965	1.967	1.973	1.971	1.968	1.977	1.977	1.969	1.489
Mn	0.935	0.946	0.972	0.953	0.942	0.941	0.942	0.939	0.943	0.941	1.406
Ca	0.013	0.012	0.013	0.013	0.013	0.013	0.013	0.013	0.012	0.013	0.047
Mg	0.019	0.018	0.015	0.016	0.016	0.017	0.019	0.027	0.015	0.021	0.042
X-total	2.943	2.973	2.965	2.950	2.944	2.943	2.942	2.956	2.947	2.944	2.984
Y-site											
Cr	0.000	0.000	0.000	0.000	0.000	0.000	0.000	0.000	0.000	0.000	0.000
Al	2.048	2.040	2.036	2.053	2.030	2.046	2.045	2.035	2.031	2.045	2.035
Y-total	2.048	2.040	2.036	2.053	2.030	2.046	2.045	2.035	2.031	2.045	2.035
Z-site											
Si	2.989	2.980	2.986	2.982	3.002	2.991	2.992	2.992	2.999	2.991	2.972
Ti	0.000	0.000	0.001	0.000	0.000	0.001	0.001	0.001	0.000	0.000	0.001
Z-total	2.989	2.980	2.987	2.983	3.003	2.991	2.993	2.993	2.999	2.992	2.972
spss.%	31.979	32.003	32.947	32.494	32.181	32.175	32.223	32.054	32.164	32.206	47.809
grss.%	0.433	0.397	0.440	0.448	0.435	0.440	0.444	0.452	0.420	0.431	1.581
alm.%	67.587	67.600	66.613	67.058	67.384	67.385	67.333	67.494	67.416	67.363	50.610

Table 15 cont.

Sample	EM1-1-d	EM1-1-d	EM1-1-d	EM1-1-d	EM1-2-b-1	EM1-2-b-2	EM1-2-b-3	EM1-2-b-4	EM1-2-b-5	EM1-2-b-6	EM2-1a-1
P_2O_5	0.12	0.11	0.10	0.09	0.10	0.12	0.12	0.09	0.10	0.13	0.12
SiO_2	36.60	36.58	36.61	36.57	36.59	36.59	36.77	36.62	36.60	36.60	36.57
TiO_2	0.00	0.01	0.01	0.02	0.00	0.01	0.00	0.01	0.01	0.01	0.01
Al_2O_3	21.33	21.29	21.30	22.28	21.31	21.29	21.30	21.29	21.29	21.32	21.28
FeO	22.00	21.87	21.95	21.85	21.25	21.39	21.41	21.51	21.48	21.49	21.45
MnO	20.33	20.41	20.36	20.43	21.10	21.08	21.10	21.07	21.09	21.06	20.99
CaO	0.53	0.51	0.49	0.46	0.49	0.47	0.46	0.51	0.48	0.48	0.46
MgO	0.30	0.31	0.31	0.30	0.29	0.29	0.31	0.30	0.23	0.24	0.31
F	0.03	0.03	0.03	0.03	0.03	0.03	0.03	0.03	0.03	0.04	0.03
Subtotal	101.25	101.12	101.16	102.02	101.15	101.29	101.50	101.43	101.30	101.36	101.22
O=F	0.01	0.01	0.01	0.01	0.01	0.01	0.01	0.01	0.01	0.01	0.01
Total	101.24	101.11	101.15	102.01	101.14	101.27	101.49	101.42	101.29	101.35	101.20
X-site											
Fe	1.493	1.486	1.491	1.469	1.443	1.452	1.450	1.459	1.458	1.458	1.457
Mn	1.398	1.405	1.401	1.391	1.452	1.449	1.447	1.447	1.450	1.447	1.444
Ca	0.046	0.045	0.042	0.039	0.042	0.041	0.039	0.044	0.041	0.041	0.040
Mg	0.036	0.037	0.038	0.036	0.035	0.035	0.037	0.036	0.028	0.030	0.038
X-total	2.974	2.973	2.972	2.935	2.973	2.978	2.973	2.987	2.978	2.977	2.979
Y-site											
Cr	0.000	0.000	0.000	0.000	0.000	0.000	0.000	0.000	0.000	0.000	0.000
Al	2.041	2.039	2.039	2.110	2.041	2.037	2.032	2.035	2.038	2.038	2.037
Y-total	2.041	2.039	2.039	2.110	2.041	2.037	2.032	2.035	2.038	2.038	2.037
Z-site											
Si	2.970	2.972	2.974	2.939	2.972	2.970	2.977	2.970	2.972	2.969	2.970
Ti	0.000	0.000	0.001	0.001	0.000	0.001	0.000	0.001	0.000	0.001	0.001
Z-total	2.970	2.973	2.974	2.940	2.972	2.971	2.977	2.971	2.972	2.970	2.970
spss.%	47.582	47.855	47.747	47.984	49.424	49.252	49.279	49.054	49.160	49.113	49.107
grss.%	1.581	1.518	1.447	1.352	1.446	1.401	1.344	1.499	1.407	1.404	1.346
alm.%	50.838	50.626	50.805	50.664	49.131	49.348	49.377	49.447	49.433	49.483	49.547

Table 15 cont.

Sample	EM2-1a-2	EM2-1a-3	EM2-1a-4	EM2-2-c-1	EM2-2-c-2	EM2-2-c-3	EM2-2-c-4	EM2-2-c-5	EM2-2-c-6	HVY1-1-a-1	HVY1-1-a-2
P_2O_5	0.15	0.09	0.10	0.09	0.11	0.11	0.09	0.10	0.10	0.07	0.07
SiO_2	36.61	36.60	36.45	36.50	36.52	36.51	36.53	36.49	36.54	36.31	36.31
TiO_2	0.01	0.00	0.00	0.01	0.01	0.01	0.01	0.01	0.01	0.01	0.00
Al_2O_3	21.28	21.30	20.98	21.34	21.35	21.41	21.40	21.39	21.40	20.56	20.54
FeO	21.46	21.51	21.75	21.32	21.30	21.30	21.29	21.37	21.36	31.67	31.63
MnO	20.99	20.96	20.82	21.11	21.09	20.98	20.97	21.01	20.98	11.09	10.96
CaO	0.44	0.40	0.38	0.51	0.50	0.51	0.51	0.51	0.52	0.26	0.25
MgO	0.29	0.28	0.21	0.28	0.29	0.23	0.25	0.26	0.27	0.02	0.03
F	0.03	0.02	0.02	0.03	0.03	0.03	0.03	0.04	0.03	0.03	0.03
Subtotal	101.25	101.16	100.72	101.19	101.20	101.10	101.09	101.18	101.20	100.01	99.82
O=F	0.01	0.01	0.01	0.01	0.01	0.01	0.01	0.02	0.01	0.01	0.01
Total	101.24	101.15	100.71	101.18	101.18	101.09	101.08	101.16	101.19	100.00	99.81
X-site											
Fe	1.456	1.462	1.487	1.449	1.447	1.448	1.447	1.452	1.450	2.187	2.187
Mn	1.443	1.442	1.442	1.453	1.451	1.444	1.444	1.446	1.443	0.776	0.768
Ca	0.038	0.035	0.034	0.045	0.043	0.044	0.045	0.044	0.045	0.023	0.022
Mg	0.035	0.034	0.026	0.034	0.035	0.028	0.031	0.032	0.033	0.003	0.003
X-total	2.973	2.973	2.988	2.981	2.976	2.965	2.966	2.973	2.971	2.987	2.979
Y-site											
Cr	0.000	0.000	0.000	0.000	0.000	0.000	0.000	0.000	0.000	0.000	0.000
Al	2.036	2.040	2.022	2.044	2.044	2.051	2.050	2.048	2.049	2.000	2.002
Y-total	2.036	2.040	2.022	2.044	2.044	2.051	2.050	2.048	2.049	2.000	2.002
Z-site											
Si	2.972	2.974	2.980	2.966	2.967	2.967	2.969	2.965	2.968	2.998	3.001
Ti	0.001	0.000	0.000	0.000	0.001	0.001	0.000	0.001	0.001	0.001	0.000
Z-total	2.972	2.974	2.980	2.967	2.967	2.968	2.970	2.966	2.968	2.998	3.001
spss.%	49.127	49.073	48.676	49.321	49.334	49.191	49.186	49.137	49.105	25.984	25.789
grss.%	1.294	1.197	1.133	1.513	1.477	1.498	1.519	1.512	1.537	0.756	0.738
alm.%	49.579	49.730	50.192	49.166	49.190	49.311	49.295	49.351	49.359	73.260	73.473

Table 15 cont.

Sample	HVY4-1b-1-1	HVY4-1b-1-2	HVY4-1b-1-3	HVY4-1b-1-4	HVY4-1b-1-5	TM1-k-1	TM1-k-2	TM1-k-3	TM1-k-4	TM1-k-5	TM1-k-6
P_2O_5	0.10	0.09	0.09	0.11	0.12	0.07	0.08	0.07	0.06	0.07	0.06
SiO_2	36.30	36.28	36.30	36.28	36.28	36.27	36.30	36.28	36.31	36.23	36.27
TiO_2	0.00	0.00	0.00	0.00	0.00	0.00	0.00	0.00	0.00	0.00	0.00
Al_2O_3	20.50	20.52	20.49	20.53	20.49	20.50	20.51	20.51	20.48	20.50	20.53
FeO	31.89	31.90	31.89	31.91	31.95	30.78	30.80	30.72	30.75	30.81	30.76
MnO	10.78	10.82	10.67	11.01	10.89	12.11	12.09	12.23	12.20	12.21	12.09
CaO	0.30	0.28	0.30	0.28	0.28	0.43	0.46	0.41	0.39	0.45	0.45
MgO	0.04	0.03	0.03	0.03	0.03	0.02	0.02	0.02	0.02	0.02	0.02
F	0.02	0.02	0.02	0.02	0.02	0.02	0.03	0.03	0.03	0.02	0.03
Subtotal	99.93	99.95	99.80	100.16	100.06	100.21	100.28	100.28	100.25	100.31	100.22
O=F	0.01	0.01	0.01	0.01	0.01	0.01	0.01	0.01	0.01	0.01	0.01
Total	99.92	99.94	99.79	100.16	100.05	100.20	100.27	100.26	100.24	100.30	100.21
X-site											
Fe	2.203	2.204	2.205	2.202	2.206	2.124	2.123	2.119	2.121	2.125	2.122
Mn	0.754	0.757	0.747	0.769	0.762	0.846	0.844	0.854	0.852	0.853	0.845
Ca	0.026	0.025	0.027	0.024	0.025	0.038	0.040	0.036	0.035	0.040	0.040
Mg	0.005	0.004	0.004	0.003	0.003	0.003	0.002	0.002	0.003	0.002	0.003
X-total	2.989	2.990	2.983	2.999	2.995	3.011	3.010	3.011	3.010	3.020	3.009
Y-site											
Cr	0.000	0.000	0.000	0.000	0.000	0.000	0.000	0.000	0.000	0.000	0.000
Al	1.996	1.998	1.997	1.996	1.993	1.993	1.992	1.993	1.991	1.992	1.996
Y-total	1.996	1.998	1.997	1.996	1.993	1.993	1.992	1.993	1.991	1.992	1.996
Z-site											
Si	2.999	2.997	3.001	2.993	2.995	2.992	2.992	2.992	2.994	2.988	2.991
Ti	0.000	0.000	0.000	0.000	0.000	0.000	0.000	0.000	0.000	0.000	0.000
Z-total	2.999	2.997	3.001	2.993	2.995	2.992	2.992	2.992	2.994	2.988	2.991
spss.%	25.279	25.361	25.092	25.682	25.453	28.132	28.069	28.391	28.323	28.267	28.103
grss.%	0.887	0.836	0.892	0.817	0.834	1.275	1.342	1.210	1.155	1.320	1.317
alm.%	73.834	73.803	74.016	73.501	73.713	70.593	70.589	70.400	70.522	70.412	70.580

Table 15 cont.

Sample	HVY1-1-a-3	HVY1-1-a-4	HVY1-1-a-5	HVY3-2-1	HVY3-2-2	HVY3-2-3	HVY3-2-4	HVY3-2-5	HVY3-2-6	HVY3-2-7	HVY3-2-8
P_2O_5	0.07	0.07	0.08	0.06	0.06	0.07	0.05	0.06	0.05	0.07	0.04
SiO_2	36.30	36.31	36.29	36.31	36.39	36.29	36.29	36.31	36.28	36.38	36.30
TiO_2	0.00	0.01	0.00	0.00	0.00	0.00	0.00	0.01	0.00	0.00	0.00
Al_2O_3	20.53	20.48	20.50	20.48	20.53	20.54	20.51	20.53	20.49	20.50	20.46
FeO	31.66	31.52	31.46	28.71	28.67	30.43	30.45	30.38	30.36	30.38	30.28
MnO	11.00	11.21	11.33	14.32	14.33	12.78	12.80	12.78	12.82	12.72	12.73
CaO	0.24	0.30	0.28	0.29	0.26	0.19	0.19	0.24	0.26	0.31	0.32
MgO	0.03	0.02	0.03	0.03	0.03	0.03	0.03	0.03	0.04	0.04	0.03
F	0.03	0.03	0.03	0.02	0.03	0.02	0.02	0.02	0.02	0.02	0.03
Subtotal	99.87	99.96	100.00	100.23	100.30	100.35	100.35	100.36	100.32	100.43	100.19
O=F	0.01	0.01	0.01	0.01	0.01	0.01	0.01	0.01	0.01	0.01	0.01
Total	99.85	99.95	99.99	100.22	100.29	100.34	100.34	100.35	100.31	100.42	100.18
X-site											
Fe	2.188	2.178	2.173	1.981	1.975	2.098	2.100	2.094	2.094	2.092	2.090
Mn	0.770	0.785	0.793	1.001	1.000	0.892	0.894	0.892	0.896	0.887	0.890
Ca	0.021	0.027	0.025	0.026	0.023	0.017	0.017	0.021	0.023	0.028	0.028
Mg	0.004	0.003	0.004	0.004	0.003	0.003	0.004	0.004	0.005	0.005	0.003
X-total	2.983	2.992	2.995	3.011	3.001	3.010	3.014	3.011	3.017	3.011	3.012
Y-site											
Cr	0.000	0.000	0.000	0.000	0.000	0.000	0.000	0.000	0.000	0.000	0.000
Al	2.000	1.995	1.996	1.991	1.993	1.996	1.993	1.994	1.992	1.990	1.990
Y-total	2.000	1.995	1.996	1.991	1.993	1.996	1.993	1.994	1.992	1.990	1.990
Z-site											
Si	3.000	3.000	2.997	2.995	2.997	2.991	2.992	2.992	2.992	2.995	2.996
Ti	0.000	0.000	0.000	0.000	0.000	0.000	0.000	0.000	0.000	0.000	0.000
Z-total	3.000	3.000	2.997	2.995	2.997	2.991	2.992	2.992	2.992	2.995	2.996
spss.%	25.848	26.247	26.503	33.278	33.357	29.668	29.696	29.671	29.729	29.508	29.583
grss.%	0.716	0.888	0.834	0.858	0.754	0.561	0.552	0.693	0.751	0.915	0.938
alm.%	73.436	72.864	72.662	65.864	65.889	69.771	69.752	69.636	69.520	69.576	69.480

Table 15 cont.

Sample	TM1-k-7	TM1-k-8	TM1-i-1	TM1-i-2	TM1-i-3	TM2-5-1	TM2-5-2	TM2-5-3	TM2-5-4	TM4-1-c-1	TM4-1-c-2
P_2O_5	0.96	0.06	0.09	0.09	0.08	0.10	0.09	0.10	0.10	0.07	0.07
SiO_2	36.27	36.30	36.30	36.32	35.33	36.34	36.34	36.38	36.36	36.34	36.37
TiO_2	0.00	0.00	0.00	0.00	0.00	0.00	0.00	0.00	0.00	0.00	0.00
Al_2O_3	20.53	20.51	20.49	20.50	20.56	20.51	20.49	20.53	20.54	20.49	20.51
FeO	30.75	30.64	20.41	30.37	30.41	30.51	30.45	30.38	30.41	30.78	30.73
MnO	12.31	12.28	12.46	12.51	12.53	12.40	12.33	12.45	12.48	12.09	12.11
CaO	0.49	0.35	0.29	0.31	0.33	0.38	0.38	0.41	0.38	0.41	0.40
MgO	0.03	0.03	0.02	0.02	0.02	0.02	0.02	0.02	0.02	0.02	0.04
F	0.03	0.02	0.03	0.03	0.03	0.02	0.02	0.03	0.02	0.02	0.02
Subtotal	101.37	100.18	90.08	100.15	99.29	100.28	100.12	100.29	100.33	100.23	100.25
O=F	0.01	0.01	0.01	0.01	0.01	0.01	0.01	0.01	0.01	0.01	0.01
Total	101.36	100.17	90.07	100.13	99.28	100.28	100.11	100.28	100.32	100.22	100.24
X-site											
Fe	2.091	2.114	1.495	2.095	2.125	2.102	2.101	2.092	2.094	2.123	2.118
Mn	0.848	0.858	0.924	0.874	0.887	0.865	0.862	0.868	0.871	0.844	0.845
Ca	0.043	0.030	0.027	0.028	0.030	0.034	0.033	0.036	0.034	0.036	0.036
Mg	0.003	0.004	0.003	0.002	0.002	0.002	0.002	0.002	0.003	0.003	0.004
X-total	2.984	3.007	2.449	2.999	3.043	3.004	2.998	3.000	3.002	3.006	3.003
Y-site											
Cr	0.000	0.000	0.000	0.000	0.000	0.000	0.000	0.000	0.000	0.000	0.000
Al	1.967	1.994	2.115	1.993	2.025	1.992	1.992	1.993	1.994	1.991	1.992
Y-total	1.967	1.994	2.115	1.993	2.025	1.992	1.992	1.993	1.994	1.991	1.992
Z-site											
Si	2.948	2.995	3.179	2.996	2.951	2.994	2.997	2.996	2.994	2.996	2.997
Ti	0.000	0.000	0.000	0.000	0.000	0.000	0.000	0.000	0.000	0.000	0.000
Z-total	2.948	2.995	3.179	2.996	2.951	2.994	2.997	2.996	2.994	2.996	2.997
spss.%	28.432	28.581	37.768	29.166	29.159	28.830	28.767	28.976	29.035	28.115	28.187
grss.%	1.443	1.016	1.120	0.920	0.980	1.126	1.112	1.213	1.127	1.212	1.189
alm.%	70.125	70.404	61.112	69.914	69.861	70.043	70.121	69.811	69.838	70.673	70.624

Table 15 cont.

Sample	TM4-1-c-3	TM4-1-c-4
P_2O_5	0.06	0.06
SiO_2	36.35	36.34
TiO_2	0.00	0.00
Al_2O_3	20.51	20.53
FeO	30.74	30.70
MnO	12.05	12.00
CaO	0.39	0.41
MgO	0.03	0.03
F	0.01	0.02
Subtotal	100.14	100.08
O=F	0.01	0.01
Total	100.13	100.08
X-site		
Fe	2.121	2.118
Mn	0.842	0.839
Ca	0.034	0.036
Mg	0.003	0.003
X-total	3.000	2.996
Y-site		
Cr	0.000	0.000
Al	1.994	1.996
Y-total	1.994	1.996
Z-site		
Si	2.998	2.998
Ti	0.000	0.000
Z-total	2.998	2.998
spss.%	28.084	28.016
grss.%	1.147	1.214
alm.%	70.768	70.770

Biotite

Table 16: Biotite composition from garnet boundary layers.

sample	MT6-4-b-1	MT6-4-b-2	MT6-4-b-3	MT2-3-m-1	MT2-3-m-2	MT2-3-m-3	BT1-b-2-1	BT1-b-2-2	BT1-b-2-3	BT1-b-2-4	BT1-b-2-5
SiO_2	38.01	37.97	38.11	37.75	37.56	37.75	36.21	36.31	36.39	36.30	36.41
TiO_2	0.43	0.45	0.49	0.48	0.50	0.49	1.32	1.28	1.40	1.31	1.22
Al_2O_3	26.22	26.59	27.21	21.01	20.99	21.04	18.79	18.98	19.21	19.09	19.10
FeO	17.09	17.11	17.20	17.40	17.43	17.44	20.98	20.83	20.66	20.60	20.61
MnO	0.11	0.09	0.08	0.07	0.07	0.07	0.89	0.90	0.87	0.90	0.92
MgO	0.25	0.33	0.34	6.57	6.54	6.00	0.24	0.19	0.21	0.22	0.21
CaO	0.10	0.09	0.10	0.10	0.08	0.09	0.06	0.07	0.06	0.05	0.06
Rb_2O	0.23	0.21	0.20	0.14	0.12	0.11	0.03	0.02	0.02	0.03	0.02
Cs_2O	0.04	0.03	0.03	0.02	0.02	0.02	0.00	0.00	0.00	0.00	0.00
Na_2O	0.59	0.64	0.61	0.48	0.56	0.57	0.44	0.39	0.41	0.41	0.40
K_2O	8.11	8.10	8.14	8.20	8.11	8.23	9.21	9.41	9.41	9.29	9.31
H_2O calc	3.76	3.80	3.82	3.76	3.74	3.72	2.99	3.11	3.11	3.03	3.06
F	0.33	0.30	0.34	0.33	0.35	0.37	1.32	1.09	1.12	1.27	1.20
Subtotal	95.27	95.70	96.69	96.30	96.06	95.90	92.50	92.59	92.88	92.50	92.54
O=F	0.14	0.12	0.14	0.14	0.15	0.16	0.56	0.46	0.47	0.53	0.51
Total	95.13	95.58	96.55	96.16	95.92	95.75	91.94	92.13	92.40	91.97	92.03

Table 16 cont.

apfu	MT6-4-b-1	MT6-4-b-2	MT6-4-b-3	MT2-3-m-1	MT2-3-m-2	MT2-3-m-3	BT1-b-2-1	BT1-b-2-2	BT1-b-2-3	BT1-b-2-4	BT1-b-2-5
Si	5.818	5.782	5.743	5.782	5.769	5.810	6.005	6.005	5.990	6.003	6.015
Ti	0.050	0.051	0.056	0.055	0.058	0.056	0.165	0.159	0.173	0.163	0.152
Al	4.731	4.773	4.833	3.794	3.801	3.817	3.672	3.700	3.728	3.721	3.720
Fe	2.188	2.180	2.167	2.229	2.239	2.245	2.910	2.881	2.843	2.849	2.848
Mn	0.014	0.012	0.011	0.009	0.009	0.008	0.125	0.126	0.121	0.126	0.129
Mg	0.056	0.076	0.077	1.500	1.498	1.375	0.060	0.047	0.051	0.055	0.052
Ca	0.016	0.015	0.017	0.016	0.013	0.014	0.011	0.012	0.010	0.009	0.011
Rb	0.023	0.021	0.019	0.014	0.012	0.011	0.003	0.003	0.002	0.003	0.002
Cs	0.002	0.002	0.002	0.001	0.001	0.001	0.000	0.000	0.000	0.000	0.000
Na	0.175	0.190	0.179	0.142	0.166	0.169	0.143	0.126	0.131	0.132	0.128
K	1.584	1.573	1.565	1.603	1.590	1.616	1.949	1.986	1.976	1.960	1.963
OH	3.838	3.857	3.836	3.839	3.832	3.818	3.307	3.429	3.415	3.338	3.373
F	0.161	0.142	0.163	0.161	0.168	0.182	0.693	0.571	0.585	0.662	0.627
^{IV}Al	2.182	2.218	2.257	2.218	2.231	2.190	1.995	1.995	2.010	1.997	1.985
^{VI}Al	2.550	2.555	2.575	1.577	1.571	1.627	1.676	1.704	1.718	1.724	1.735
Sum Tetrahedral	8.000	8.000	8.000	8.000	8.000	8.000	8.000	8.000	8.000	8.000	8.000
Sum Octahedral	4.858	4.873	4.886	5.369	5.375	5.312	4.936	4.918	4.908	4.917	4.916
Sum x-site	1.800	1.801	1.782	1.776	1.782	1.812	2.106	2.126	2.120	2.103	2.104
Sum w-site	4.000	4.000	4.000	4.000	4.000	4.000	4.000	4.000	4.000	4.000	4.000
Fe/(Fe+Mg)	0.975	0.966	0.966	0.598	0.599	0.620	0.980	0.984	0.982	0.981	0.982

Table 16 cont.

sample	BT1-b-2-6	BT2-a-1	BT2-a-2	BT2-a-3	BT2-a-4	BT3-f-1	BT3-f-2	BT3-f-3	BT3-f-4	BT3-g-1	BT3-g-2
SiO_2	36.41	36.43	36.36	36.41	36.35	37.78	37.79	37.86	37.79	37.83	37.89
TiO_2	1.31	1.39	1.87	1.68	1.51	1.98	2.22	1.99	2.09	2.11	2.11
Al_2O_3	19.09	18.92	18.97	18.89	18.89	18.32	18.46	18.57	18.61	18.88	18.90
FeO	20.56	20.89	20.92	20.88	20.92	24.22	24.16	24.21	24.00	23.70	23.76
MnO	0.98	1.00	1.06	0.98	0.99	0.98	0.99	1.11	1.33	0.99	0.97
MgO	0.23	0.23	0.21	0.22	0.23	0.32	0.36	0.34	0.37	0.40	0.38
CaO	0.07	0.98	0.09	0.09	0.08	0.12	0.14	0.14	0.17	0.20	0.19
Rb_2O	0.03	0.04	0.03	0.03	0.02	0.03	0.03	0.03	0.03	0.02	0.02
Cs_2O	0.00	0.00	0.00	0.00	0.00	0.00	0.00	0.00	0.00	0.00	0.00
Na_2O	0.36	0.50	0.52	0.46	0.51	0.52	0.56	0.52	0.57	0.50	0.57
K_2O	9.51	9.54	9.49	9.51	9.34	9.89	10.00	9.93	9.88	10.04	10.10
H_2O calc	3.07	3.07	2.99	3.02	2.95	3.22	3.26	3.25	3.26	3.31	3.30
F	1.19	1.27	1.43	1.33	1.45	1.22	1.19	1.20	1.20	1.09	1.14
Subtotal	92.81	94.27	93.94	93.50	93.25	98.61	99.14	99.16	99.29	99.08	99.34
O=F	0.50	0.53	0.60	0.56	0.61	0.51	0.50	0.51	0.50	0.46	0.48
Total	92.31	93.73	93.33	92.94	92.64	98.10	98.64	98.66	98.79	98.62	98.86

Table 16 cont.

apfu	BT1-b-2-6	BT2-a-1	BT2-a-2	BT2-a-3	BT2-a-4	BT3-f-1	BT3-f-2	BT3-f-3	BT3-f-4	BT3-g-1	BT3-g-2
Si	6.004	5.950	5.949	5.979	5.985	5.960	5.929	5.938	5.921	5.921	5.919
Ti	0.163	0.171	0.230	0.207	0.187	0.235	0.262	0.235	0.246	0.249	0.248
Al	3.710	3.642	3.658	3.656	3.667	3.407	3.414	3.433	3.437	3.482	3.480
Fe	2.835	2.853	2.863	2.867	2.881	3.196	3.170	3.176	3.144	3.102	3.104
Mn	0.137	0.138	0.146	0.137	0.138	0.131	0.132	0.148	0.177	0.131	0.129
Mg	0.057	0.057	0.052	0.055	0.057	0.075	0.083	0.080	0.086	0.093	0.089
Ca	0.012	0.172	0.016	0.015	0.014	0.021	0.024	0.024	0.028	0.034	0.032
Rb	0.003	0.004	0.003	0.004	0.002	0.003	0.003	0.003	0.003	0.002	0.002
Cs	0.000	0.000	0.000	0.000	0.000	0.000	0.000	0.000	0.000	0.000	0.000
Na	0.114	0.158	0.166	0.145	0.163	0.160	0.169	0.159	0.172	0.151	0.172
K	2.001	1.988	1.982	1.992	1.963	1.991	2.002	1.988	1.976	2.005	2.013
OH	3.379	3.346	3.260	3.307	3.244	3.390	3.410	3.405	3.406	3.460	3.435
F	0.621	0.654	0.740	0.693	0.756	0.610	0.590	0.595	0.594	0.540	0.565
^{IV}Al	1.996	2.050	2.051	2.021	2.015	2.040	2.071	2.062	2.079	2.079	2.081
^{VI}Al	1.715	1.592	1.608	1.635	1.652	1.367	1.343	1.371	1.358	1.403	1.398
Sum Tetrahedral	8.000	8.000	8.000	8.000	8.000	8.000	8.000	8.000	8.000	8.000	8.000
Sum Octahedral	4.906	4.811	4.900	4.900	4.916	5.004	4.991	5.011	5.011	4.977	4.968
Sum x-site	2.131	2.322	2.167	2.156	2.143	2.174	2.198	2.174	2.179	2.192	2.219
Sum w-site	4.000	4.000	4.000	4.000	4.000	4.000	4.000	4.000	4.000	4.000	4.000
Fe/(Fe+Mg)	0.980	0.980	0.982	0.981	0.981	0.977	0.974	0.975	0.973	0.971	0.972

Table 16 cont.

sample	BT3-g-3	BT2-a-1	BT2-a-2	BT2-a-3	BT2-a-4	BT2-a-5	HVY1-1-c-1	HVY1-1-c-2	HVY1-1-c-3	HVY1-1-c-4
SiO_2	37.88	37.70	37.74	37.81	37.80	37.80	37.72	37.83	37.76	37.69
TiO_2	2.13	2.11	1.98	2.11	2.20	2.12	0.22	0.26	0.30	0.32
Al_2O_3	18.86	18.57	18.51	18.61	18.67	18.70	26.94	27.09	26.93	26.94
FeO	23.73	23.95	23.98	23.89	24.01	23.98	17.90	17.81	17.68	18.33
MnO	0.94	1.22	1.20	1.22	1.27	1.23	0.51	0.48	0.47	0.56
MgO	0.35	0.30	0.22	0.25	0.25	0.24	2.72	2.58	2.33	2.29
CaO	0.21	0.14	0.15	0.14	0.15	0.15	0.21	0.19	0.23	0.25
Rb_2O	0.02	0.03	0.03	0.03	0.03	0.03	0.02	0.02	0.02	0.02
Cs_2O	0.00	0.00	0.00	0.00	0.00	0.00	0.00	0.00	0.00	0.00
Na_2O	0.54	0.50	0.51	0.51	0.49	0.48	0.46	0.43	0.42	0.41
K_2O	10.09	9.78	9.95	10.11	10.09	9.98	10.06	9.92	10.11	9.89
H_2O calc	3.31	3.31	3.26	3.24	3.26	3.24	3.82	3.83	3.84	3.83
F	1.11	1.06	1.15	1.22	1.20	1.23	0.57	0.55	0.49	0.52
Subtotal	99.18	98.66	98.67	99.15	99.42	99.17	101.15	101.00	100.59	101.08
O=F	0.47	0.44	0.48	0.51	0.50	0.52	0.24	0.23	0.21	0.22
Total	98.72	98.21	98.19	98.64	98.91	98.65	100.91	100.77	100.38	100.86

Table 16 cont.

apfu	BT3-g-3	BT2-a-1	BT2-a-2	BT2-a-3	BT2-a-4	BT2-a-5	HVY1-1-c-1	HVY1-1-c-2	HVY1-1-c-3	HVY1-1-c-4
Si	5.924	5.933	5.948	5.933	5.918	5.927	5.534	5.547	5.562	5.538
Ti	0.251	0.250	0.235	0.249	0.259	0.250	0.025	0.028	0.033	0.036
Al	3.476	3.444	3.439	3.442	3.445	3.456	4.659	4.682	4.676	4.667
Fe	3.104	3.152	3.161	3.136	3.143	3.145	2.196	2.184	2.177	2.253
Mn	0.125	0.163	0.160	0.162	0.168	0.163	0.064	0.060	0.058	0.070
Mg	0.083	0.070	0.051	0.059	0.059	0.057	0.595	0.563	0.512	0.502
Ca	0.036	0.023	0.025	0.024	0.025	0.026	0.033	0.030	0.037	0.040
Rb	0.002	0.003	0.003	0.003	0.003	0.003	0.002	0.002	0.002	0.002
Cs	0.000	0.000	0.000	0.000	0.000	0.000	0.000	0.000	0.000	0.000
Na	0.163	0.152	0.154	0.155	0.148	0.145	0.129	0.123	0.121	0.117
K	2.013	1.965	2.000	2.025	2.016	1.997	1.882	1.856	1.900	1.855
OH	3.453	3.475	3.429	3.397	3.407	3.390	3.737	3.744	3.769	3.758
F	0.546	0.525	0.571	0.603	0.593	0.610	0.262	0.255	0.230	0.242
^{IV}Al	2.076	2.067	2.052	2.067	2.082	2.073	2.466	2.453	2.438	2.462
^{VI}Al	1.400	1.377	1.387	1.375	1.363	1.383	2.193	2.228	2.238	2.205
Sum Tetrahedral	8.000	8.000	8.000	8.000	8.000	8.000	8.000	8.000	8.000	8.000
Sum Octahedral	4.962	5.012	4.993	4.981	4.992	4.998	5.072	5.064	5.019	5.066
Sum x-site	2.214	2.143	2.183	2.208	2.192	2.170	2.047	2.011	2.059	2.014
Sum w-site	4.000	4.000	4.000	4.000	4.000	4.000	4.000	4.000	4.000	4.000
Fe/(Fe+Mg)	0.974	0.978	0.984	0.981	0.982	0.982	0.787	0.795	0.809	0.818

'zinnwaldite' Micas

Table 17: compositions of Li-calculated zinnwaldites from fracture filling micas in garnets from the garnet line at Mt. Mica

sample	MT4-1-b-1	MT4-1-b-2	MT4-1-b-3	MT2-3-c-1	MT2-3-c-2	MT2-3-c-3	MT1-1-f-1	MT1-1-f-2	MT1-1-f-3	MT1-1-f-4	MT1-1-h-1
SiO_2	45.21	45.23	45.30	45.34	45.29	45.37	45.33	45.39	45.44	45.34	45.42
TiO_2	0.17	0.13	0.10	0.11	0.09	0.09	0.09	0.11	0.09	0.09	0.08
Al_2O_3	32.46	32.40	32.31	31.21	31.32	31.33	32.66	32.68	32.70	32.72	32.80
FeO	3.87	4.02	3.93	5.09	4.89	4.95	3.65	3.56	3.62	3.70	3.76
MnO	0.32	0.29	0.31	0.56	0.49	0.53	0.29	0.32	0.33	0.34	0.40
MgO	0.10	0.09	0.09	0.02	0.04	0.03	0.09	0.09	0.09	0.08	0.08
CaO	0.03	0.03	0.04	0.02	0.03	0.04	0.04	0.04	0.04	0.04	0.03
Rb_2O	1.43	1.23	1.12	0.89	0.98	0.89	1.11	1.30	1.31	1.28	1.11
Cs_2O	0.44	0.48	0.51	0.22	0.19	0.18	0.34	0.24	0.35	0.42	0.34
Li_2O calc.	2.62	2.62	2.62	2.62	2.62	2.62	2.62	2.62	2.62	2.62	2.62
Na_2O	0.54	0.56	0.56	0.34	0.33	0.35	0.60	0.60	0.57	0.64	0.59
K_2O	8.34	8.33	8.22	8.78	8.83	8.73	8.57	8.56	8.62	8.45	8.77
H_2O calc	3.88	3.82	3.69	3.80	3.79	3.76	3.69	3.77	3.68	3.65	3.76
F	1.22	1.28	1.30	1.01	1.04	1.11	1.32	1.43	1.37	1.43	1.22
Subtotal	100.64	100.52	100.11	100.03	99.93	100.00	100.40	100.69	100.83	100.82	100.99
O=F	0.51	0.54	0.55	0.43	0.44	0.47	0.56	0.60	0.58	0.60	0.51
Total	100.13	99.99	99.56	99.60	99.50	99.53	99.85	100.09	100.26	100.22	100.48

Table 17 cont.

sample	MT4-1-b-1	MT4-1-b-2	MT4-1-b-3	MT2-3-c-1	MT2-3-c-2	MT2-3-c-3	MT1-1-f-1	MT1-1-f-2	MT1-1-f-3	MT1-1-f-4	MT1-1-h-1
apfu											
Si	6.086	6.095	6.125	6.161	6.157	6.161	6.106	6.094	6.107	6.098	6.092
Ti	0.017	0.013	0.010	0.012	0.009	0.009	0.009	0.011	0.009	0.009	0.008
Al	5.149	5.146	5.150	4.999	5.018	5.014	5.185	5.171	5.180	5.187	5.185
Fe	0.436	0.453	0.445	0.579	0.556	0.562	0.411	0.399	0.407	0.416	0.422
Mn	0.037	0.033	0.036	0.064	0.057	0.061	0.033	0.036	0.038	0.039	0.045
Mg	0.020	0.018	0.019	0.004	0.009	0.007	0.018	0.018	0.018	0.017	0.017
Ca	0.005	0.005	0.006	0.003	0.004	0.006	0.006	0.006	0.005	0.006	0.005
Rb	0.124	0.107	0.097	0.078	0.086	0.078	0.096	0.112	0.114	0.111	0.096
Cs	0.025	0.028	0.030	0.013	0.011	0.010	0.020	0.013	0.020	0.024	0.019
Li	1.418	1.420	1.425	1.432	1.432	1.431	1.419	1.415	1.416	1.417	1.413
Na	0.142	0.145	0.148	0.090	0.088	0.092	0.157	0.155	0.147	0.168	0.153
K	1.433	1.432	1.419	1.522	1.532	1.513	1.472	1.466	1.479	1.451	1.500
OH	3.481	3.434	3.326	3.446	3.433	3.404	3.319	3.379	3.301	3.272	3.363
F	0.521	0.545	0.556	0.435	0.447	0.477	0.562	0.607	0.581	0.610	0.519
^{IV}Al	1.914	1.905	1.875	1.839	1.843	1.839	1.894	1.906	1.893	1.902	1.908
^{VI}Al	3.236	3.241	3.275	3.159	3.175	3.175	3.291	3.265	3.288	3.286	3.278
Sum Tetrahedral	8.000	8.000	8.000	8.000	8.000	8.000	8.000	8.000	8.000	8.000	8.000
Sum Octahedral	5.164	5.179	5.209	5.249	5.239	5.245	5.182	5.144	5.176	5.184	5.183
Sum x-site	1.729	1.717	1.699	1.706	1.721	1.700	1.751	1.752	1.765	1.759	1.773
Fe+Mn+Ti-VIAl	-2.746	-2.741	-2.785	-2.505	-2.554	-2.543	-2.838	-2.819	-2.833	-2.822	-2.802

Table 17 cont.

sample	MT1-1-h-2	MT1-1-h-3
SiO_2	45.40	45.39
TiO_2	0.08	0.08
Al_2O_3	32.89	32.90
FeO	3.67	3.63
MnO	0.38	0.34
MgO	0.09	0.08
CaO	0.03	0.03
Rb_2O	1.11	1.20
Cs_2O	0.33	0.38
Li_2O calc.	2.62	2.62
Na_2O	0.60	0.59
K_2O	8.57	8.60
H_2O calc	3.67	3.73
F	1.40	1.28
Subtotal	100.84	100.86
O=F	0.59	0.54
Total	100.25	100.32

Table 17 cont.

sample	MT1-1-h-2	MT1-1-h-3
apfu		
Si	6.093	6.093
Ti	0.008	0.008
Al	5.203	5.205
Fe	0.412	0.408
Mn	0.044	0.039
Mg	0.018	0.015
Ca	0.004	0.004
Rb	0.096	0.104
Cs	0.019	0.022
Li	1.414	1.414
Na	0.156	0.152
K	1.467	1.473
OH	3.288	3.338
F	0.594	0.544
^{IV}Al	1.907	1.907
^{VI}Al	3.296	3.298
Sum Tetrahedral	8.000	8.000
Sum Octahedral	5.191	5.183
Sum x-site	1.742	1.755
Fe+Mn+Ti-VIAl	-2.832	-2.843

K-feldspar

Table 18: K-feldspar compositions from various garnet boundary layers in Oxford County, Maine pegmatites.

Sample	MT4-1-a-1	MT4-1-a-2	MT4-1-a-3	MA14-1-d-6	MA14-1-d-7	MA14-1-d-8	MA14-1-d-9	MA14-1-d-10
SiO_2	64.40	64.43	64.40	64.40	64.40	64.41	64.41	64.39
TiO_2	0.00	0.01	0.00	0.01	0.01	0.01	0.01	0.01
Al_2O_3	18.23	18.30	18.32	18.29	18.32	18.33	18.30	18.30
FeO	0.63	0.58	0.73	0.31	0.12	0.16	0.32	0.37
CaO	0.01	0.01	0.01	0.00	0.01	0.00	0.01	0.02
Cs_2O	0.00	0.00	0.00	0.00	0.00	0.00	0.00	0.00
Rb_2O	0.23	0.30	0.32	0.21	0.19	0.18	0.20	0.18
K_2O	15.68	15.51	15.56	15.51	15.56	15.44	15.51	15.48
Na_2O	0.00	0.00	0.00	0.23	0.22	0.12	0.19	0.20
Total	99.19	99.14	99.35	98.97	98.83	98.65	98.96	98.94
apfu								
Si	3.001	3.001	2.998	3.002	3.004	3.006	3.003	3.002
Ti	0.000	0.000	0.000	0.000	0.000	0.000	0.000	0.000
Al	1.002	1.005	1.005	1.005	1.007	1.009	1.005	1.006
Fe	0.025	0.023	0.029	0.012	0.005	0.006	0.013	0.014
Ca	0.001	0.000	0.000	0.000	0.001	0.000	0.001	0.001
Cs	0.000	0.000	0.000	0.000	0.000	0.000	0.000	0.000
Rb	0.007	0.009	0.010	0.006	0.006	0.005	0.006	0.005
K	0.932	0.922	0.924	0.923	0.926	0.920	0.923	0.921
Na	0.000	0.000	0.000	0.021	0.020	0.011	0.017	0.018
Ab%	0.000	0.000	0.000	2.222	2.130	1.148	1.836	1.924
An%	0.059	0.049	0.043	0.000	0.058	0.000	0.064	0.122
Or%	99.941	99.951	99.957	97.778	97.812	98.852	98.101	97.954

Table 18 cont.

Sample	MA14-1-d-11	TM2-1-3	TM2-1-4	TM4-1-a-1	TM4-1-a-2	TM4-1-a-3	EM1-1-6	EM1-1-7
SiO_2	64.42	64.70	64.72	64.71	64.72	64.69	65.44	65.38
TiO_2	0.01	0.00	0.01	0.00	0.00	0.01	0.00	0.01
Al_2O_3	18.28	18.31	18.23	18.32	18.34	18.33	18.16	18.20
FeO	0.40	0.00	0.00	0.00	0.00	0.00	0.00	0.00
CaO	0.04	0.00	0.00	0.00	0.00	0.00	0.01	0.00
Cs_2O	0.00	0.00	0.00	0.00	0.00	0.00	0.00	0.00
Rb_2O	0.18	0.07	0.05	0.05	0.04	0.05	0.11	0.11
K_2O	15.50	16.55	16.60	16.58	16.52	16.55	16.06	15.90
Na_2O	0.19	0.46	0.51	0.53	0.48	0.51	0.45	0.51
Total	99.03	100.08	100.11	100.19	100.11	100.14	100.22	100.11
apfu								
Si	3.002	2.995	2.997	2.994	2.995	2.994	3.014	3.013
Ti	0.000	0.000	0.000	0.000	0.000	0.000	0.000	0.000
Al	1.004	0.999	0.995	0.999	1.000	1.000	0.986	0.988
Fe	0.016	0.000	0.000	0.000	0.000	0.000	0.000	0.000
Ca	0.002	0.000	0.000	0.000	0.000	0.000	0.000	0.000
Cs	0.000	0.000	0.000	0.000	0.000	0.000	0.000	0.000
Rb	0.005	0.002	0.001	0.002	0.001	0.001	0.003	0.003
K	0.921	0.977	0.981	0.979	0.975	0.977	0.943	0.935
Na	0.017	0.041	0.045	0.048	0.043	0.046	0.041	0.046
Ab%	1.815	4.020	4.419	4.665	4.262	4.465	4.118	4.648
An%	0.234	0.000	0.000	0.000	0.000	0.000	0.045	0.000
Or%	97.951	95.980	95.581	95.335	95.738	95.535	95.837	95.352

Table 18 cont.

Sample	EM1-1e-8	EM1-1-9	EM1-1-10	EM1-1-11	BT2-a-1	BT2-a-2	BT2-a-3	BT2-a-4	BT2-a-5
SiO_2	65.41	65.52	65.49	65.49	65.39	65.33	65.40	65.39	65.41
TiO_2	0.01	0.00	0.00	0.01	0.01	0.01	0.01	0.01	0.01
Al_2O_3	18.17	18.16	18.21	18.16	18.15	18.17	18.20	18.10	18.17
FeO	0.00	0.00	0.00	0.00	0.00	0.00	0.00	0.00	0.00
CaO	0.00	0.00	0.00	0.00	0.00	0.01	0.01	0.00	0.00
Cs_2O	0.00	0.00	0.00	0.00	0.00	0.00	0.01	0.02	0.00
Rb_2O	0.10	0.11	0.11	0.11	0.08	0.09	0.09	0.09	0.08
K_2O	15.97	15.99	16.02	16.01	15.99	16.12	16.10	16.10	16.08
Na_2O	0.47	0.49	0.47	0.50	0.41	0.29	0.33	0.43	0.46
Total	100.11	100.26	100.30	100.27	100.04	100.03	100.16	100.13	100.21
apfu									
Si	3.014	3.015	3.013	3.014	3.015	3.014	3.013	3.015	3.013
Ti	0.000	0.000	0.000	0.000	0.000	0.000	0.000	0.000	0.000
Al	0.987	0.985	0.988	0.985	0.987	0.988	0.988	0.984	0.986
Fe	0.000	0.000	0.000	0.000	0.000	0.000	0.000	0.000	0.000
Ca	0.000	0.000	0.000	0.000	0.000	0.001	0.000	0.000	0.000
Cs	0.000	0.000	0.000	0.000	0.000	0.000	0.000	0.000	0.000
Rb	0.003	0.003	0.003	0.003	0.002	0.003	0.003	0.003	0.002
K	0.939	0.939	0.941	0.940	0.941	0.949	0.947	0.947	0.945
Na	0.042	0.044	0.042	0.045	0.037	0.026	0.030	0.038	0.041
Ab%	4.256	4.433	4.285	4.556	3.767	2.677	3.028	3.901	4.124
An%	0.000	0.000	0.000	0.000	0.000	0.056	0.045	0.000	0.000
Or%	95.744	95.567	95.715	95.444	96.233	97.267	96.927	96.099	95.876

Plagioclase Feldspar

Table 19: Plagioclase feldspar compositions from various garnet line boundary layers in Oxford County, Maine pegmatites.

Sample	MT6-1-c-1	MT6-1-c-2	MT6-1-c-3	MT6-1-c-4	MT6-1-a-1	MT6-1-a-2	MT6-1-a-3	MA14-1-d-1
SiO_2	67.76	67.80	67.77	67.70	67.82	67.79	67.81	67.81
TiO_2	0.00	0.00	0.00	0.00	0.00	0.00	0.00	0.00
Al_2O_3	19.78	19.79	19.80	19.77	19.71	19.82	19.81	19.81
FeO	0.00	0.00	0.00	0.00	0.00	0.00	0.00	0.00
CaO	0.01	0.01	0.01	0.02	0.02	0.01	0.02	0.11
Cs_2O	0.00	0.00	0.00	0.00	0.00	0.00	0.00	0.00
Rb_2O	0.00	0.00	0.00	0.00	0.00	0.00	0.00	0.00
K_2O	0.21	0.20	0.19	0.21	0.23	0.22	0.18	0.12
Na_2O	10.98	11.00	10.91	11.03	10.91	10.89	10.97	10.79
Total	98.74	98.80	98.69	98.72	98.70	98.73	98.79	98.64
apfu								
Si	2.990	2.990	2.991	2.989	2.994	2.991	2.990	2.992
Ti	0.000	0.000	0.000	0.000	0.000	0.000	0.000	0.000
Al	1.029	1.029	1.030	1.029	1.026	1.031	1.030	1.030
Fe	0.000	0.000	0.000	0.000	0.000	0.000	0.000	0.000
Ca	0.000	0.000	0.001	0.001	0.001	0.001	0.001	0.005
Cs	0.000	0.000	0.000	0.000	0.000	0.000	0.000	0.000
Rb	0.000	0.000	0.000	0.000	0.000	0.000	0.000	0.000
K	0.012	0.011	0.011	0.012	0.013	0.012	0.010	0.007
Na	0.940	0.941	0.934	0.944	0.934	0.932	0.938	0.923
Ab	98.701	98.791	98.809	98.684	98.518	98.653	98.812	98.705
An	0.045	0.040	0.065	0.079	0.110	0.060	0.115	0.566
Or	1.254	1.170	1.126	1.237	1.372	1.287	1.073	0.728

Table 19 cont.

Sample	MA14-1-d-2	MA14-1-d-3	MA14-1-d-4	MA14-1-d-5	EM1-1-1	EM1-1-2	EM1-1-3	EM1-1e-4
SiO_2	67.84	67.83	67.81	67.81	67.76	67.81	67.77	67.75
TiO_2	0.00	0.00	0.00	0.00	0.00	0.00	0.00	0.00
Al_2O_3	19.81	19.82	19.80	19.80	19.81	19.79	19.81	19.80
FeO	0.00	0.00	0.00	0.00	0.00	0.00	0.00	0.00
CaO	0.22	0.12	0.17	0.21	0.22	0.20	0.23	0.19
Cs_2O	0.00	0.00	0.00	0.00	0.00	0.00	0.00	0.00
Rb_2O	0.00	0.00	0.00	0.00	0.00	0.00	0.00	0.00
K_2O	0.19	0.17	0.20	0.17	0.04	0.05	0.05	0.04
Na_2O	10.71	10.81	10.77	10.71	10.40	10.33	10.35	10.35
Total	98.78	98.75	98.74	98.71	98.24	98.17	98.21	98.13
apfu								
Si	2.991	2.991	2.991	2.991	2.996	2.999	2.997	2.998
Ti	0.000	0.000	0.000	0.000	0.000	0.000	0.000	0.000
Al	1.030	1.030	1.029	1.030	1.033	1.032	1.033	1.033
Fe	0.000	0.000	0.000	0.000	0.000	0.000	0.000	0.000
Ca	0.010	0.006	0.008	0.010	0.011	0.009	0.011	0.009
Cs	0.000	0.000	0.000	0.000	0.000	0.000	0.000	0.000
Rb	0.000	0.000	0.000	0.000	0.000	0.000	0.000	0.000
K	0.011	0.009	0.011	0.010	0.002	0.003	0.003	0.002
Na	0.916	0.924	0.921	0.916	0.892	0.886	0.888	0.888
Ab	97.734	98.397	97.963	97.906	98.563	98.670	98.467	98.758
An	1.119	0.609	0.840	1.066	1.162	1.029	1.214	0.997
Or	1.147	0.994	1.198	1.028	0.274	0.302	0.319	0.245

Table 19 cont.

Sample	EM1-1-5	EM2-2-i-1	EM2-2-i-2	EM2-2-i-3	EM2-2-i-4	HVY1-d-1	HVY1-d-2	HVY1-d-3
SiO_2	67.81	67.70	67.75	67.73	67.68	66.10	66.10	66.09
TiO_2	0.00	0.00	0.00	0.00	0.00	0.00	0.00	0.00
Al_2O_3	19.80	19.80	19.82	19.82	19.83	21.88	21.89	21.87
FeO	0.00	0.00	0.00	0.00	0.00	0.00	0.00	0.00
CaO	0.19	0.42	0.42	0.48	0.41	2.97	2.95	2.83
Cs_2O	0.00	0.00	0.00	0.00	0.00	0.00	0.00	0.00
Rb_2O	0.00	0.00	0.00	0.00	0.00	0.00	0.00	0.00
K_2O	0.06	0.06	0.06	0.04	0.04	0.02	0.02	0.02
Na_2O	10.44	10.21	10.26	10.20	10.24	9.78	9.80	9.84
Total	98.31	98.19	98.31	98.28	98.19	100.74	100.77	100.66
apfu								
Si	2.997	2.996	2.995	2.995	2.995	2.881	2.880	2.882
Ti	0.000	0.000	0.000	0.000	0.000	0.000	0.000	0.000
Al	1.032	1.033	1.033	1.033	1.034	1.124	1.124	1.124
Fe	0.000	0.000	0.000	0.000	0.000	0.000	0.000	0.000
Ca	0.009	0.020	0.020	0.023	0.019	0.139	0.138	0.132
Cs	0.000	0.000	0.000	0.000	0.000	0.000	0.000	0.000
Rb	0.000	0.000	0.000	0.000	0.000	0.000	0.000	0.000
K	0.003	0.003	0.003	0.002	0.002	0.001	0.001	0.001
Na	0.895	0.876	0.879	0.874	0.878	0.827	0.828	0.832
Ab	98.608	97.419	97.424	97.176	97.609	85.538	85.607	86.218
An	1.013	2.230	2.194	2.548	2.134	14.335	14.261	13.673
Or	0.379	0.351	0.381	0.276	0.257	0.127	0.132	0.110

Table 19 cont.

Sample	HVY3-1-1	HVY3-1-2	HVY3-1-3	HVY3-1-4	HVY3-1-5	TM2-1-1	TM2-1-2	BT1-a-4-1
SiO_2	67.59	67.68	67.83	67.66	67.54	68.51	68.50	67.80
TiO_2	0.00	0.00	0.00	0.00	0.00	0.00	0.00	
Al_2O_3	20.21	20.09	19.91	20.10	20.23	19.61	19.55	19.81
FeO	0.00	0.00	0.00	0.00	0.00	0.00	0.00	
CaO	0.89	0.79	0.59	0.81	0.95	0.21	0.20	0.03
Cs_2O	0.00	0.00	0.00	0.00	0.00	0.00	0.00	
Rb_2O	0.00	0.00	0.00	0.00	0.00	0.00	0.00	
K_2O	0.07	0.06	0.08	0.07	0.06	0.06	0.07	0.09
Na_2O	11.19	11.23	11.34	11.16	11.09	11.61	11.55	10.78
Total	99.94	99.84	99.76	99.79	99.87	100.01	99.87	98.51
apfu								
Si	2.959	2.964	2.973	2.964	2.958	2.991	2.994	2.994
Ti	0.000	0.000	0.000	0.000	0.000	0.000	0.000	0.000
Al	1.043	1.037	1.029	1.038	1.045	1.009	1.007	1.031
Fe	0.000	0.000	0.000	0.000	0.000	0.000	0.000	
Ca	0.042	0.037	0.028	0.038	0.044	0.010	0.009	0.002
Cs	0.000	0.000	0.000	0.000	0.000	0.000	0.000	0.000
Rb	0.000	0.000	0.000	0.000	0.000	0.000	0.000	0.000
K	0.004	0.003	0.005	0.004	0.003	0.003	0.004	0.005
Na	0.950	0.953	0.964	0.948	0.942	0.983	0.979	0.923
Ab	95.436	95.942	96.778	95.763	95.173	98.658	98.662	99.322
An	4.199	3.726	2.767	3.847	4.482	0.995	0.939	0.163
Or	0.365	0.332	0.455	0.390	0.345	0.347	0.399	0.515

Table 19 cont.

Sample	BT1-a-4-2	BT1-a-4-3	BT1-a-4-4	BT1-a-4-5	BT1-a-4-6	BT2-a-1	BT1-a-4-2	BT1-a-4-3
SiO_2	67.73	67.78	67.80	67.80	67.83	67.77	67.81	67.80
TiO_2								
Al_2O_3	19.82	19.79	19.78	19.87	19.86	19.80	19.80	19.81
FeO								
CaO	0.03	0.04	0.06	0.05	0.06	0.22	0.26	0.30
Cs_2O								
Rb_2O								
K_2O	0.13	0.09	0.06	0.07	0.08	0.07	0.06	0.04
Na_2O	10.83	10.82	10.91	10.87	10.84	10.29	10.40	10.41
Total	98.55	98.53	98.60	98.67	98.68	98.15	98.33	98.36
apfu								
Si	2.992	2.993	2.993	2.990	2.991	2.999	2.997	2.996
Ti	0.000	0.000	0.000	0.000	0.000	0.000	0.000	0.000
Al	1.032	1.030	1.029	1.033	1.032	1.033	1.031	1.032
Fe								
Ca	0.001	0.002	0.003	0.003	0.003	0.011	0.012	0.014
Cs	0.000	0.000	0.000	0.000	0.000	0.000	0.000	0.000
Rb	0.000	0.000	0.000	0.000	0.000	0.000	0.000	0.000
K	0.007	0.005	0.003	0.004	0.005	0.004	0.003	0.002
Na	0.928	0.927	0.934	0.930	0.927	0.883	0.891	0.892
Ab	99.064	99.261	99.368	99.312	99.176	98.418	98.284	98.164
An	0.142	0.208	0.302	0.268	0.318	1.173	1.337	1.563
Or	0.794	0.531	0.330	0.421	0.506	0.409	0.379	0.273

Table 19 cont.

Sample	BT1-a-4-4	BT1-a-4-5	BT3-e-1	BT3-e-2	BT3-e-3	BT3-e-4
SiO_2	67.83	67.78	67.81	67.79	67.80	67.78
TiO_2						
Al_2O_3	19.79	19.78	19.82	19.80	19.84	19.80
FeO						
CaO	0.34	0.32	0.17	0.21	0.19	0.23
Cs_2O						
Rb_2O						
K_2O	0.04	0.04	0.06	0.06	0.06	0.05
Na_2O	10.48	10.45	10.29	10.31	10.31	10.30
Total	98.49	98.36	98.15	98.17	98.20	98.16
apfu						
Si	2.995	2.995	2.999	2.999	2.998	2.998
Ti	0.000	0.000	0.000	0.000	0.000	0.000
Al	1.030	1.030	1.033	1.032	1.034	1.033
Fe						
Ca	0.016	0.015	0.008	0.010	0.009	0.011
Cs	0.000	0.000	0.000	0.000	0.000	0.000
Rb	0.000	0.000	0.000	0.000	0.000	0.000
K	0.002	0.002	0.003	0.003	0.003	0.003
Na	0.897	0.895	0.883	0.884	0.884	0.883
Ab	97.977	98.104	98.746	98.507	98.638	98.465
An	1.777	1.661	0.907	1.103	1.010	1.221
Or	0.246	0.235	0.347	0.390	0.353	0.315

Tourmaline

Table 20: Tourmaline compositions from garnet line boundary layers in Oxford County, Maine pegmatites.

Sample	MT2-3-d-1	MT2-3-d-2	MT2-3-d-3	MT1-2-b-1	MT1-2-b-2	MT1-2-b-3	MT1-2-b-4	MT1-2-d-1	MT1-2-d-2	MT1-2-d-3
SiO_2	36.59	36.50	36.55	36.58	36.56	35.02	35.11	36.57	36.62	36.60
TiO_2	0.01	0.01	0.01	0.01	0.01	0.02	0.02	0.01	0.01	0.01
B_2O_3 calc.	10.95	10.73	10.76	10.82	10.82	10.28	10.30	10.82	10.84	10.85
Al_2O_3	38.33	38.22	38.29	39.50	39.51	34.12	34.07	39.32	39.35	39.43
FeO	5.65	5.56	5.72	4.65	4.79	12.99	13.17	3.78	4.01	3.98
MnO	1.10	1.10	1.09	1.12	0.99	0.68	0.88	1.57	1.45	1.49
MgO										
CaO	0.42	0.48	0.50	0.12	0.10	0.09	0.09	0.43	0.39	0.45
Li_2O calc.	1.77	1.39	1.39	1.37	1.37	0.53	0.50	1.52	1.50	1.51
Na_2O	2.11	2.09	2.15	2.10	2.12	2.18	2.20	2.22	2.19	2.23
K_2O	0.03	0.03	0.03	0.02	0.02	0.03	0.03	0.02	0.03	0.02
H_2O calc.	3.31	3.21	3.22	3.27	3.28	3.12	3.15	3.27	3.25	3.27
F	1.00	1.04	1.05	0.99	0.97	0.90	0.87	0.98	1.05	1.01
Subtotal	101.29	100.37	100.76	100.55	100.53	99.94	100.37	100.52	100.69	100.86
O=F	0.42	0.44	0.44	0.42	0.41	0.38	0.36	0.41	0.44	0.42
Total	100.87	99.93	100.32	100.13	100.12	99.56	100.01	100.11	100.25	100.44
apfu										
Si	5.803	5.902	5.895	5.867	5.866	5.915	5.915	5.863	5.866	5.853
Ti	0.001	0.002	0.002	0.001	0.001	0.002	0.002	0.001	0.001	0.001
B	2.999	2.997	2.996	2.996	2.996	2.996	2.996	2.996	2.996	2.996
Al	7.166	7.285	7.278	7.468	7.470	6.792	6.764	7.431	7.429	7.433
Fe	0.750	0.752	0.771	0.624	0.642	1.834	1.855	0.507	0.537	0.533
Mn	0.148	0.151	0.148	0.152	0.134	0.097	0.125	0.213	0.197	0.201
Mg	0.000	0.000	0.000	0.000	0.000	0.000	0.000	0.000	0.000	0.000
Ca	0.072	0.083	0.086	0.021	0.017	0.016	0.016	0.074	0.067	0.077
Li	1.131	0.905	0.902	0.884	0.884	0.357	0.337	0.981	0.966	0.974
Na	0.649	0.656	0.674	0.653	0.658	0.713	0.719	0.689	0.680	0.692
K	0.007	0.006	0.006	0.004	0.005	0.006	0.007	0.004	0.006	0.005
H	3.498	3.467	3.463	3.499	3.510	3.520	3.539	3.502	3.471	3.492
F	0.502	0.533	0.537	0.501	0.490	0.480	0.461	0.498	0.529	0.508

Table 20 cont.

Sample	MT6-1-7-1	MT6-1-7-2	MT6-1-7-3	MT6-1h-1	MT6-1h-2	MT6-1-t-1	MT6-1-t-2	MT6-1-t-3	MT1-1A-1	mt1-1A-2
SiO_2	35.21	35.17	35.20	35.31	35.29	36.01	35.97	35.99	36.68	36.50
TiO_2	0.01	0.01	0.01	0.01	0.01	0.01	0.01	0.01	0.01	0.01
B_2O_3 calc.	10.34	10.33	10.38	10.43	10.42	10.64	10.63	10.63	10.79	10.75
Al_2O_3	34.46	34.43	34.88	35.10	34.99	37.77	37.68	37.80	38.78	38.70
FeO	13.11	13.09	13.21	12.98	13.17	6.07	6.12	6.09	4.99	4.99
MnO	0.34	0.36	0.30	0.33	0.34	0.99	0.87	0.86	0.98	0.99
MgO	0.00	0.00	0.00	0.00	0.00	0.00	0.00	0.00	0.00	0.00
CaO	0.09	0.11	0.08	0.11	0.10	0.55	0.63	0.59	0.53	0.48
Li_2O calc.	0.56	0.56	0.51	0.56	0.54	1.36	1.39	1.37	1.46	1.43
Na_2O	2.21	2.19	2.09	2.19	2.17	2.21	2.19	2.20	2.00	1.98
K_2O	0.02	0.03	0.03	0.03	0.03	0.03	0.04	0.02	0.02	0.02
H_2O calc.	3.18	3.13	3.16	3.21	3.20	3.29	3.29	3.25	3.21	3.20
F	0.83	0.93	0.90	0.82	0.83	0.82	0.80	0.89	1.10	1.09
Subtotal	100.38	100.34	100.76	101.10	101.08	99.73	99.62	99.70	100.55	100.14
O=F	0.35	0.39	0.38	0.35	0.35	0.35	0.34	0.37	0.46	0.46
Total	100.02	99.94	100.38	100.75	100.73	99.39	99.28	99.33	100.08	99.68

Table 20 cont.

Sample	MT6-1-7-1	MT6-1-7-2	MT6-1-7-3	MT6-1h-1	MT6-1h-2	MT6-1-t-1	MT6-1-t-2	MT6-1-t-3	MT1-1A-1	mt1-1A-2
apfu										
Si	5.910	5.908	5.886	5.878	5.881	5.875	5.874	5.873	5.898	5.893
Ti	0.002	0.001	0.002	0.002	0.001	0.001	0.002	0.001	0.001	0.001
B	2.996	2.995	2.997	2.996	2.996	2.996	2.996	2.995	2.996	2.996
Al	6.817	6.819	6.874	6.886	6.872	7.263	7.253	7.271	7.351	7.365
Fe	1.841	1.840	1.848	1.807	1.835	0.828	0.836	0.832	0.671	0.673
Mn	0.049	0.051	0.042	0.047	0.048	0.136	0.121	0.119	0.134	0.135
Mg	0.000	0.000	0.000	0.000	0.000	0.000	0.000	0.000	0.000	0.000
Ca	0.017	0.020	0.015	0.020	0.019	0.097	0.111	0.103	0.092	0.084
Li	0.378	0.377	0.346	0.377	0.360	0.894	0.911	0.899	0.942	0.930
Na	0.720	0.714	0.678	0.707	0.699	0.700	0.695	0.696	0.623	0.621
K	0.005	0.007	0.005	0.007	0.006	0.005	0.009	0.005	0.004	0.005
H	3.557	3.504	3.522	3.567	3.560	3.575	3.588	3.542	3.440	3.443
F	0.443	0.496	0.478	0.433	0.440	0.425	0.412	0.458	0.560	0.557

Table 20 cont.

Sample	mt1-1A-3	mt1-1A-4	mt1-1N-1	mt1-1N-2	mt1-1N-3	mt1-1N-4	mt1-1N-5	mt1-1N-6	MT10-1	MT10 -2
SiO_2	36.52	36.48	36.48	36.54	36.52	36.51	36.58	36.50	36.45	36.41
TiO_2	0.01	0.01	0.01	0.01	0.01	0.01	0.01	0.01	0.02	0.02
B_2O_3 calc.	10.75	10.76	10.75	10.76	10.73	10.74	10.76	10.68	10.76	10.76
Al_2O_3	38.68	38.88	38.78	38.78	38.70	38.70	38.71	38.69	38.47	38.50
FeO	5.00	4.89	4.90	4.79	4.65	5.02	5.11	5.09	4.99	5.01
MnO	0.89	0.90	1.01	1.11	1.09	0.67	0.57	0.61	1.38	1.31
MgO	0.00	0.00	0.00	0.00	0.00	0.00	0.00	0.00	0.00	0.00
CaO	0.51	0.51	0.45	0.45	0.40	0.45	0.42	0.44	0.40	0.41
Li_2O calc.	1.45	1.43	1.41	1.43	1.43	1.47	1.48	1.42	1.43	1.43
Na_2O	2.01	1.89	1.91	1.99	1.89	2.01	2.11	2.12	2.20	2.18
K_2O	0.03	0.02	0.03	0.03	0.03	0.03	0.02	0.03	0.02	0.03
H_2O calc.	3.18	3.14	3.24	3.24	3.24	3.18	3.19	3.19	3.25	3.24
F	1.12	1.21	1.00	1.01	0.98	1.12	1.11	1.09	0.98	1.00
Subtotal	100.15	100.12	99.97	100.13	99.68	99.91	100.08	99.88	100.34	100.31
O=F	0.47	0.51	0.42	0.42	0.41	0.47	0.47	0.46	0.41	0.42
Total	99.68	99.61	99.55	99.71	99.27	99.44	99.61	99.42	99.93	99.89

Table 20 cont.

Sample	mt1-1A-3	mt1-1A-4	mt1-1N-1	mt1-1N-2	mt1-1N-3	mt1-1N-4	mt1-1N-5	mt1-1N-6	MT10-1	MT10 -2
apfu										
Si	5.896	5.888	5.893	5.895	5.909	5.900	5.902	5.904	5.885	5.882
Ti	0.001	0.001	0.001	0.001	0.001	0.001	0.002	0.001	0.003	0.002
B	2.995	2.996	2.997	2.996	2.997	2.997	2.996	2.983	3.000	3.000
Al	7.359	7.395	7.384	7.374	7.380	7.372	7.363	7.377	7.322	7.330
Fe	0.676	0.661	0.662	0.646	0.629	0.679	0.690	0.689	0.674	0.677
Mn	0.122	0.123	0.138	0.152	0.150	0.092	0.077	0.084	0.188	0.180
Mg	0.000	0.000	0.000	0.000	0.000	0.000	0.000	0.000	0.000	0.000
Ca	0.088	0.088	0.079	0.077	0.070	0.078	0.073	0.077	0.069	0.071
Li	0.942	0.929	0.919	0.928	0.928	0.953	0.964	0.925	0.927	0.929
Na	0.629	0.592	0.599	0.623	0.593	0.630	0.661	0.665	0.689	0.683
K	0.005	0.004	0.006	0.006	0.007	0.005	0.005	0.006	0.004	0.007
H	3.427	3.382	3.487	3.485	3.498	3.427	3.433	3.442	3.501	3.487
F	0.573	0.618	0.513	0.515	0.502	0.573	0.567	0.558	0.499	0.512

Table 20 cont.

Sample	MT10 -3	MT10-4	MT10 -5	MT10-6	MT10 -7	MT10-8	MT10-9	EM1-1-d-1	EM1-1-d-2	EM1-1-d-3
SiO_2	36.39	36.43	36.47	36.44	36.41	36.36	36.40	36.45	36.50	36.45
TiO_2	0.02	0.02	0.08	0.09	0.11	0.09	0.09	0.89	0.93	0.87
B_2O_3 calc.	10.75	10.76	10.40	10.40	10.40	10.39	10.40	10.38	10.38	10.37
Al_2O_3	38.48	38.46	32.77	32.80	32.93	32.98	33.02	32.66	32.56	32.66
FeO	5.11	5.21	12.98	12.77	12.59	12.46	12.54	10.34	10.45	10.30
MnO	1.20	1.23	0.85	0.86	0.88	0.90	0.86	0.22	0.25	0.22
MgO	0.00	0.00	0.01	0.01	0.02	0.02	0.01	0.78	0.61	0.70
CaO	0.43	0.40	0.09	0.10	0.10	0.09	0.10	0.03	0.04	0.05
Li_2O calc.	1.43	1.42	0.90	0.93	0.92	0.91	0.90	1.16	1.20	1.18
Na_2O	2.17	2.21	2.28	2.31	2.29	2.30	2.20	2.21	2.19	2.21
K_2O	0.03	0.03	0.02	0.02	0.02	0.02	0.03	0.04	0.03	0.04
H_2O calc.	3.25	3.29	3.18	3.18	3.18	3.19	3.19	3.16	3.15	3.18
F	0.98	0.89	0.87	0.86	0.87	0.84	0.83	0.89	0.90	0.86
Subtotal	100.26	100.35	100.88	100.74	100.71	100.55	100.58	99.23	99.20	99.10
O=F	0.41	0.38	0.36	0.36	0.36	0.36	0.35	0.37	0.38	0.36
Total	99.85	99.97	100.52	100.38	100.34	100.20	100.23	98.85	98.82	98.73

Table 20 cont.

Sample	MT10 -3	MT10-4	MT10 -5	MT10-6	MT10 -7	MT10-8	MT10-9	EM1-1-d-1	EM1-1-d-2	EM1-1-d-3
apfu										
Si	5.881	5.882	6.091	6.089	6.082	6.078	6.083	6.096	6.108	6.100
Ti	0.003	0.003	0.010	0.011	0.014	0.012	0.011	0.112	0.117	0.110
B	3.000	3.000	2.999	2.999	2.999	2.999	2.999	2.998	2.998	2.998
Al	7.329	7.319	6.451	6.460	6.483	6.500	6.504	6.437	6.422	6.443
Fe	0.691	0.704	1.813	1.784	1.758	1.742	1.753	1.447	1.462	1.442
Mn	0.164	0.168	0.121	0.121	0.124	0.128	0.122	0.031	0.036	0.032
Mg	0.000	0.000	0.003	0.002	0.005	0.004	0.003	0.193	0.151	0.175
Ca	0.075	0.070	0.016	0.018	0.018	0.016	0.017	0.006	0.008	0.009
Li	0.932	0.925	0.603	0.622	0.615	0.615	0.606	0.777	0.811	0.797
Na	0.681	0.692	0.737	0.749	0.741	0.746	0.712	0.718	0.711	0.719
K	0.006	0.005	0.005	0.004	0.004	0.005	0.006	0.009	0.007	0.008
H	3.498	3.544	3.542	3.548	3.542	3.553	3.560	3.531	3.522	3.547
F	0.502	0.456	0.457	0.452	0.457	0.446	0.440	0.469	0.478	0.453

Table 20 cont.

Sample	EM1-1-d-4	EM1-1-d-5	EM1-2-b-1	EM1-2-b-2	EM1-2-b-3	EM1-2-b-4	EM2-2-f-1	EM2-2-f-2	EM2-2-f-3	EM2-2-f-4
SiO_2	36.51	36.40	36.54	36.51	36.60	36.54	36.48	36.42	36.40	36.57
TiO_2	0.88	0.82	0.68	0.65	0.71	0.60	0.21	0.23	0.30	0.22
B_2O_3 calc.	10.38	10.35	10.34	10.34	10.36	10.35	10.31	10.30	10.31	10.32
Al_2O_3	32.60	32.60	32.54	32.51	32.50	32.54	32.66	32.68	32.65	32.66
FeO	10.42	10.39	10.41	10.33	10.45	10.39	10.81	10.87	10.91	10.80
MnO	0.19	0.18	0.20	0.21	0.21	0.20	0.12	0.12	0.11	0.13
MgO	0.71	0.68	0.57	0.67	0.65	0.66	0.32	0.34	0.31	0.32
CaO	0.03	0.04	0.04	0.04	0.03	0.04	0.06	0.06	0.05	0.05
Li_2O calc.	1.19	1.17	1.25	1.23	1.23	1.24	1.28	1.24	1.26	1.30
Na_2O	2.24	2.12	2.10	2.11	2.10	2.22	2.22	2.15	2.34	2.25
K_2O	0.04	0.04	0.03	0.03	0.04	0.03	0.04	0.04	0.04	0.05
H_2O calc.	3.17	3.14	3.17	3.19	3.16	3.16	3.19	3.17	3.18	3.20
F	0.88	0.91	0.85	0.80	0.87	0.87	0.78	0.81	0.81	0.76
Subtotal	99.23	98.83	98.72	98.61	98.91	98.86	98.48	98.42	98.68	98.61
O=F	0.37	0.38	0.36	0.34	0.37	0.36	0.33	0.34	0.34	0.32
Total	98.86	98.45	98.37	98.27	98.55	98.49	98.15	98.08	98.34	98.29

Table 20 cont.

Sample	EM1-1-d-4	EM1-1-d-5	EM1-2-b-1	EM1-2-b-2	EM1-2-b-3	EM1-2-b-4	EM2-2-f-1	EM2-2-f-2	EM2-2-f-3	EM2-2-f-4
apfu										
Si	6.106	6.109	6.134	6.133	6.135	6.130	6.146	6.141	6.129	6.151
Ti	0.110	0.104	0.085	0.081	0.090	0.076	0.027	0.029	0.037	0.027
B	2.998	2.998	2.998	2.998	2.998	2.998	2.998	2.998	2.998	2.998
Al	6.425	6.449	6.439	6.438	6.421	6.434	6.484	6.495	6.480	6.475
Fe	1.457	1.459	1.462	1.452	1.464	1.458	1.523	1.533	1.537	1.519
Mn	0.027	0.025	0.028	0.030	0.030	0.028	0.018	0.017	0.016	0.018
Mg	0.177	0.169	0.142	0.168	0.162	0.165	0.081	0.084	0.078	0.079
Ca	0.006	0.007	0.007	0.007	0.006	0.007	0.010	0.010	0.009	0.008
Li	0.802	0.793	0.842	0.829	0.831	0.837	0.865	0.839	0.851	0.880
Na	0.725	0.688	0.683	0.687	0.681	0.723	0.726	0.704	0.764	0.734
K	0.009	0.009	0.007	0.007	0.009	0.007	0.009	0.008	0.009	0.010
H	3.536	3.520	3.551	3.575	3.538	3.541	3.583	3.571	3.568	3.595
F	0.464	0.480	0.449	0.425	0.462	0.459	0.417	0.429	0.432	0.405

Table 20 cont.

Sample	EM2-2-f-5	BT3-e-1	BT3-e-2	BT3-e-3	BT3-e-4	BT3-e-5	BT3-g-1	BT3-g-2	BT3-g-3	BT3-g-4
SiO_2	36.56	36.69	36.55	36.66	36.60	36.61	36.57	36.61	36.64	36.56
TiO_2	0.21	0.03	0.04	0.03	0.04	0.04	0.06	0.04	0.04	0.05
B_2O_3 calc.	10.32	10.81	10.79	10.82	10.83	10.83	10.80	10.80	10.80	10.79
Al_2O_3	32.65	38.21	38.33	38.35	38.40	38.37	38.09	38.10	38.10	38.09
FeO	10.86	6.33	6.40	6.30	6.32	6.30	6.64	6.59	6.58	6.73
MnO	0.12	0.23	0.20	0.20	0.19	0.19	0.16	0.18	0.12	0.15
MgO	0.29	0.32	0.33	0.41	0.42	0.43	0.44	0.38	0.41	0.37
CaO	0.05	0.68	0.60	0.62	0.61	0.60	0.56	0.54	0.50	0.50
Li_2O calc.	1.30	1.38	1.35	1.37	1.38	1.37	1.35	1.36	1.35	1.33
Na_2O	2.22	1.90	1.91	1.99	2.10	2.10	2.11	2.13	2.09	2.07
K_2O	0.04	0.03	0.02	0.03	0.03	0.03	0.03	0.03	0.03	0.03
H_2O calc.	3.18	3.25	3.25	3.27	3.31	3.28	3.69	3.27	3.27	3.27
F	0.81	1.01	0.99	0.97	0.90	0.96	0.08	0.97	0.96	0.96
Subtotal	98.60	100.87	100.76	101.02	101.13	101.11	100.56	101.01	100.89	100.90
O=F	0.34	0.43	0.42	0.41	0.38	0.40	0.03	0.41	0.40	0.40
Total	98.26	100.44	100.35	100.61	100.75	100.70	100.53	100.61	100.48	100.50

Table 20 cont.

Sample	EM2-2-f-5	BT3-e-1	BT3-e-2	BT3-e-3	BT3-e-4	BT3-e-5	BT3-g-1	BT3-g-2	BT3-g-3	BT3-g-4
apfu										
Si	6.152	5.901	5.884	5.886	5.872	5.876	5.883	5.890	5.898	5.889
Ti	0.027	0.004	0.005	0.004	0.005	0.005	0.007	0.005	0.005	0.007
B	2.998	3.001	3.000	3.000	3.000	3.001	3.000	3.000	3.000	3.001
Al	6.476	7.244	7.276	7.258	7.262	7.258	7.223	7.224	7.228	7.232
Fe	1.528	0.852	0.862	0.846	0.848	0.846	0.894	0.886	0.886	0.907
Mn	0.017	0.032	0.027	0.027	0.025	0.026	0.021	0.024	0.017	0.021
Mg	0.073	0.077	0.079	0.099	0.101	0.104	0.106	0.092	0.099	0.090
Ca	0.008	0.117	0.103	0.107	0.105	0.103	0.096	0.094	0.086	0.086
Li	0.877	0.893	0.871	0.883	0.891	0.883	0.871	0.883	0.872	0.861
Na	0.725	0.592	0.597	0.619	0.653	0.654	0.659	0.666	0.653	0.647
K	0.009	0.007	0.005	0.006	0.006	0.006	0.006	0.005	0.006	0.005
H	3.567	3.485	3.496	3.508	3.543	3.515	3.957	3.504	3.513	3.512
F	0.433	0.515	0.503	0.491	0.455	0.485	0.042	0.495	0.487	0.487

Table 20 cont.

Sample	BT3-g-5	HVY1-d-1	HVY1-d-2	HVY1-d-3	HVY1-d-4	TM3-1-c-1	TM3-1-c-2	TM3-1-c-3	TM3-1-f-1	TM3-1-f-2
SiO_2	36.61	35.60	35.55	35.51	35.60	36.38	36.39	36.40	36.36	36.41
TiO_2	0.04	0.13	0.15	0.13	0.14	0.04	0.05	0.03	0.03	0.02
B_2O_3 calc.	10.81	10.36	10.34	10.33	10.36	10.69	10.68	10.69	10.66	10.66
Al_2O_3	38.23	33.65	33.69	33.67	33.72	37.88	37.79	37.79	37.85	37.79
FeO	6.63	12.22	12.20	12.23	12.13	5.63	5.56	5.72	5.61	5.56
MnO	0.13	0.02	0.02	0.02	0.03	1.11	1.09	1.21	1.09	1.00
MgO	0.38	1.00	0.97	1.00	1.01	0.00	0.00	0.00	0.00	0.00
CaO	0.54	0.16	0.14	0.13	0.15	0.29	0.28	0.26	0.23	0.21
Li_2O calc.	1.34	0.57	0.55	0.53	0.57	1.39	1.40	1.37	1.35	1.38
Na_2O	2.10	2.10	2.03	2.01	2.10	2.27	2.25	2.31	2.12	2.18
K_2O	0.02	0.03	0.02	0.02	0.02	0.02	0.02	0.01	0.02	0.03
H_2O calc.	3.26	3.30	3.27	3.30	3.28	3.27	3.24	3.26	3.28	3.28
F	1.00	0.58	0.62	0.56	0.62	0.89	0.93	0.90	0.83	0.84
Subtotal	101.10	99.72	99.55	99.46	99.73	99.88	99.68	99.98	99.43	99.36
O=F	0.42	0.24	0.26	0.23	0.26	0.38	0.39	0.38	0.35	0.35
Total	100.68	99.47	99.29	99.22	99.47	99.50	99.28	99.60	99.08	99.01

Table 20 cont.

Sample	BT3-g-5	HVY1-d-1	HVY1-d-2	HVY1-d-3	HVY1-d-4	TM3-1-c-1	TM3-1-c-2	TM3-1-c-3	TM3-1-f-1	TM3-1-f-2
apfu										
Si	5.884	5.974	5.974	5.972	5.971	5.912	5.922	5.915	5.926	5.935
Ti	0.005	0.017	0.018	0.017	0.018	0.005	0.006	0.004	0.003	0.003
B	3.000	3.000	3.000	3.000	3.000	3.000	3.000	3.000	3.000	3.000
Al	7.243	6.657	6.673	6.675	6.667	7.255	7.250	7.239	7.271	7.260
Fe	0.892	1.716	1.714	1.720	1.702	0.766	0.757	0.777	0.765	0.757
Mn	0.018	0.003	0.003	0.003	0.004	0.153	0.150	0.167	0.151	0.139
Mg	0.090	0.250	0.244	0.252	0.252	0.000	0.000	0.000	0.000	0.000
Ca	0.094	0.028	0.025	0.024	0.026	0.051	0.048	0.046	0.041	0.037
Li	0.865	0.384	0.374	0.360	0.385	0.909	0.915	0.898	0.884	0.905
Na	0.654	0.683	0.662	0.655	0.683	0.714	0.711	0.728	0.670	0.689
K	0.004	0.007	0.005	0.005	0.004	0.004	0.003	0.003	0.005	0.006
H	3.492	3.694	3.669	3.704	3.670	3.541	3.519	3.536	3.570	3.569
F	0.507	0.306	0.331	0.296	0.329	0.459	0.481	0.464	0.430	0.430

Table 20 cont.

Sample	TM4-1-c-1	TM4-1-c-2	TM4-1-c-3
SiO_2	36.40	36.38	36.37
TiO_2	0.02	0.02	0.02
B_2O_3 calc.	10.71	10.72	10.71
Al_2O_3	38.32	38.38	38.33
FeO	4.98	5.01	5.03
MnO	1.22	1.20	1.29
MgO	0.00	0.00	0.00
CaO	0.23	0.25	0.27
Li_2O calc.	1.41	1.41	1.39
Na_2O	2.20	2.19	2.12
K_2O	0.03	0.04	0.05
H_2O calc.	3.24	3.22	3.22
F	0.96	1.01	1.01
Subtotal	99.74	99.82	99.80
O=F	0.40	0.42	0.42
Total	99.34	99.39	99.37
apfu			
Si	5.905	5.899	5.901
Ti	0.003	0.002	0.002
B	3.000	3.000	3.000
Al	7.327	7.335	7.330
Fe	0.676	0.679	0.683
Mn	0.168	0.165	0.177
Mg	0.000	0.000	0.000
Ca	0.041	0.044	0.046
Li	0.922	0.920	0.906
Na	0.692	0.689	0.666
K	0.007	0.008	0.011
H	3.509	3.482	3.483
F	0.490	0.517	0.517

Columbite-group Minerals

Table 21: Columbite-group mineral compositions from garnet boundary layers in Oxford County, Maine pegmatites.

Sample	MT2-3-f-1	MT2-3-f-2	MT2-3-f-3	MT2-3-f-4	MT2-3-f-5	MT2-3-f-6	MT2-3-f-7	MT1-2-f-1	MT1-2-f-2	MT1-2-f-3	MT1-2-f-4
Nb_2O_5	37.90	38.23	29.44	29.41	24.90	25.01	24.98	37.66	37.56	37.45	37.60
Ta_2O_5	45.23	45.09	53.67	53.56	59.41	59.34	59.22	45.32	45.23	45.44	45.23
UO_2	0.00	0.00	0.00	0.00	0.00	0.00	0.00	0.02	0.02	0.02	0.04
SiO_2	0.04	0.07	0.09	0.10	0.06	0.09	0.08	0.02	0.01	0.00	0.00
TiO_2	0.00	0.00	0.00	0.00	0.00	0.00	0.00	0.00	0.00	0.00	0.00
SnO_2	0.12	0.11	0.14	0.12	0.14	0.12	0.10	0.03	0.01	0.01	0.08
Al_2O_3	0.00	0.00	0.00	0.00	0.00	0.00	0.00	0.00	0.00	0.00	0.00
FeO	5.78	5.89	4.76	4.62	5.99	6.11	5.90	6.34	6.22	5.95	5.76
MnO	11.68	11.60	11.89	11.89	10.21	10.32	10.29	11.11	11.34	11.62	11.78
CaO	0.00	0.00	0.00	0.00	0.00	0.00	0.00	0.00	0.00	0.00	0.00
Total	100.75	100.99	99.99	99.69	100.71	100.98	100.56	100.51	100.40	100.50	100.49
A-site											
Fe	1.311	1.331	1.136	1.106	1.458	1.482	1.436	1.443	1.419	1.356	1.312
Mn	2.682	2.654	2.874	2.881	2.519	2.535	2.539	2.562	2.619	2.683	2.717
Mg	0.000	0.000	0.000	0.000	0.000	0.000	0.000	0.000	0.000	0.000	0.000
A-total	3.993	3.984	4.010	3.987	3.976	4.018	3.975	4.005	4.037	4.039	4.029
B-site											
Sn	0.013	0.012	0.016	0.014	0.017	0.014	0.011	0.003	0.001	0.001	0.009
Ta	3.336	3.312	4.165	4.167	4.705	4.682	4.692	3.355	3.353	3.368	3.350
Nb	4.647	4.669	3.798	3.805	3.278	3.280	3.291	4.634	4.628	4.615	4.629
B-total	7.996	7.993	7.979	7.986	8.000	7.976	7.994	7.993	7.982	7.984	7.988
Mn/(Mn+Fe)	0.672	0.666	0.717	0.723	0.633	0.631	0.639	0.640	0.649	0.664	0.674
Ta/(Ta+Nb)	0.418	0.415	0.523	0.523	0.589	0.588	0.588	0.420	0.420	0.422	0.420

Table 21 cont.

Sample	MT1-2-f-5	EM1-1-f-1	EM1-1-f-2	EM1-1-f-3	EM1-1-f-4	EM1-1-f-5	EM1-1-f-6	EM1-1-f-7	EM1-1-f-8	EM1-1-f-9
Nb_2O_5	37.23	71.34	71.50	71.43	63.56	63.50	63.57	44.95	44.96	44.86
Ta_2O_5	45.64	8.99	9.09	9.56	17.01	16.99	16.97	35.95	35.94	35.99
UO_2	0.03	0.02	0.03	0.03	0.05	0.05	0.05	0.06	0.66	0.06
SiO_2	0.01	0.03	0.03	0.03	0.03	0.01	0.04	0.06	0.06	0.04
TiO_2	0.00	0.27	0.24	0.27	0.19	0.20	0.19	0.10	0.10	0.10
SnO_2	0.03	0.12	0.09	0.13	0.10	0.13	0.13	0.21	0.18	0.19
Al_2O_3	0.00	0.23	0.05	0.01	0.03	0.02	0.02	0.03	0.03	0.03
FeO	6.09	12.90	12.67	12.78	12.67	12.54	12.52	4.32	4.10	4.42
MnO	10.98	5.78	5.90	5.84	6.31	6.39	6.40	13.78	13.80	13.68
CaO	0.00	0.00	0.00	0.00	0.00	0.00	0.00	0.00	0.01	0.00
Total	100.03	99.68	99.62	100.08	99.95	99.83	99.89	99.46	99.83	99.38
A-site										
Fe	1.397	2.503	2.464	2.479	2.547	2.525	2.518	0.952	0.902	0.976
Mn	2.549	1.136	1.163	1.148	1.285	1.303	1.304	3.078	3.078	3.058
Mg	0.000	0.000	0.000	0.000	0.000	0.000	0.000	0.000	0.000	0.000
A-total	3.946	3.640	3.627	3.627	3.832	3.828	3.822	4.030	3.980	4.033
B-site										
Sn	0.004	0.011	0.009	0.012	0.009	0.012	0.013	0.022	0.019	0.020
Ta	3.402	0.567	0.575	0.603	1.112	1.112	1.110	2.577	2.574	2.584
Nb	4.613	7.486	7.517	7.491	6.907	6.910	6.911	5.357	5.352	5.353
B-total	8.018	8.064	8.100	8.106	8.028	8.034	8.033	7.956	7.945	7.957
Mn/(Mn+Fe)	0.646	0.312	0.321	0.317	0.335	0.340	0.341	0.764	0.773	0.758
Ta/(Ta+Nb)	0.424	0.070	0.071	0.074	0.139	0.139	0.138	0.325	0.325	0.326

Zircon Table 22: Zircon compositions from garnet boundary layer in Oxford County, Maine pegmatites.

Sample	MA14-1-H-1	MA14-1-H-2	MA14-1-H-3	MA14-1-H-4	MA14-1-H-5	MA13-1-h-1	MA13-1-h-2	MA13-1-h-3	MA13-1-h-4	MA2-1-4-1	MA2-1-4-2	MA2-1-4-3
ZrO_2	64.43	64.39	64.28	64.31	64.28	64.56	64.49	62.25	62.56	64.22	64.31	64.28
SiO_2	32.32	32.28	32.44	32.31	32.33	32.44	32.39	30.09	30.01	32.46	32.48	32.44
HfO_2	2.89	2.78	2.67	2.80	2.78	2.92	3.01	2.89	2.78	3.03	3.06	3.10
UO_2	0.09	0.11	0.09	0.09	0.08	0.07	0.07	0.03	0.03	0.07	0.07	0.08
FeO	0.81	0.92	0.67	0.73	0.82	0.32	0.45	0.41	0.44	0.45	0.52	0.98
CaO	0.03	0.02	0.03	0.06	0.08	0.04	0.05	0.04	0.05	0.03	0.05	0.04
Al_2O_3	0.05	0.05	0.06	0.04	0.06	0.04	0.05	0.05	0.04	0.03	0.05	0.05
MnO	0.10	0.09	0.08	0.11	0.09	0.07	0.08	0.06	0.07	0.09	0.09	0.07
ThO_2	0.32	0.39	0.29	0.23	0.31	0.29	0.27	0.27	0.23	0.21	0.24	0.21
Total	101.06	101.03	100.61	100.69	100.84	100.76	100.86	96.11	96.20	100.60	100.86	101.26
apfu												
Zr	0.965	0.965	0.964	0.965	0.964	0.968	0.967	0.985	0.990	0.964	0.963	0.961
Si	0.993	0.992	0.998	0.995	0.994	0.997	0.996	0.977	0.974	0.999	0.998	0.994
Hf	0.025	0.024	0.023	0.025	0.024	0.026	0.026	0.027	0.026	0.027	0.027	0.027
U	0.001	0.001	0.001	0.001	0.001	0.000	0.000	0.000	0.000	0.000	0.000	0.001
Fe	0.021	0.024	0.017	0.019	0.021	0.008	0.012	0.011	0.012	0.012	0.013	0.025
Ca	0.001	0.001	0.001	0.002	0.003	0.001	0.002	0.001	0.002	0.001	0.002	0.001
Al	0.002	0.002	0.002	0.002	0.002	0.002	0.002	0.002	0.002	0.001	0.002	0.002
Mn	0.003	0.002	0.002	0.003	0.002	0.002	0.002	0.002	0.002	0.002	0.002	0.002
Th	0.002	0.003	0.002	0.002	0.002	0.002	0.002	0.002	0.002	0.001	0.002	0.001
X-site	0.993	0.993	0.990	0.992	0.991	0.996	0.995	1.014	1.017	0.993	0.992	0.990
Y-site	0.993	0.992	0.998	0.995	0.994	0.997	0.996	0.977	0.974	0.999	0.998	0.994

Table 22 cont.

Sample	MA2-1-4-4	BT1-a-3-1	BT1-a-3-2	BT1-a-3-3	BT1-a-3-4	BT1-a-3-5	BT3-e-1	BT3-e-2	BT3-e-3	BT3-e-4	BT3-e-5	EM1-2-a-1
ZrO_2	62.31	64.22	64.30	64.33	64.20	64.31	64.22	64.30	64.30	64.31	64.30	63.83
SiO_2	32.51	32.33	32.41	32.35	32.41	32.37	32.40	32.37	32.60	32.57	32.61	32.19
HfO_2	2.98	3.21	3.28	3.22	3.78	3.55	3.19	3.18	3.10	3.19	3.20	3.68
UO_2	0.07	0.00	0.02	0.01	0.02	0.03	0.02	0.02	0.02	0.01	0.02	0.87
FeO	0.46	0.03	0.03	0.03	0.04	0.04	0.05	0.05	0.04	0.05	0.06	0.09
CaO	0.04	0.04	41.00	0.03	0.06	0.05	0.06	0.05	0.05	0.05	0.05	0.08
Al_2O_3	0.05	0.02	0.02	0.04	0.03	0.04	0.04	0.04	0.04	0.04	0.03	0.05
MnO	0.08	0.06	0.05	0.05	0.06	0.06	0.05	0.06	0.06	0.07	0.05	0.12
ThO_2	0.24	0.07	0.07	0.07	0.08	0.07	0.09	0.09	0.09	0.09	0.08	0.12
Total	98.73	99.99	141.19	100.14	100.69	100.53	100.11	100.16	100.29	100.39	100.39	101.04

Table 22 cont.

	MA2-1-4-4	BT1-a-3-1	BT1-a-3-2	BT1-a-3-3	BT1-a-3-4	BT1-a-3-5	BT3-e-1	BT3-e-2	BT3-e-3	BT3-e-4	BT3-e-5	EM1-2-a-1
apfu												
Zr	0.948	0.969	0.723	0.969	0.964	0.967	0.967	0.968	0.965	0.965	0.965	0.961
Si	1.014	1.000	0.747	0.999	0.998	0.998	1.001	1.000	1.004	1.002	1.003	0.994
Hf	0.027	0.028	0.022	0.028	0.033	0.031	0.028	0.028	0.027	0.028	0.028	0.032
U	0.000	0.000	0.000	0.000	0.000	0.000	0.000	0.000	0.000	0.000	0.000	0.006
Fe	0.012	0.001	0.001	0.001	0.001	0.001	0.001	0.001	0.001	0.001	0.001	0.002
Ca	0.001	0.001	1.013	0.001	0.002	0.002	0.002	0.002	0.002	0.002	0.001	0.003
Al	0.002	0.001	0.001	0.001	0.001	0.002	0.002	0.001	0.001	0.001	0.001	0.002
Mn	0.002	0.001	0.001	0.001	0.002	0.002	0.001	0.002	0.001	0.002	0.001	0.003
Th	0.002	0.001	0.000	0.001	0.001	0.000	0.001	0.001	0.001	0.001	0.001	0.001
X-site	0.977	0.998	0.745	0.998	0.998	0.999	0.996	0.997	0.993	0.994	0.994	1.000
Y-site	1.014	1.000	0.747	0.999	0.998	0.998	1.001	1.000	1.004	1.002	1.003	0.994

Table 22 cont.

Sample	EM1-2-a-2	EM1-2-a-3	EM1-2-a-4	EM2-2-c-1	EM2-2-c-2	EM2-2-c-3	EM2-2-7-1	EM2-2-7-2	EM2-2-7-3	MT6-1-u-1	MT6-1-u-2	MT6-1-u-3
ZrO_2	64.78	64.01	64.01	63.92	63.79	63.82	63.80	63.78	63.80	64.23	64.17	64.23
SiO_2	32.19	32.09	32.17	32.33	32.21	32.27	32.30	32.26	32.24	32.21	32.19	32.31
HfO_2	4.09	4.11	4.01	3.56	3.90	3.78	3.67	3.63	3.57	3.01	3.22	2.98
UO_2	0.70	0.79	0.79	0.21	0.23	0.20	0.16	0.16	0.15	0.04	0.04	0.03
FeO	0.10	0.08	0.09	0.12	0.09	0.10	0.13	0.14	0.14	0.01	0.02	0.01
CaO	0.08	0.07	0.08	0.11	0.09	0.11	0.13	0.12	0.13	0.04	0.05	0.04
Al_2O_3	0.06	0.05	0.07	0.08	0.09	0.12	0.04	0.05	0.06	0.02	0.02	0.00
MnO	0.14	0.15	0.14	0.10	0.12	0.14	0.09	0.10	0.09	0.09	0.04	0.05
ThO_2	0.14	0.15	0.14	0.17	0.15	0.21	0.21	0.18	0.20	0.10	0.09	0.09
Total	102.28	101.50	101.49	100.60	100.68	100.75	100.54	100.42	100.37	99.76	99.84	99.74

Table 22 cont.

Sample	EM1-2-a-2	EM1-2-a-3	EM1-2-a-4	EM2-2-c-1	EM2-2-c-2	EM2-2-c-3	EM2-2-7-1	EM2-2-7-2	EM2-2-7-3	MT6-1-u-1	MT6-1-u-2	MT6-1-u-3
apfu												
Zr	0.967	0.962	0.961	0.962	0.961	0.960	0.961	0.962	0.962	0.971	0.970	0.970
Si	0.985	0.989	0.991	0.997	0.995	0.995	0.998	0.997	0.997	0.999	0.998	1.001
Hf	0.036	0.036	0.035	0.031	0.034	0.033	0.032	0.032	0.032	0.027	0.029	0.026
U	0.005	0.005	0.005	0.001	0.002	0.001	0.001	0.001	0.001	0.000	0.000	0.000
Fe	0.003	0.002	0.002	0.003	0.002	0.003	0.003	0.004	0.004	0.000	0.001	0.000
Ca	0.002	0.002	0.003	0.004	0.003	0.003	0.004	0.004	0.004	0.001	0.002	0.001
Al	0.002	0.002	0.002	0.003	0.003	0.004	0.002	0.002	0.002	0.001	0.001	0.000
Mn	0.004	0.004	0.004	0.003	0.003	0.004	0.002	0.003	0.002	0.002	0.001	0.001
Th	0.001	0.001	0.001	0.001	0.001	0.001	0.002	0.001	0.001	0.001	0.001	0.001
X-site	1.009	1.005	1.003	0.996	0.998	0.996	0.996	0.996	0.996	0.999	1.000	0.998
Y-site	0.985	0.989	0.991	0.997	0.995	0.995	0.998	0.997	0.997	0.999	0.998	1.001

Table 22 cont.

Sample	MT6-1-u-4	MT6-1-a-1	MT6-1-a-2	MT6-1-a-3	MT6-1-a-4	MT6-1-a-5	MT6-1-a-6	MT4-1-d-1	MT4-1-d-2	MT4-1-d-3	MT1-2-c-1	MT1-2-c-2
ZrO_2	64.21	64.23	64.30	64.24	61.11	62.09	64.33	63.97	63.83	63.90	64.12	64.21
SiO_2	32.27	32.33	32.28	32.31	30.12	30.21	32.34	32.22	32.41	32.18	32.29	32.31
HfO_2	2.99	3.40	3.34	3.29	3.46	3.51	3.49	3.23	3.42	3.34	3.22	3.24
UO_2	0.03	0.02	0.02	0.02	0.01	0.01	0.03	0.03	0.04	0.03	0.03	0.03
FeO	0.02	0.02	0.02	0.02	0.78	0.62	0.01	0.79	0.70	0.66	0.00	0.01
CaO	0.03	0.03	0.03	0.02	1.33	1.09	0.02	0.01	0.00	0.00	0.00	0.00
Al_2O_3	0.01	0.03	0.02	0.03	0.03	0.04	0.02	0.03	0.04	0.02	0.03	0.03
MnO	0.06	0.04	0.04	0.04	0.89	0.99	0.05	0.03	0.02	0.02	0.01	0.01
ThO_2	0.09	0.10	0.09	0.09	0.05	0.06	0.10	0.07	0.07	0.07	0.07	0.07
Total	99.71	100.20	100.14	100.07	97.78	98.63	100.39	100.37	100.53	100.23	99.77	99.91

Table 22 cont.

Sample	MT6-1-u-4	MT6-1-a-1	MT6-1-a-2	MT6-1-a-3	MT6-1-a-4	MT6-1-a-5	MT6-1-a-6	MT4-1-d-1	MT4-1-d-2	MT4-1-d-3	MT1-2-c-1	MT1-2-c-2
apfu												
Zr	0.971	0.968	0.970	0.969	0.956	0.964	0.968	0.964	0.960	0.964	0.969	0.969
Si	1.000	0.999	0.998	0.999	0.966	0.962	0.998	0.996	0.999	0.996	1.001	1.000
Hf	0.026	0.030	0.029	0.029	0.032	0.032	0.031	0.028	0.030	0.029	0.029	0.029
U	0.000	0.000	0.000	0.000	0.000	0.000	0.000	0.000	0.000	0.000	0.000	0.000
Fe	0.001	0.000	0.000	0.001	0.021	0.017	0.000	0.020	0.018	0.017	0.000	0.000
Ca	0.001	0.001	0.001	0.001	0.046	0.037	0.001	0.000	0.000	0.000	0.000	0.000
Al	0.000	0.001	0.001	0.001	0.001	0.002	0.001	0.001	0.001	0.001	0.001	0.001
Mn	0.001	0.001	0.001	0.001	0.024	0.027	0.001	0.001	0.001	0.001	0.000	0.000
Th	0.001	0.001	0.001	0.001	0.000	0.000	0.001	0.001	0.000	0.000	0.000	0.000
X-site	0.998	0.999	1.000	0.999	0.988	0.996	1.000	0.993	0.990	0.995	0.998	0.999
Y-site	1.000	0.999	0.998	0.999	0.966	0.962	0.998	0.996	0.999	0.996	1.001	1.000

Table 22 cont.

Sample	MT1-2-c-3	MT1-2-c-4	MT1-2-c-5	MT6-1-u-1	MT6-1-u-2	TM2-1-c-1	TM2-1-c-2	TM2-1-c-3	TM4-1-c-1	TM4-1-c-2	TM4-1-c-3
ZrO_2	64.20	61.23	60.89	64.03	64.21	63.87	63.79	63.84	63.90	63.79	63.89
SiO_2	32.20	30.43	30.12	32.28	32.34	32.30	32.30	32.41	32.35	32.41	32.45
HfO_2	3.18	3.22	3.22	3.12	2.98	3.36	3.40	3.30	3.01	2.98	3.11
UO_2	0.03	0.01	0.01	0.03	0.03	0.18	0.17	0.17	0.11	0.11	0.09
FeO	0.01	2.12	1.98	0.01	0.01	0.09	0.11	0.11	0.21	0.10	0.14
CaO	0.00	1.22	2.32	0.00	0.00	0.18	0.17	0.16	0.32	0.29	0.27
Al_2O_3	0.04	0.07	0.05	0.02	0.02	0.11	0.21	0.09	0.09	0.08	0.15
MnO	0.01	0.32	0.34	0.01	0.01	0.22	0.18	0.17	0.19	0.15	0.23
ThO_2	0.06	0.05	0.05	0.05	0.05	0.31	0.27	0.31	0.28	0.26	0.25
Total	99.73	98.70	98.97	99.54	99.65	100.62	100.61	100.56	100.46	100.17	100.58

Table 22 cont.

Sample	MT1-2-c-3	MT1-2-c-4	MT1-2-c-5	MT6-1-u-1	MT6-1-u-2	TM2-1-c-1	TM2-1-c-2	TM2-1-c-3	TM4-1-c-1	TM4-1-c-2	TM4-1-c-3
apfu											
Zr	0.971	0.948	0.943	0.969	0.970	0.961	0.959	0.960	0.961	0.960	0.959
Si	0.999	0.967	0.956	1.002	1.002	0.996	0.996	0.999	0.997	1.001	0.998
Hf	0.028	0.029	0.029	0.028	0.026	0.030	0.030	0.029	0.026	0.026	0.027
U	0.000	0.000	0.000	0.000	0.000	0.001	0.001	0.001	0.001	0.001	0.001
Fe	0.000	0.056	0.053	0.000	0.000	0.002	0.003	0.003	0.005	0.003	0.004
Ca	0.000	0.042	0.079	0.000	0.000	0.006	0.006	0.005	0.011	0.010	0.009
Al	0.001	0.003	0.002	0.001	0.001	0.004	0.008	0.003	0.003	0.003	0.005
Mn	0.000	0.009	0.009	0.000	0.000	0.006	0.005	0.004	0.005	0.004	0.006
Th	0.000	0.000	0.000	0.000	0.000	0.002	0.002	0.002	0.002	0.002	0.002
X-site	1.000	0.978	0.972	0.997	0.997	0.994	0.992	0.992	0.990	0.989	0.988
Y-site	0.999	0.967	0.956	1.002	1.002	0.996	0.996	0.999	0.997	1.001	0.998

Apatite

Table 23: Apatite compositions from garnet boundary layers in Oxford County, Maine pegmatites.

Sample	BT1-a-1-1	BT1-a-1-2	BT1-a-1-3	BT1-a-1-4	BT1-a-1-5	BT1-a-1-6	BT2-a-1	BT2-a-2	BT2-a-3	BT2-a-4
SiO_2	0.06	0.04	0.04	0.06	0.04	0.06	0.06	0.06	0.05	0.07
Al_2O_3	0.02	0.01	0.02	0.03	0.03	0.02	0.00	0.00	0.02	0.02
FeO	0.01	0.01	0.02	0.00	0.01	0.01	0.01	0.01	0.01	0.01
MnO	0.12	0.09	0.23	1.33	1.44	1.21	0.03	0.02	0.02	0.02
MgO	0.00	0.00	0.00	0.00	0.00	0.00	0.00	0.00	0.00	0.00
SrO	0.07	0.06	0.08	0.12	0.09	0.07	0.05	0.05	0.05	0.04
CaO	0.00	0.00	0.00	0.00	0.00	0.00	0.00	0.00	0.00	0.00
P_2O_5	42.33	42.38	42.41	42.39	42.41	42.43	42.29	42.33	42.29	42.33
H_2O calc.	0.23	0.28	0.27	0.23	0.28	0.23	0.22	0.23	0.26	0.27
Cl	0.00	0.00	0.00	0.00	0.00	0.00	0.00	0.00	0.00	0.00
F	3.29	3.19	3.22	3.31	3.23	3.32	3.31	3.29	3.22	3.21
subtotal	101.75	101.69	101.89	102.93	103.14	102.99	101.73	101.60	101.51	101.51
O=F+Cl	1.39	1.34	1.36	1.39	1.36	1.40	1.39	1.39	1.36	1.35
Total	100.36	100.34	100.54	101.53	101.78	101.59	100.34	100.22	100.16	100.16

Table 23 cont.

Sample	BT1-a-1-1	BT1-a-1-2	BT1-a-1-3	BT1-a-1-4	BT1-a-1-5	BT1-a-1-6	BT2-a-1	BT2-a-2	BT2-a-3	BT2-a-4
apfu										
Si	0.005	0.004	0.004	0.005	0.004	0.005	0.005	0.005	0.004	0.005
Al	0.002	0.001	0.002	0.003	0.003	0.002	0.000	0.000	0.002	0.002
Fe	0.001	0.001	0.002	0.000	0.001	0.001	0.001	0.001	0.001	0.001
Mn	0.009	0.007	0.016	0.094	0.101	0.085	0.002	0.002	0.002	0.001
Mg	0.000	0.000	0.000	0.000	0.000	0.000	0.000	0.000	0.000	0.000
Sr	0.003	0.003	0.004	0.006	0.004	0.003	0.003	0.002	0.002	0.002
Ca	4.982	4.982	4.974	4.934	4.940	4.946	4.997	4.987	4.988	4.982
P	2.997	3.000	2.998	2.981	2.977	2.981	2.995	3.000	2.998	3.000
H	0.129	0.156	0.149	0.130	0.154	0.130	0.124	0.128	0.146	0.150
Cl	0.000	0.000	0.000	0.000	0.000	0.000	0.000	0.000	0.000	0.000
F	0.871	0.844	0.851	0.870	0.846	0.870	0.876	0.871	0.854	0.850
X-site	4.997	4.993	4.997	5.036	5.049	5.037	5.002	4.992	4.995	4.988
Y-site	2.997	3.000	2.998	2.981	2.977	2.981	2.995	3.000	2.998	3.000
Z-site	1.000	0.999	1.000	1.000	0.999	1.000	1.000	1.000	1.000	1.000

Table 23 cont.

Sample	HVY-1-d-1	HVY-1-d-2	HVY-1-d-3	TM3-a-1	TM3-a-2	TM3-a-3	TM3-a-4	TM3-a-5	TM2-b-1	TM2-b-2
SiO_2	0.03	0.03	0.03	0.07	0.09	0.08	0.07	0.32	0.11	0.11
Al_2O_3	0.00	0.00	0.00	0.00	0.00	0.00	0.00	0.00	0.00	0.00
FeO	0.00	0.00	0.00	0.01	0.00	0.01	0.01	0.01	0.00	0.00
MnO	0.01	0.01	0.01	0.04	0.04	0.02	0.05	0.07	0.10	0.11
MgO	0.00	0.00	0.00	0.00	0.00	0.00	0.00	0.00	0.00	0.00
SrO	0.02	0.03	0.03	0.08	0.06	0.06	0.01	0.03	0.03	0.03
CaO	55.60	55.68	55.71	55.49	55.51	55.58	55.53	55.50	55.40	55.41
P_2O_5	42.33	42.38	42.32	42.34	42.38	42.34	42.40	42.29	42.39	42.33
H_2O calc.	0.37	0.38	0.39	0.36	0.27	0.25	0.21	0.26	0.33	0.31
Cl										
F	3.00	2.97	2.95	3.01	3.21	3.26	3.33	3.23	3.09	3.12
subtotal	101.37	101.49	101.44	101.40	101.55	101.59	101.62	101.71	101.45	101.42
O=F+Cl	1.26	1.25	1.24	1.27	1.35	1.37	1.40	1.36	1.30	1.31
Total	100.11	100.24	100.20	100.13	100.20	100.22	100.22	100.35	100.15	100.11

Table 23 cont.

Sample	HVY-1-d-1	HVY-1-d-2	HVY-1-d-3	TM3-a-1	TM3-a-2	TM3-a-3	TM3-a-4	TM3-a-5	TM2-b-1	TM2-b-2
apfu										
Si	0.003	0.002	0.002	0.006	0.008	0.007	0.006	0.027	0.009	0.009
Al	0.000	0.000	0.000	0.000	0.000	0.000	0.000	0.000	0.000	0.000
Fe	0.000	0.000	0.000	0.000	0.000	0.000	0.000	0.000	0.000	0.000
Mn	0.001	0.001	0.001	0.003	0.003	0.002	0.004	0.005	0.007	0.008
Mg	0.000	0.000	0.000	0.000	0.000	0.000	0.000	0.000	0.000	0.000
Sr	0.001	0.002	0.002	0.004	0.003	0.003	0.000	0.002	0.001	0.001
Ca	4.989	4.990	4.996	4.978	4.975	4.983	4.977	4.966	4.966	4.971
P	3.002	3.001	2.999	3.001	3.002	2.999	3.003	2.990	3.003	3.001
H	0.206	0.213	0.218	0.203	0.150	0.138	0.118	0.147	0.182	0.173
Cl	0.000	0.000	0.000	0.000	0.000	0.000	0.000	0.000	0.000	0.000
F	0.794	0.787	0.782	0.797	0.849	0.861	0.882	0.853	0.818	0.826
X-site	4.991	4.992	4.999	4.985	4.981	4.988	4.982	4.972	4.974	4.980
Y-site	3.002	3.001	2.999	3.001	3.002	2.999	3.003	2.990	3.003	3.001
Z-site	1.000	1.000	1.000	1.000	1.000	1.000	1.000	1.000	1.000	0.999

Table 23 cont.

Sample	TM2-b-3	TM2-b-4	TM2-b-5	MA13-1-h-4	MA13-1-h-5	ma14-A-D-1	ma14-A-D-2	ma14-A-D-3	ma14-A-D-4	ma14-A-D-5
SiO_2	0.09	0.12	0.07	0.07	0.09	0.14	0.09	0.08	0.21	0.23
Al_2O_3	0.00	0.00	0.00	0.00	0.00	0.00	0.02	0.04	0.03	0.01
FeO	0.01	0.01	0.00	0.01	0.01	0.01	0.01	0.01	0.01	0.00
MnO	0.09	0.11	0.11	0.11	0.22	0.12	0.09	0.11	0.08	0.05
MgO	0.00	0.00	0.00	0.00	0.01	0.00	0.00	0.01	0.01	0.00
SrO	0.04	0.04	0.03	0.21	0.24	0.22	0.31	0.27	0.24	0.21
CaO	55.45	55.48	55.41	55.11	51.22	51.21	51.23	51.09	51.16	51.14
P_2O_5	42.31	42.39	42.38	42.01	42.11	42.11	42.09	42.01	41.98	41.98
H_2O calc.	0.27	0.33	0.32	0.30	0.32	0.37	0.42	0.35	0.37	0.42
Cl				0.28	0.34	0.26	0.23	0.19	0.23	0.20
F	3.21	3.10	3.10	3.12	2.99	2.88	2.78	2.92	2.88	2.77
subtotal	101.47	101.56	101.42	101.23	97.56	97.33	97.27	97.08	97.19	97.03
O=F+Cl	1.35	1.30	1.31	1.37	1.34	1.27	1.22	1.27	1.27	1.21
Total	100.12	100.26	100.12	99.85	96.22	96.06	96.05	95.81	95.93	95.81

Table 23 cont.

Sample	TM2-b-3	TM2-b-4	TM2-b-5	MA13-1-h-4	MA13-1-h-5	ma14-A-D-1	ma14-A-D-2	ma14-A-D-3	ma14-A-D-4	ma14-A-D-5
apfu										
Si	0.007	0.010	0.006	0.006	0.008	0.012	0.008	0.007	0.018	0.020
Al	0.000	0.000	0.000	0.000	0.000	0.000	0.002	0.004	0.003	0.001
Fe	0.000	0.000	0.000	0.001	0.001	0.001	0.001	0.001	0.001	0.000
Mn	0.007	0.008	0.008	0.008	0.016	0.009	0.007	0.008	0.006	0.004
Mg	0.000	0.000	0.000	0.000	0.001	0.000	0.000	0.001	0.001	0.000
Sr	0.002	0.002	0.001	0.010	0.012	0.011	0.016	0.014	0.012	0.011
Ca	4.976	4.970	4.970	4.968	4.737	4.739	4.743	4.741	4.739	4.741
P	3.000	3.000	3.003	2.992	3.077	3.079	3.079	3.080	3.073	3.075
H	0.149	0.182	0.179	0.171	0.183	0.213	0.240	0.200	0.211	0.242
Cl	0.000	0.000	0.000	0.039	0.050	0.037	0.034	0.028	0.033	0.029
F	0.851	0.818	0.821	0.829	0.817	0.787	0.760	0.800	0.789	0.758
X-site	4.985	4.980	4.979	4.968	4.737	4.739	4.743	4.741	4.739	4.741
Y-site	3.000	3.000	3.003	2.992	3.077	3.079	3.079	3.080	3.073	3.075
Z-site	1.000	1.000	1.000	1.000	1.000	1.000	1.000	1.000	1.000	1.000

Table 23 cont.

Sample	MA13-1-h-1	MA13-1-h-2	MA13-1-h-3	MT2-3-d-1	MT2-3-d-2	MT2-3-d-3	MT2-3-d-4	MT1-2-h-1	MT1-2-h-2	MT1-2-h-3
SiO_2	0.11	0.08	0.05	0.06	0.08	0.05	0.07	0.04	0.05	0.06
Al_2O_3	0.00	0.00	0.01	0.02	0.02	0.05	0.02	0.03	0.03	0.01
FeO	0.01	0.02	0.03	0.01	0.03	0.01	0.03	0.01	0.01	0.01
MnO	0.06	0.07	0.07	0.11	0.14	0.11	0.09	0.12	0.17	0.23
MgO	0.01	0.01	0.01	0.00	0.01	0.00	0.00	0.00	0.00	0.00
SrO	0.21	0.22	0.25	0.10	0.09	0.12	0.92	0.11	0.11	0.21
CaO	54.94	55.02	55.11	55.34	55.41	55.38	55.41	55.37	55.33	55.29
P_2O_5	42.00	41.89	42.01	41.99	42.01	42.06	41.98	41.93	42.01	41.98
H_2O calc.	0.36	0.41	0.25	0.30	0.32	0.33	0.26	0.37	0.36	0.31
Cl	0.11	0.21	0.25	0.00	0.00	0.00	0.00	0.00	0.00	0.00
F	2.99	2.89	3.22	3.11	3.08	3.06	3.21	2.98	3.01	3.10
subtotal	100.81	100.82	101.26	101.05	101.20	101.17	102.00	100.97	101.07	101.21
O=F+Cl	1.29	1.27	1.41	1.31	1.30	1.29	1.35	1.26	1.27	1.31
Total	99.53	99.56	99.85	99.74	99.90	99.88	100.65	99.71	99.80	99.90

Table 23 cont.

Sample	MA13-1-h-1	MA13-1-h-2	MA13-1-h-3	MT2-3-d-1	MT2-3-d-2	MT2-3-d-3	MT2-3-d-4	MT1-2-h-1	MT1-2-h-2	MT1-2-h-3
apfu										
Si	0.009	0.007	0.004	0.005	0.006	0.004	0.005	0.003	0.005	0.005
Al	0.000	0.000	0.001	0.002	0.002	0.005	0.002	0.003	0.003	0.001
Fe	0.001	0.001	0.002	0.001	0.002	0.001	0.002	0.001	0.001	0.001
Mn	0.004	0.005	0.005	0.008	0.010	0.008	0.006	0.009	0.012	0.017
Mg	0.001	0.001	0.001	0.000	0.001	0.000	0.000	0.000	0.000	0.000
Sr	0.010	0.011	0.012	0.005	0.004	0.006	0.045	0.006	0.005	0.010
Ca	4.963	4.973	4.970	4.992	4.991	4.988	4.980	4.997	4.988	4.985
P	2.998	2.992	2.993	2.993	2.990	2.993	2.981	2.991	2.992	2.990
H	0.202	0.228	0.142	0.171	0.180	0.188	0.148	0.205	0.200	0.175
Cl	0.016	0.030	0.035	0.000	0.000	0.000	0.000	0.000	0.000	0.000
F	0.798	0.772	0.858	0.829	0.820	0.812	0.852	0.794	0.800	0.825
X-site	4.963	4.973	4.970	5.008	5.011	5.008	5.035	5.015	5.008	5.013
Y-site	2.998	2.992	2.993	2.993	2.990	2.993	2.981	2.991	2.992	2.990
Z-site	1.000	1.000	1.000	0.999	1.000	1.000	1.000	1.000	1.000	1.000

Table 23 cont.

Sample	MT6-1-c-1	MT6-1-c-2	MT6-1-c-3
SiO_2	0.04	0.07	0.02
Al_2O_3	0.02	0.03	0.03
FeO	0.01	0.00	0.00
MnO	0.22	0.20	0.20
MgO	0.00	0.00	0.00
SrO	0.19	0.17	0.19
CaO	55.40	55.48	55.45
P_2O_5	42.01	42.11	42.09
H_2O calc.	0.31	0.27	0.32
Cl	0.00	0.00	0.00
F	3.11	3.19	3.09
subtotal	101.30	101.53	101.39
O=F+Cl	1.31	1.34	1.30
Total	99.99	100.18	100.09

Table 23 cont.

Sample	MT6-1-c-1	MT6-1-c-2	MT6-1-c-3
apfu			
Si	0.003	0.006	0.002
Al	0.002	0.003	0.003
Fe	0.001	0.000	0.000
Mn	0.015	0.014	0.014
Mg	0.000	0.000	0.000
Sr	0.009	0.008	0.009
Ca	4.990	4.986	4.988
P	2.990	2.990	2.992
H	0.172	0.153	0.179
Cl	0.000	0.000	0.000
F	0.827	0.847	0.821
X-site	5.018	5.011	5.014
Y-site	2.990	2.990	2.992
Z-site	0.999	1.000	1.000

Pollucite: Table 24: Pollucite compostions fomr garnet line boundary layers in Oxford County, Maine pegmatites.

Sample	MT4-1-A-1	MT4-1-A-2	MT4-1-A-3	MT4-1-b-1	MT4-1-b-2	MT6-1-c-1	MT6-1-c-2	MT6-1-c-3	HVY1-1-a-3-1	HVY1-1-a-3-2
SiO2	47.99	46.99	44.00	43.98	43.98	44.00	43.89	43.78	43.31	43.29
Al2O3	16.58	16.78	13.12	12.54	12.68	12.88	12.90	12.87	12.61	12.56
Fe2O3	0.24	0.12	3.25	4.95	5.39	5.62	5.69	5.45	6.07	5.81
MnO	0.09	0.30	0.27	0.27	0.25	0.23	0.29	0.28	0.19	0.19
Na2O	2.12	1.89	1.14	1.46	1.54	0.98	0.89	1.00	1.78	1.67
K2O	1.10	1.11	2.72	3.45	5.50	0.67	0.68	0.70	4.11	4.88
Rb2O	1.22	1.09	1.23	1.12	1.09	1.33	1.23	1.41	1.02	1.01
Cs2O	33.23	32.66	31.87	30.00	29.09	31.01	31.11	31.09	29.89	29.93
CaO	0.32	0.29	0.31	0.33	0.35	0.11	0.21	0.15	0.22	0.21
Total	102.8859	101.22143	97.916	98.109	99.879	96.845	96.9027	96.731	99.214302	99.551086
Si	2.114	2.101	2.104	2.083	2.052	2.098	2.093	2.095	2.043	2.043
Al	0.861	0.884	0.739	0.700	0.697	0.724	0.725	0.726	0.701	0.698
Fe	0.008	0.004	0.117	0.177	0.189	0.202	0.204	0.196	0.215	0.206
Mn	0.003	0.011	0.011	0.011	0.010	0.009	0.012	0.011	0.008	0.008
Na	0.181	0.164	0.106	0.134	0.140	0.091	0.082	0.093	0.163	0.153
K	0.062	0.063	0.166	0.208	0.327	0.040	0.041	0.043	0.247	0.294
Rb	0.035	0.031	0.038	0.034	0.033	0.041	0.038	0.043	0.031	0.030
Cs	0.624	0.623	0.650	0.606	0.579	0.630	0.633	0.635	0.601	0.602
Ca	0.015	0.014	0.016	0.017	0.017	0.006	0.011	0.007	0.011	0.011
Si/Al	2.456	2.376	2.846	2.976	2.944	2.898	2.887	2.885	2.914	2.925
$Al+Fe^{3+}$	0.869	0.888	0.856	0.877	0.886	0.925	0.929	0.922	0.916	0.905
$Si/Al+Fe^{3+}$	2.434	2.365	2.457	2.376	2.315	2.267	2.252	2.272	2.229	2.258
CRK	78.582	80.168	87.501	84.924	85.668	88.062	88.402	87.771	83.481	85.009

Table 24 cont.

	HVY1-1-a-3-3	HVY1-1-a-3-4	HVY1-1-a-3-5	HVY1-1-c-1	HVY1-1-c-2	HVY1-1-1-1	HVY1-1-1-2	HVY1-1-k-1	HVY1-1-k-2
SiO2	43.34	43.29	43.55	43.29	43.32	43.40	43.37	43.29	43.42
Al2O3	12.54	12.78	12.67	12.59	12.61	12.63	12.60	12.70	12.57
Fe2O3	5.60	5.80	5.81	5.55	5.55	4.71	6.17	5.70	5.20
MnO	0.19	0.20	0.21	0.19	0.20	0.10	0.14	0.21	0.22
Na2O	1.67	1.70	1.67	1.55	1.60	2.23	1.81	1.91	1.71
K2O	4.39	4.46	4.51	4.35	4.22	4.01	4.32	4.76	4.67
Rb2O	0.98	1.03	1.11	1.22	1.33	0.98	1.05	1.12	1.10
Cs2O	29.92	29.89	29.96	30.65	30.56	28.67	29.78	29.72	29.74
CaO	0.22	0.22	0.23	0.31	0.28	0.18	0.17	0.23	0.21
Total	98.865616	99.364956	99.729199	99.692192	99.663079	96.923103	99.41002	99.65056	98.842162
Si	2.053	2.040	2.046	2.049	2.049	2.069	2.041	2.037	2.056
Al	0.700	0.710	0.702	0.702	0.703	0.710	0.699	0.705	0.702
Fe	0.200	0.206	0.205	0.198	0.197	0.169	0.218	0.202	0.185
Mn	0.008	0.008	0.008	0.008	0.008	0.004	0.006	0.008	0.009
Na	0.153	0.155	0.152	0.143	0.147	0.206	0.165	0.174	0.157
K	0.265	0.268	0.270	0.262	0.255	0.244	0.259	0.286	0.282
Rb	0.030	0.031	0.034	0.037	0.040	0.030	0.032	0.034	0.033
Cs	0.604	0.601	0.600	0.618	0.616	0.583	0.598	0.597	0.601
Ca	0.011	0.011	0.012	0.016	0.014	0.009	0.008	0.012	0.011
Si/Al	2.932	2.873	2.916	2.918	2.914	2.914	2.922	2.892	2.931
$Al+Fe^{3+}$	0.900	0.916	0.907	0.899	0.900	0.879	0.917	0.906	0.887
$Si/Al+Fe^{3+}$	2.282	2.228	2.255	2.278	2.275	2.354	2.226	2.248	2.318
CRK	84.541	84.403	84.650	85.282	84.986	79.901	83.664	83.112	84.501

Xenotime

Table 25: Xenotime compositions from garnet line boundary layers in Oxford County, Maine pegmatites.

Sample	MT1-1-i-1	MT1-1-i-2	MT1-1-i-3	HVY-1-i-1	HVY-1-i-2	HVY-1-i-3	HVY-4-1-1	HVY-4-1-2	TM1-i-1	TM1-i-2	TM1-k-1	TM1-k-2	TM3-1-e-1	TM3-1-e-2
P_2O_5	34.84	34.78	34.82	34.83	34.80	34.80	34.78	34.80	34.87	34.86	34.86	34.83	37.31	37.22
SiO_2	0.04	0.04	0.05	0.04	0.03	0.04	0.06	0.03	0.06	0.05	0.02	0.03	0.21	0.27
ThO_2	0.01	0.01	0.02	0.01	0.02	0.00	0.01	0.01	0.00	0.01	0.01	0.01	0.02	0.02
UO_2	0.01	0.01	0.01	0.01	0.01	0.00	0.01	0.01					0.01	0.01
Al_2O_3	0.06	0.05	0.06	0.07	0.06	0.06	0.10	0.07	0.02	0.02	0.00	0.03		
Y_2O_3	50.44	50.47	50.49	50.40	50.44	50.41	50.46	50.41	50.48	50.49	50.39	50.40	50.02	50.12
Nd_2O_3	0.01	0.01	0.01	0.00	0.02	0.01	0.02	0.02	0.01	0.02	0.02	0.03		
Sm_2O_3	0.11	0.09	0.10	0.03	0.00	0.04	0.05	0.05	0.03	0.04	0.05	0.05	0.06	0.06
Gd_2O_3	2.25	2.33	2.29	2.83	2.62	2.70	2.78	2.80	2.89	2.82	2.79	2.85	2.13	2.21
Dy_2O_3	0.92	1.00	1.05	0.88	0.84	0.84	0.88	0.86	0.90	0.88	0.90	0.90	4.33	4.12
Ho_2O_3	0.61	0.65	0.63	0.67	0.71	0.70	0.73	0.72	0.75	0.72	0.78	0.76	0.79	0.76
Er_2O_3	1.89	1.99	1.07	2.01	1.91	1.98	1.94	2.09	1.99	2.07	2.10	2.09	2.21	2.31
Yb_2O_3	3.45	4.51	3.44	3.21	3.09	3.12	3.01	3.07	2.89	2.87	2.79	2.77	3.11	3.31
FeO	0.41	0.40	0.38	0.27	0.32	0.26	0.23	0.24	0.17	0.16	0.20	0.18	0.04	0.04
MnO				0.01	0.01	0.01	0.01	0.01	0.01	0.01			0.03	0.04
CaO	0.08	0.08	0.06	0.10	0.12	0.16	0.13	0.11	0.08	0.09	0.12	0.16	0.12	0.11
Total	95.12	96.44	94.49	95.39	95.01	95.13	95.21	95.32	95.17	95.10	95.04	95.10	100.39	100.59

Table 25 cont.

Sample	MT1-1-i-1	MT1-1-i-2	MT1-1-i-3	HVY-1-i-1	HVY-1-i-2	HVY-1-i-3	HVY-4-1-1	HVY-4-1-2	TM1-i-1	TM1-i-2	TM1-k-1	TM1-k-2	TM3-1-e-1	TM3-1-e-2
apfu														
P	0.992	0.985	0.994	0.990	0.991	0.991	0.990	0.990	0.992	0.992	0.993	0.992	1.006	1.004
Si	0.001	0.001	0.002	0.001	0.001	0.001	0.002	0.001	0.002	0.002	0.001	0.001	0.007	0.008
Th	0.000	0.000	0.000	0.000	0.000	0.000	0.000	0.000	0.000	0.000	0.000	0.000	0.000	0.000
U	0.000	0.000	0.000	0.000	0.000	0.000	0.000	0.000	0.000	0.000	0.000	0.000	0.000	0.000
Al	0.002	0.002	0.002	0.003	0.002	0.002	0.004	0.003	0.001	0.001	0.000	0.001	0.000	0.000
Y	0.902	0.899	0.906	0.901	0.903	0.902	0.902	0.902	0.903	0.904	0.903	0.902	0.848	0.849
Nd	0.000	0.000	0.000	0.000	0.000	0.000	0.000	0.000	0.000	0.000	0.000	0.000	0.000	0.000
Sm	0.001	0.001	0.001	0.000	0.000	0.001	0.001	0.001	0.000	0.000	0.001	0.001	0.001	0.001
Gd	0.025	0.026	0.026	0.032	0.029	0.030	0.031	0.031	0.032	0.031	0.031	0.032	0.023	0.023
Dy	0.010	0.011	0.011	0.010	0.009	0.009	0.009	0.009	0.010	0.010	0.010	0.010	0.044	0.042
Ho	0.007	0.007	0.007	0.007	0.008	0.007	0.008	0.008	0.008	0.008	0.008	0.008	0.008	0.008
Er	0.020	0.021	0.011	0.021	0.020	0.021	0.021	0.022	0.021	0.022	0.022	0.022	0.022	0.023
Yb	0.035	0.046	0.035	0.033	0.032	0.032	0.031	0.032	0.030	0.029	0.029	0.028	0.030	0.032
Fe	0.012	0.011	0.011	0.007	0.009	0.007	0.007	0.007	0.005	0.004	0.006	0.005	0.001	0.001
Mn	0.000	0.000	0.000	0.000	0.000	0.000	0.000	0.000	0.000	0.000	0.000	0.000	0.001	0.001
Ca	0.003	0.003	0.002	0.004	0.004	0.006	0.005	0.004	0.003	0.003	0.004	0.006	0.004	0.004

Monazite

Table 26: Monazite compostions from garnet boundary layers in Oxford County, Maine pegmaites.

Sample	MT6-2-1	MT6-2-2	MT6-2-3	MA2-1-1	MA2-1-2	MA2-1-3	BT-3-1	BT-3-2	BT-3-3	TM1-d-1	TM1-d-2	TM3-1-c-1	TM3-1-c-2
P_2O_5	29.68	29.57	29.56	29.47	29.63	29.78	29.89	30.04	29.88	29.88	29.91	29.98	30.09
SiO_2	1.61	1.65	1.67	1.44	1.50	1.61	0.98	1.09	1.00	0.72	0.78	0.98	0.98
ThO_2	10.40	10.43	10.45	10.22	10.24	10.21	7.90	8.02	8.10	6.56	6.45	7.23	7.19
UO_2	0.87	0.85	0.88	0.82	0.84	0.82	0.30	0.33	0.34	0.34	0.28	0.41	0.39
Al_2O_3	0.05	0.07	0.08	0.09	0.08	0.07	0.04	0.05	0.05	0.02	0.04	0.04	0.05
Y_2O_3	2.67	2.64	2.70	1.88	1.91	1.81	1.21	1.22	1.20	0.98	0.95	0.87	0.92
La_2O_3	8.11	8.09	8.12	8.33	8.29	8.33	9.89	9.83	9.87	10.09	10.00	10.35	10.29
Ce_2O_3	22.82	22.72	22.67	22.56	22.62	22.55	23.87	23.88	23.78	23.78	23.68	23.87	24.01
Pr_2O_3	2.32	2.28	2.30	2.11	2.09	2.20	3.43	3.55	3.43	3.38	3.44	3.41	3.40
Nd_2O_3	14.44	14.51	14.52	14.78	14.64	14.56	13.23	13.34	13.56	12.92	13.01	13.21	13.27
Sm_2O_3	3.89	4.03	3.78	3.89	3.93	3.71	3.63	3.73	3.63	3.89	3.78	3.98	4.01
Eu_2O_3	0.08	0.09	0.11	0.10	0.07	0.08	0.21	0.20	0.20	0.19	0.19	0.20	0.20
Gd_2O_3	2.34	2.12	1.89	1.99	1.98	2.01	2.78	2.78	2.62	2.67	2.54	2.88	2.91
Tb_2O_3	1.00	1.09	0.91	0.98	0.88	0.92	0.78	0.78	0.68	0.80	0.67	0.81	0.99
Dy_2O_3	0.00	0.00	0.00	0.00	0.00	0.00	0.00	0.00	0.00	0.00	0.00	0.00	0.00
Yb_2O_3	0.20	0.20	0.19	0.16	0.18	0.14	0.17	0.15	0.14	0.12	0.13	0.10	0.12
FeO	0.11	0.09	0.10	0.13	0.19	0.18	0.21	0.22	0.24	0.18	0.21	0.23	0.26
MnO	0.00	0.00	0.00	0.00	0.00	0.00	0.00	0.00	0.00	0.12	0.09	0.03	0.04
MgO	0.11	0.10	0.09	0.10	0.09	0.09	0.06	0.06	0.07	0.02	0.02	0.02	0.03
CaO	0.89	0.90	0.92	1.21	1.22	1.21	0.54	0.56	0.56	0.43	0.39	0.41	0.40
PbO	0.14	0.14	0.14	0.14	0.14	0.14	0.45	0.44	0.44	0.34	0.30	0.36	0.41
total	101.73	101.57	101.08	100.40	100.52	100.42	99.57	100.27	99.79	97.46	96.86	99.39	99.95

Table 26 cont.

Sample	MT6-2-1	MT6-2-2	MT6-2-3	MA2-1-1	MA2-1-2	MA2-1-3	BT-3-1	BT-3-2	BT-3-3	TM1-d-1	TM1-d-2	TM3-1-c-1	TM3-1-c-2
apfu													
A-site													
Th	0.091	0.091	0.091	0.090	0.090	0.089	0.070	0.071	0.072	0.059	0.058	0.064	0.064
U	0.007	0.007	0.008	0.007	0.007	0.007	0.003	0.003	0.003	0.003	0.002	0.004	0.003
Al	0.002	0.003	0.004	0.004	0.004	0.003	0.002	0.002	0.002	0.001	0.002	0.002	0.002
Y	0.054	0.054	0.055	0.039	0.039	0.037	0.025	0.025	0.025	0.021	0.020	0.018	0.019
La	0.115	0.115	0.115	0.119	0.118	0.118	0.143	0.141	0.142	0.148	0.147	0.149	0.148
Ce	0.320	0.319	0.319	0.320	0.320	0.318	0.342	0.339	0.340	0.346	0.345	0.342	0.342
Pr	0.032	0.032	0.032	0.030	0.029	0.031	0.049	0.050	0.049	0.049	0.050	0.049	0.048
Nd	0.198	0.199	0.199	0.205	0.202	0.200	0.185	0.185	0.189	0.183	0.185	0.185	0.185
Sm	0.051	0.053	0.050	0.052	0.052	0.049	0.049	0.050	0.049	0.053	0.052	0.054	0.054
Eu	0.001	0.001	0.002	0.001	0.001	0.001	0.003	0.003	0.003	0.003	0.003	0.003	0.003
Gd	0.030	0.027	0.024	0.026	0.025	0.026	0.036	0.036	0.034	0.035	0.033	0.037	0.038
Tb	0.000	0.000	0.000	0.000	0.000	0.000	0.000	0.000	0.000	0.000	0.000	0.000	0.000
Dy	0.012	0.013	0.011	0.012	0.011	0.011	0.010	0.010	0.009	0.010	0.009	0.010	0.012
Yb	0.002	0.002	0.002	0.002	0.002	0.002	0.002	0.002	0.002	0.001	0.002	0.001	0.001
Fe	0.004	0.003	0.003	0.004	0.006	0.006	0.007	0.007	0.008	0.006	0.007	0.008	0.008
Mn	0.000	0.000	0.000	0.000	0.000	0.000	0.000	0.000	0.000	0.004	0.003	0.001	0.001
Mg	0.006	0.006	0.005	0.006	0.005	0.005	0.003	0.003	0.004	0.001	0.001	0.001	0.002
Ca	0.037	0.037	0.038	0.050	0.050	0.050	0.023	0.023	0.023	0.018	0.017	0.017	0.017
Pb	0.001	0.001	0.001	0.001	0.001	0.001	0.005	0.005	0.005	0.004	0.003	0.004	0.004
A-total	0.964	0.964	0.961	0.969	0.964	0.955	0.955	0.955	0.958	0.946	0.938	0.949	0.952
B-site													
P	0.962	0.961	0.962	0.967	0.969	0.971	0.990	0.987	0.988	1.004	1.007	0.993	0.992
Si	0.062	0.063	0.064	0.056	0.058	0.062	0.038	0.042	0.039	0.029	0.031	0.038	0.038
B-total	1.024	1.024	1.026	1.023	1.027	1.033	1.028	1.029	1.027	1.033	1.038	1.032	1.030

Scheelite and Wolframite: Table 27: Scheelite and wolframite compositions from garnet boundary layers in Oxford County, Maine pegmatites.

Sample	MT2-3-a-1	MT2-3-a-2	MT2-3-a-3	MT2-3-a-4	MT2-3-a-5	MT1-1-a-1	MT1-1-a-2	MT1-1-a-3
WO_3	75.32	75.68	75.72	75.52	75.83	74.78	74.80	74.79
Nb_2O_5	0.01	0.00	0.01	0.01	0.01	0.01	0.01	0.02
Ta_2O_5	0.01	0.00	0.00	0.01	0.01	0.01	0.02	0.02
TiO_2	0.12	0.01	0.01	0.00	0.00			
SiO_2						0.19	0.09	0.14
SnO_2	0.02	0.01	0.01	0.02	0.02			
Al_2O_3	0.02	0.06	0.05	0.00	0.00	0.04	0.03	0.01
FeO	12.78	11.81	11.61	2.92	3.22	0.11	0.10	0.13
MnO	11.45	12.43	12.72	22.12	22.01	0.09	0.10	0.11
MgO	0.11	0.09	0.08	0.03	0.12			
CaO						19.14	18.99	19.16
Total	99.85	100.08	100.22	100.63	101.23	94.38	94.15	94.38
apfu								
W	0.984	0.987	0.986	0.979	0.976	0.978	0.982	0.979
Nb	0.000	0.000	0.000	0.000	0.000	0.000	0.000	0.000
Ta	0.000	0.000	0.000	0.000	0.000	0.000	0.000	0.000
Ti	0.005	0.000	0.000	0.000	0.000	0.000	0.000	0.000
Si	0.000	0.000	0.000	0.000	0.000	0.010	0.005	0.007
Sn	0.000	0.000	0.000	0.000	0.000	0.000	0.000	0.000
Al	0.001	0.003	0.003	0.000	0.000	0.002	0.002	0.001
Fe	0.539	0.497	0.488	0.122	0.134	0.005	0.004	0.006
Mn	0.489	0.530	0.541	0.937	0.926	0.004	0.004	0.004
Mg	0.008	0.007	0.006	0.002	0.009	0.000	0.000	0.000
Ca	0.000	0.000	0.000	0.000	0.000	1.035	1.031	1.036

Vita:

Myles Felch was born in Manchester, NH on June 2, 1989. He lived in Maine for nineteen years and attended the University of Maine at Farmington, graduating in 2012 with a B.A. in Geology. His graduate studies began in the fall of 2012 at the University of New Orleans, where he became a member of the MP2 research group.